

THE UNIVERSITY OF MICHIGAN  
INDUSTRY PROGRAM OF THE COLLEGE OF ENGINEERING

HEAT TRANSFER FROM HIGH TEMPERATURE GASES  
INSIDE CIRCULAR TUBES

Herbert Edmund Zellnik

A dissertation submitted in partial  
fulfillment of the requirements for the degree of  
Doctor of Philosophy in the University of Michigan  
1956.

September, 1956

IP-177



#### ACKNOWLEDGEMENT

We wish to express our appreciation to the author for permission to give this thesis limited distribution under the Industry Program of the College of Engineering.



## ACKNOWLEDGEMENTS

The author is greatly indebted to his doctoral committee, who generously provided valuable advice and assistance. In particular, the author appreciated the guidance of Professor S. W. Churchill, the chairman of the doctoral committee, whose active interest and helpful suggestions were a major factor in the completion of this work.

Professor L. Thomassen's advice and assistance in technical details concerning thermocouples and thermocouple location was of great help to the author.

The author wishes to thank W. J. M. Douglas for assistance in many of the experimental details, as well as for many valuable suggestions, and also G. P. Colpitts, M. T. Tayyabkhan, and K. S. Sanvordenker for their help, suggestions, and moral support.

Help in the preparation of this report by the Industry Program is gratefully acknowledged. The author is also indebted to the men of the Chemical Engineering Department shops, without whose aid the equipment would never have been built or kept in running condition.

The author gratefully acknowledges the financial assistance received by him from the American Cyanamid Company for one year and the Sinclair Oil Refining Company for two years, without which this work would have been virtually impossible.



TABLE OF CONTENTS

	<u>Page</u>
ACKNOWLEDGEMENT . . . . .	ii
AUTHOR'S ACKNOWLEDGEMENTS . . . . .	iii
LIST OF ILLUSTRATIONS . . . . .	vi
LIST OF TABLES . . . . .	viii
NOMENCLATURE . . . . .	ix
ABSTRACT . . . . .	xiii
INTRODUCTION . . . . .	1
REVIEW OF THEORY AND PRIOR WORK . . . . .	5
Fluid Flow Theory and Forced Convective Heat Transfer in Tubes . . . . .	6
Effect of Temperature Level and Radial Temperature Distribution on Heat Transfer . . . . .	11
Local Rates of Heat Transfer with Special Emphasis on the Entrance Section of Circular Tubes . . . . .	18
High Temperature Experimental Techniques for Local Coefficients . . . . .	20
APPARATUS . . . . .	22
Electric Resistance Furnace and Adiabatic Sections . . . . .	24
Gas Supply and Measuring System . . . . .	34
Cooling Water System . . . . .	38
Heat Transfer Test Unit . . . . .	39
MATERIALS . . . . .	45
Gas . . . . .	45
Test Object . . . . .	45
Thermocouples in Test Object . . . . .	45
EXPERIMENTAL THEORY . . . . .	46
Measurement of Rate of Heat Transfer . . . . .	46
Discussion of Assumptions . . . . .	51
Analysis of Radiation Effects . . . . .	53
Turbulence Level and Velocity Profiles . . . . .	55
Flow Measurement with Inconel Orifice Meter . . . . .	56
EXPERIMENTAL PROCEDURE . . . . .	60
Preliminary Experimental Work . . . . .	60
Preparations for a Run . . . . .	61
Variables Measured during an Experimental Run and Experimental Range . . . . .	62

TABLE OF CONTENTS (Cont.)

	<u>Page</u>
Specifications for Acceptable Runs . . . . .	63
Location of Thermocouples in Test Object and Calibration of Equipment . . . . .	65
DISCUSSION OF FACTORS AFFECTING ACCURACY OF EXPERIMENTAL RESULTS . . . . .	68
Location of Thermocouples in Test Object . . . . .	68
Gas Temperature Measurement. . . . .	71
Minor Clogging of Screens. . . . .	75
Gas Flow Rate. . . . .	76
Net Temperature Differences on the Water Side. . . . .	76
Thermal Properties of Air. . . . .	77
EXPERIMENTAL RESULTS. . . . .	79
DISCUSSION AND INTERPRETATIONS OF RESULTS . . . . .	97
Correlations Based on Use of Bulk Temperature for Evaluating Properties. . . . .	97
Effect of Evaluating Properties at Varying Reference Temperatures . . . . .	104
Comparisons with Prior Work. . . . .	116
CONCLUSIONS . . . . .	123
APPENDIX A. ORIGINAL AND PROCESSED DATA. . . . .	124
APPENDIX B. DATA PROCESSING. . . . .	129
APPENDIX C. DERIVATIONS AND PROOFS . . . . .	135
APPENDIX D. PROPERTIES OF MATERIALS AND CALIBRATIONS . . . . .	147
APPENDIX E. SOURCES OF EQUIPMENT AND MATERIALS . . . . .	151
BIBLIOGRAPHY. . . . .	153



LIST OF ILLUSTRATIONS

<u>Figure</u>		<u>Page</u>
1	General Views of Apparatus. . . . .	23
2	Furnace Detail. . . . .	26
3	View of Test Object and Adiabatic Sections. . . . .	30
4	Detail of Adiabatic Sections and Top Furnace Assembly. . . . .	31
5	Schematic Diagram of Flow Systems . . . . .	37
6	Detail of Test Object . . . . .	41
7	Thermocouple Wiring Diagram . . . . .	43
8	Comparison Between Methods of Estimating Local Bulk Temperature . . . . .	74
9a	Correlation of Local Heat Transfer Data and Deter- mination of Effect of Temperature Level for L/D = 1.5, Properties Evaluated at Bulk Temperature . . . . .	89
9b	Correlation of Local Heat Transfer Data and Deter- mination of Effect of Temperature Level for L/D = 4, Properties Evaluated at Bulk Temperature .	90
9c	Correlation of Local Heat Transfer Data and Deter- mination of Effect of Temperature Level for L/D = 7, Properties Evaluated at Bulk Temperature .	91
9d	Correlation of Local Heat Transfer Data and Deter- mination of Effect of Temperature Level for L/D = 10, Properties Evaluated at Bulk Temperature.	92
9e	Correlation of Local Heat Transfer Data and Deter- mination of Effect of Temperature Level for L/D = 1.5, Properties Evaluated at Film Temperature . . . . .	93
10	Correlation of Local Heat Transfer Coefficients at L/D = 10 as a Function of Mass Velocity . . . . .	94
11	Summary of Heat Balances. . . . .	95
12	Comparison of Present Data with Curve Derived from Boelter, et al. . . . .	96

LIST OF ILLUSTRATIONS (Cont.)

<u>Figure</u>		<u>Page</u>
13	Sketch of Normalized Heat Transfer Rate Profiles in Inlet Region for Various Methods of Correlation.	102
14	Plot of Reference Temperature Adjustment Function for Film Temperature. . . . .	111
15	Diagram of Reference Temperature Adjustment Func- tion for Various Reference Temperatures . . . . .	111
16	Effect of Temperature Level for Heating and Cooling . . . . .	118
17	Graphical Calculations for Run No. 46 . . . . .	133
18	Geometric Interchange Factor for Radiation Emitted from the End of a Cylinder to the Cylinder Walls. .	137
19	Illustration of Conformal Mapping Procedure . . . .	142
20	Calibration Curve for Inconel Orifice . . . . .	148
21	Calibration Curve for Air Rotameter . . . . .	149
22	Calibration Curve of TC-7 in the Test Object. . . .	150

LIST OF TABLES

<u>Table</u>		<u>Page</u>
Ia	Summary of Original and Processed Data for L/D = 1.5 . . . . .	124
Ib	Summary of Original and Processed Data for L/D = 4 . . . . .	125
Ic	Summary of Original and Processed Data for L/D = 7 . . . . .	126
Id	Summary of Original and Processed Data for L/D = 10. . . . .	127
II	Summary of Operating Conditions and Heat Balances .	128
III	Composition and Thermal Conductivity of Inconel . .	147
IV	Sources of Equipment and Materials. . . . .	151



## NOMENCLATURE

- A = area,  $\text{ft}^2$
- a = multiplicative constant in convection equations
- b = Reynolds number exponent
- C = arbitrary constant in solution of radial conduction equation,  $^{\circ}\text{F}$
- $C_o$  = orifice coefficient, dimensionless
- c = constants in orifice equations
- c = Prandtl number exponent
- $c_p$  = specific heat at constant pressure,  $\text{Btu/lb } ^{\circ}\text{F}$
- D = diameter, ft
- $D_{o20}$  = diameter of inconel orifice at  $20^{\circ}\text{C}$ , ft
- d = exponent on dimensionless group (L/D)
- E = dimensionless distance equal to L/r
- F = geometry factor in radiation equation, dimensionless
- $\bar{F}$  = geometry factor in radiation equation corrected for emissivity, dimensionless
- f = exponent on dimensionless group ( $v/v_c$ )
- f = function of
- G = mass velocity,  $\text{lbs/hr ft}^2$
- h = heat transfer coefficient,  $\text{Btu/hr ft}^2 ^{\circ}\text{F}$
- K = constant in Boelter's equation for  $h_{av}$ , dimensionless
- k = thermal conductivity,  $\text{Btu/hr ft } ^{\circ}\text{F}$
- L = length, distance from tube inlet, ft
- M = Mach number, ( $v/v_c$ ), dimensionless
- m = exponent on dimensionless group ( $T_b/T_s$ )
- n = arbitrary exponent that has to be evaluated

$Nu$  = Nusselt number,  $(hD/k)$ , dimensionless  
 $Pr$  = Prandtl number,  $(c_p\mu/k)$ , dimensionless  
 $q$  = heat transfer rate, Btu/hr  
 $r$  = radial coordinate of a cylinder, feet or mils  
 $Re$  = Reynolds number,  $(DG/\mu)$ , dimensionless  
 $S$  = complex constant in conformal transformation  
 $St$  = Stanton number,  $(h/c_pG)$ , dimensionless  
 $T$  = real constant in conformal transformation  
 $T$  = absolute temperature, °R  
 $t$  = temperature, °F  
 $t'$  = temperature derived from straight line method, °F  
 $U, U', U''$  = abscissa of points in  $W, W',$  and  $W''$  planes, respectively  
 $V$  = transformed  $\Theta$  coordinate in complex plane  
 $v$  = linear velocity, ft/hr  
 $v_c$  = sonic velocity, ft/hr  
 $W$  = weight rate of flow, lbs/hr  
 $W, W', W''$  = points in transformed complex plane longitudinal coordinate  
 $Z$  = longitudinal coordinate of cylinder, ft  
 $Z', Z''$  = transformed  $Z$  coordinates in  $W'$  and  $W''$  planes  
 $z$  = coefficient in reference temperature equation, dimensionless  
 $\alpha$  = proportional to  
 $\alpha$  = temperature coefficient of thermal conductivity,  $1/^\circ\text{F}$   
 $\alpha_T$  = expansion factor of orifice (length at  $T$ /length at  $20^\circ\text{C}$ )  
 $\beta$  = modified orifice coefficient  
 $\Gamma$  = dimensionless function of reference and bulk temperatures  
 $\gamma$  = exponent, equal to  $(0.8\xi - \nu)$   
 $\Delta$  = finite difference (state 2 minus state 1)  
 $\delta$  = exponent on  $(T_b/T_s)$  adjustment term

- $\epsilon$  = emissivity for thermal radiation, dimensionless  
 $\eta$  = approximate power to which both  $\mu$  and  $k$  are supposed to vary  
 $\Theta$  = angular coordinate, radians  
 $\theta$  = time, hour  
 $\lambda$  = multiplicative constant for reference temperature adjustment, dimensionless  
 $\mu$  = viscosity, lb/ ft hr  
 $\nu$  = power of temperature to which viscosity varies  
 $\xi$  = power of temperature to which thermal conductivity varies  
 $\pi$  = ratio of circumference to diameter of circle, dimensionless  
 $\rho$  = density, lbs/ft<sup>3</sup>  
 $\sigma$  = Stefan-Boltzmann constant for thermal radiation, Btu/hr ft<sup>2</sup>  
           Btu/hr ft<sup>2</sup> °R<sup>4</sup>  
 $\phi_i$  = function of particular property in question

### Subscripts

- $av$  = average  
 $b$  = bulk of fluid (usually refers to local condition)  
 $c$  = convection  
 $e$  = exit  
 $f$  = film (arithmetic average)  
 $g$  = gas  
 $i$  = inlet  
 $i$  = reference state (for thermal conductivity only)  
 $m$  = integrated mean  
 $o$  = orifice  
 $o$  = at outside surface of inconel tube  
 $r$  = reference for properties

r = radiation  
s = at inside surface of inconel tube  
t = total  
w = water  
0,1,2 = arbitrary states or positions  
10 = at L/D = 10

### Abbreviations

div = divergence of  
gpm = gallons per minute  
grad = gradient of  
KVA = Kilovoltampere  
lb = pound  
log = common logarithm (base = 10)  
ln = natural logarithm (base = e)  
mil = 0.001 inch  
psia = absolute pressure, lb/in<sup>2</sup>  
psig = gauge pressure, lb/in<sup>2</sup>  
SCFM = standard cubic feet per minute  
S.D. = standard deviation  
< = less than  
> = greater than  
≈ = approximately equal to



## ABSTRACT

The local rates of convective heat transfer from a high temperature gas stream to a cold tube wall were measured in the inlet region of a circular tube for the case of an initially flat velocity and flat temperature profile.

Air, at inlet temperatures from 480° to 2000°F and flow rates corresponding to bulk Reynolds numbers up to 22,000, was passed through a water-cooled inconel tube, whose surface was kept at about 100°F.

Local rates of heat transfer were obtained at distances corresponding to 1.5, 4, 7, and 10 tube diameters from the inlet of the tube, by means of measuring the radial temperature profiles in each of four thermally isolated annular sectors of the tube wall. From each radial temperature profile, the thermal flux and the extrapolated inside wall temperature were obtained from the classical equation for conduction, which, together with a knowledge of the local bulk gas temperature, permitted the local heat transfer coefficient to be computed. The results obtained at 10 tube diameters from the inlet were essentially the same as for fully developed flow and hence were equivalent to the results that would have been obtained for a long tube after the entrance effects had become negligible.

The local rates of heat transfer obtained were correlated in the form of

$$\text{Nu} = a \text{Re}^{0.8} \text{Pr}^{1/3} (T_p/T_s)^m$$

where

a = constant, which varies with distance down the tube but asymptotically approaches a value of 0.023 after ten tube diameters from the inlet.

$T_b$  = absolute bulk gas temperature, °R.

$T_s$  = absolute temperature of cold surface, °R.

$m$  = exponent on term which accounts for effect of temperature level

Re = Reynolds Number, Pr = Prandtl Modulus, Nu = Nusselt Number.

The effect of evaluating the thermal properties at different reference temperatures was also studied, and the experimental results indicate the following:

1) There is no significant effect of temperature level on the correlations, i.e.,  $m \approx 0$ , if the thermal properties in the dimensionless groups are evaluated at the bulk temperature. Hence, the  $(T_b/T_s)$  term can be deleted completely, thus reducing the equation given above to the form of existing correlations based on experiments with small temperature differences.

2) If the thermal properties are evaluated at the surface temperature rather than the bulk gas temperature, the results indicate that inclusion of the term  $(T_b/T_s)^{0.33}$  is necessary, and this adequately accounts for the effects of temperature level; however, a factor of the form  $(T_b/T_s)^m$  can never successfully account for the effects of temperature level if the properties are referred to the film temperature.

3) Even though  $\underline{a}$  varies down the length of the tube,  $\underline{m}$  does not and is purely a function of the reference temperature used. Hence, the effect of temperature level does not vary down the length of the tube.

Thus, existing correlations based on low temperature work have been shown to be adequate for high temperature applications if the properties are evaluated at the bulk gas temperature. Agreement between the results of this study and those of previous investigations, wherever experimental ranges overlap, is excellent.

## INTRODUCTION

Convective heat transfer between a gas stream and the walls of a circular tube has many important commercial applications and hence has been the subject of intense theoretical and experimental investigation for well over three quarters of a century.

Since so many branches of engineering, as well as applied physics, have contributed to this field of investigation, it is not surprising to find such a diversity of scope, purpose, and method, in the various investigations. A wide range of variables has been encompassed by the work of previous investigators, but yet the assembled information is quite incomplete in many areas of present interest, such as high temperatures, high vacuum, and intense pressure.

Many investigators realized that temperature level had an effect on heat transfer, and expressions to account for this phenomenon were developed, either from purely theoretical considerations or from actual experimental measurements. Until recently, however, most of the experiments for cooling gases inside circular tubes were carried out near room temperature with only comparatively small temperature differences across the film. One of the notable early exceptions was Groeber,<sup>12</sup> who passed air heated up to 600°F through a bare horizontal tube whose outside surface was directly exposed to the air and noticed that the heat transfer coefficient increased with temperature level.

Most of the high temperature work reported in the literature is for heat addition, results for wall temperatures up to 2500°F and  $T_s/T_b$  ratios of 3.5 having been reported. The most definitive work to date on the effect of large wall to gas temperature differences is that

of Humble, et al.<sup>16</sup> Their work is primarily concerned with the heating of gases, though a few heat extraction runs were taken for inlet air temperatures up to a maximum of 1040°F. For a large range of Reynolds numbers, they passed air through electrically heated inconel and platinum tubes of various length to diameter ratios, the wall temperatures going up to as high as 2600°F and the temperature differences across the film up to 2000°F. Only average coefficients were measured and an integrated average wall temperature was used in evaluating the mean temperature difference between the gas and the wall. As was expected, a decrease in the Nusselt number was observed as the ratio  $T_s/T_b$  increased, but the effect of  $T_s/T_b$  was explicitly eliminated in their final correlations by using a modified Reynolds number. In their few cooling runs, however, they noticed that there was no effect of temperature level if they correlated in terms of the properties evaluated at the bulk temperature. This fact, as well as previous theoretical analyses, clearly point out the fact that it cannot be expected that data on heat transfer coefficients obtained for heating can also be used to predict those for cooling, especially when radial temperature differences are great.

A possible source of error in Humble, et al.'s work is that, because they used only average wall and bulk temperatures and computed only average coefficients, a variation in the effect of temperature level down the length of the tube, especially in the inlet section, might go unnoticed if there were a compensating effect. Furthermore, no data has as yet been published which indicates whether there is any significant change in the variation of heat transfer coefficients down the length of the tube in the inlet section as compared to the results obtained at low temperatures.

Because of the paucity of high temperature cooling data, and the limited temperature ranges covered by prior work, it is apparent that an extension of our present knowledge into these high temperature ranges would fill a much needed gap. Neglect of this region is probably not only due to the experimental difficulties encountered in obtaining a high temperature gas stream and in materials of construction, but also possibly to a general failure to realize that temperature difference may be a significant factor in affecting heat transfer. It was therefore felt advisable to undertake an investigations which would go up to gas temperature of 2000°F.

This experimental study was set up with four main objectives in mind:

- 1) To determine if temperature level affected the known low temperature variation of Nusselt number with  $L/D$  in the inlet section of a tube.

- 2) To determine whether the effects of temperature level varied down the length of the tube.

- 3) To investigate the effect of temperature level on the Nusselt number for the case of high temperature heat extraction.

- 4) To determine the best form of an overall correlation to account for the effects of temperature level.

Standard apparatus and techniques for experimental work at high gas temperatures and for the measurement of local coefficients does not exist; however, a technique for measuring local coefficients, developed by Churchill,<sup>5</sup> even though for a different geometry, is applicable to this case, and was successfully utilized. Other aspects of Churchill's

work were also found analogous to this one, and his method of gas temperature measurement was successfully applied to the present work.

The present investigation covers a considerable range of gas temperatures and a small, but reasonable, range of Reynolds numbers. The reason that only a small range of Reynolds numbers was used is that it was felt that the effect of flow rate on the heat transfer coefficient had already been defined on the basis of the extensive prior work in the fields of heat transfer and fluid flow. The inside surface of the heat transfer tube was kept at a relatively constant temperature. The effects of tube diameter and gas properties having been well defined by previous studies, experiments were limited to a single tube diameter and a single gas.

Experimental data and correlations are presented for the local coefficients measured at four points down the tube, corresponding to  $L/D = 1.5, 4, 7,$  and  $10$ . For all practical purposes, the results at  $L/D = 10$  may be considered as equal to that which would be obtained in a long tube after the entrance effects become negligible. The experimental apparatus and techniques are described in detail, and pertinent aspects of previous studies are described and discussed.

The experimental program covered a temperature range in which practically no data have been reported, especially for local coefficients, and hence fulfills a great need by extending our knowledge of the effects of high temperature level on heat transfer.

## REVIEW OF THEORY AND PRIOR WORK

The topics of heat transfer and fluid flow have been the subject of intense theoretical and experimental investigation for well over three quarters of a century. Convective heat transfer inside circular tubes has been a widely studied field, and good general summaries of the past work may be found in McAdams<sup>18</sup> and Groeber, et al.<sup>13</sup> However, the exact effect of temperature level on the heat transfer coefficient for the cooling of high temperature gases inside circular tubes has not yet been precisely determined since most of the previous work has been done at temperatures below 500°F, with only a few experimenters reaching gas temperatures of 1000°F. Because the temperature region encountered in this investigation is one in which relatively little work has been done, the experimental and theoretical aspects of previous studies are reviewed in the light of how they affect the development and interpretation of the present study. This review will be divided into three main sections, namely:

- 1) Fluid Flow Theory and Forced Convective Heat Transfer Inside Tubes,
- 2) Effects of Temperature Level and Distribution on Heat Transfer,
- 3) Local Rates of Heat Transfer in the Entrance Section.

In general, the theoretical and experimental work as well as the experimental technique pertinent to that topic will be discussed in each of the appropriate sub-sections and will be treated simultaneously.

Fluid Flow Theory and Forced Convective Heat Transfer Inside Tubes

Before going more closely into the problem at hand, namely the effect of temperature level upon heat transfer, it is necessary to look at the fundamental work in heat transfer upon which present heat transfer theory and correlation depends. Only the work of previous investigators which has a bearing on the present study will be surveyed.

Convective heat transfer and fluid flow theory are intimately related. If the complete fluctuating temperature, velocity and density distribution of a fluid flowing inside a pipe are known, then the heat transfer, pressure drop, average bulk velocity, etc. can in theory be calculated from purely mathematical considerations. For the case of laminar flow, the momentum, energy, and continuity equations of fluid dynamics can be solved to give the temperature and velocity fields if constant fluid properties are assumed. This case was originally studied by Graetz and extended by Nusselt and others, and the work is well reviewed in Groeber, et al.<sup>13</sup> The assumption of constant fluid properties, however, holds only if the temperature changes encountered are comparatively small.

Turbulent flow through a tube becomes complex to analyze since the flow pattern, according to the boundary layer concept, is assumed to be composed to a laminar sub-layer, a buffer zone (recently eliminated in an analysis by Deissler<sup>6</sup>), and a turbulent zone. A purely mathematical approach to the problem is also much more difficult because portions of the fluid move about in random fashion. Since a transverse velocity gradient exists, momentum is accordingly transferred from one portion of the fluid to another, and a shear stress, in addition to the viscous



shear, is produced. Expressions for this "eddy" shear stress have been derived and applied by von Karman,<sup>29</sup> Bakhmeteff,<sup>2</sup> Deissler,<sup>6</sup> and others. A similar correction factor for thermal conductivity, the "eddy" conductivity, is also required to attack the problem analytically. Because of the uncertainties in theory, the simplifying assumptions required to arrive at an analytic solution, as well as the difficulty in applying the unwieldy mathematical expressions proposed by theoreticians, it has become common engineering practice to fit empirical correlations to convective heat transfer data. These correlations are functions of characteristic dimensionless groups which have been derived either from putting the Navier-Stokes equations into dimensionless form or from a dimensional analysis of the fluid flow problem after the variables to be considered have been selected. The most commonly encountered of these groups are:

<u>Name</u>	<u>Symbol</u>	<u>Equation</u>
Reynolds Number	Re	$Dv\rho/\mu$ or $DG/\mu$
Prandtl Number	Pr	$c_p\mu/k$
Nusselt Number	Nu	$hD/k$
Graetz Number	Gz	$Wc_p/kL$

Two other dimensionless groups, derivable from the above, often appear in the literature. These are the Stanton number,  $St = Nu/RePr = h/c_pG$ , and the Peclet number,  $Pe = RePr = DGc_p/k$ . Other dimensionless ratios such as  $L/D$ ,  $v/v_c$ ,  $T_s/T_b$ , etc. also may be found in correlations to account for tube length, high velocities, and temperature level, respectively. Each dimensionless group has a physical meaning pertinent to the problem. The Reynolds number, for instance, is the ratio of the

inertia to the friction forces and is the criterion of flow behavior,  $Re < 2100$  denoting laminar flow and  $Re > 10,000$  indicating the completely developed turbulent flow regime.

For the general case, dimensional analysis suggests that forced convective heat transfer data can be correlated in terms of a number of dimensionless groups, i.e.,

$$Nu = f \left( Re, Pr, \frac{L}{D}, \frac{T_s}{T_b}, \frac{v}{v_c} \text{ ----- etc.} \right) \quad (1)$$

or

$$St = f \left( Re, Pr, \frac{L}{D}, \frac{T_s}{T_b}, \frac{v}{v_c} \text{ ----- etc.} \right) \quad (2)$$

The groups such as  $\frac{L}{D}, \frac{T_s}{T_b}, \frac{v}{v_c}$  are included to account for the effects of additionally introduced variables that may be relevant to the problem at hand. It then is assumed that the above functions can be expressed in terms of power series of the dimensionless groups, the first term of each series being the predominant one. From this it follows that

$$Nu = a (Re)^b (Pr)^c \left[ \left( \frac{L}{D} \right)^d \left( \frac{T_s}{T_b} \right)^m \text{ --- etc.} \right] \quad (3)$$

or

$$St = a (Re)^{b-1} (Pr)^{c-1} \left[ \left( \frac{L}{D} \right)^d \left( \frac{T_s}{T_b} \right)^m \text{ --- etc.} \right] \quad (4)$$

Based on extensive data, McAdams<sup>18</sup> recommends a value of 0.8 for  $b$ , the exponent of  $Re$  in equation (3). For  $c$ , the  $Pr$  exponent, all researchers agree on some value between 0.3 and 0.4,  $1/3$  often being recommended for both heating and cooling. The multiplicative constant which critically depends on  $b$  and  $c$ , as evaluated by various investigators, ranged from a low of 0.023 to a high of 0.028, 0.023 being the recommended value. Summarizing, McAdams recommends the following relationship for gases inside tubes:

$$(hD/k) = 0.023 (DG/\mu)^{0.8} (c_p\mu/k)^{0.4} \quad (5)$$

The data on which the above correlation was based were all for relatively low temperatures and heat fluxes, the maximum experimental temperature being 600°F. McAdams also states that the exact effect of the Pr for gases is hard to evaluate because this group is hardly affected by gross variations in temperature and pressure.

Many investigators noted that tube length was a decided variable in correlating overall heat transfer coefficients. This is due to the variation of the local Nusselt number down the length of the tube while the boundary layer is forming, and an analysis of the entrance section itself and the associated experimental work may be found in a separate section of this report. Dimensional analysis leads to the introduction of a group  $(\frac{L}{D})^n$  as a factor in equations (3) and (4). Nusselt<sup>20</sup> suggested a value for n of -0.054 for  $\frac{L}{D}$  up to 200, while Humble, et al.<sup>16</sup> found that a value of -0.1 correlated their data very well for  $15 < \frac{L}{D} < 120$ . If, for small values of  $\frac{L}{D}$ , the result of studies from a flat plate in turbulent flow are applied, then n would be -0.2 (see reference 13). A recent theoretical analysis by Deissler<sup>9</sup> sheds some light on the confusion of what the proper exponent is. From a solution of the heat flow equations for a thermal boundary layer, and assuming the equality of the eddy diffusivities for momentum and heat transfer, he constructed theoretical curves on logarithmic coordinates for the variation of  $Nu_{av}$  with  $\frac{L}{D}$  for various values of Re. For  $6 < \frac{L}{D} < 60$ , a line of slope -0.1 would account extremely well for the tube length effect, though for values of  $\frac{L}{D} > 60$  the slope decreases and for  $\frac{L}{D} < 6$  the slope increases. Thus, the proper exponent of  $\frac{L}{D}$  is itself

a function of the length of the tube, and indicates why  $(\frac{L}{D})^n$  is a poor form to use. In a way, this corroborates as well as explains the differences in the various values proposed by previous investigators.

A factor which many early investigators overlooked was the effect of turbulence level on the heat transfer coefficient. Even now, there is disagreement as to exactly what the effect is for the inside of circular tubes. Boelter, et al.<sup>3</sup> claims that there is no appreciable effect of turbulence level on their data, yet their curves do denote about a ten percent increase in heat transfer coefficient when turbulence promoting screens were used. Ramey, et al.,<sup>24</sup> on the other hand, found that the turbulence and local velocity distortions induced by the jet-type entrance of gases from a mixing device increased heat transfer coefficients by better than 300 percent. Since turbulence level is difficult to measure, it is difficult to obtain results with it as an operating variable; however, recently, some techniques have been devised by Baines and Peterson<sup>1</sup> and others by which the turbulence level of a fluid issuing from a series of screens can be predicted as a function of Re and screen variables. This will be discussed in more detail in the section on experimental theory. It hence seems evident that as an aid to future investigators, an attempt should be made to define the turbulence level at which the heat transfer experiments were carried out.

Other factors such as Mach number, surface temperature variation, roughness, and free convection effects may affect turbulent heat transfer, but these will not be reviewed in detail here because they have no direct bearing on the present investigation. The extremely important factors of temperature level, temperature distribution, and the variation

of local rates in the entrance sections have been deferred for special consideration in the next two sections of this report, in which they and the associated experimental work will be treated in detail.

### Effect of Temperature Level and Radial Temperature Distribution on Heat Transfer

Many investigators realized that temperature level and distribution had an effect on heat transfer and expressions to account for this phenomenon were developed, either from purely theoretical considerations or from actual experimental measurements; however, the maximum temperatures at which experiments for cooling gases inside circular tubes were carried out were mainly for low temperature differences between the bulk gas and the wall temperatures, although a few experimenters did go up to gas temperatures of about 1000°F. These will be discussed later.

A direct mathematical attack on the problem is complicated by the fact that for high temperature differences between the bulk and the wall the fluid properties such as viscosity, thermal conductivity, density, etc. vary considerably and hence the velocity and temperature distributions differ greatly from the idealized "isothermal" case. In gases, a flattening of the velocity profile is obtained for heating while a peaking of the profile at the center of the tube is obtained for heat extraction. (The reverse is true for liquids since their viscosity decreases with temperature.) Due to the different nature of the flow pattern for heating and cooling, it cannot be expected that data on heat transfer coefficients obtained for heating can also be used to predict those for cooling, especially when the radial temperature differences are great. The findings of most investigators in the field has been that the heat transfer coefficient increases with temperature level

for the cooling of high temperature gases and decreases for heat addition to gases. The exact effect of the temperature level on the heat transfer coefficient for cooling has not yet been accurately determined, and below, as an example, are enumerated various empirical relations as to the quantitative effect of heat extraction that were suggested prior to 1931, as cited in McAdams:<sup>18</sup>

<u>Date</u>	<u>Author</u>	<u>h varies, as</u>
1919	Weber	$(c_p)_g T_g^{1/2}$
1924	Fessenden	$(c_p)_g T_g/T_f$
1927	Dixon	$(c_p)_g T_f^{2/3}$
1930	Nusselt	$(c_p)_s (T_g/T_s)^{1/3}$
1931	Reynolds Analogy	$(c_p)_g \mu_g^{0.2}$

---

NOTE: Absolute temperature is represented by T, with subscripts s for surface, g for gas, and f for film:  
 $T_f = T_g + T_s/2.$

In one of the earliest experiments to determine the exact effect of temperature level on the heat transfer coefficient, Groeber<sup>12</sup> passed heated air through a base horizontal steel tube whose outside surface was directly exposed to air. This caused the tube wall temperature to rise as the inlet air temperature was increased. For a wide range of flow rates, the air temperature was varied between 212° and 600°F, the resulting range of wall temperatures being 167° and 482°F respectively. Groeber noticed a definite increase in the heat transfer coefficient at higher temperatures, and proposed a correlation which was dependent on both the wall and bulk temperatures, though not in a ratio form.

As pointed out previously, convective heat transfer coefficients are generally correlated in the form

$$(hD/k) = a (DG/\mu)^b (c_p\mu/k)^c \left[ \left(\frac{L}{D}\right)^d \left(\frac{v}{v_c}\right)^f \text{---etc.} \right] \quad (6)$$

or

$$(h/c_p G) = a (DG/\mu)^{b-1} (c_p\mu/k)^{c-1} \left[ \left(\frac{L}{D}\right)^d \left(\frac{v}{v_c}\right)^f \text{---etc.} \right] \quad (7)$$

where the terms in brackets account for the effect of tube length, the Mach number, temperature, and others. Though the Prandtl number,  $c_p\mu/k$ , of gases varies only slightly with temperature, the Nusselt number,  $hD/k$ , and the Reynolds number,  $DG/\mu$ , depend upon the temperature at which  $k$  and  $\mu$  are evaluated. Because for gases, the variations of  $\mu$  and  $k$  are very similar and can be approximated by the expression

$$\left(\frac{\mu_2}{\mu_1}\right) = \left(\frac{k_2}{k_1}\right) = \left(\frac{T_2}{T_1}\right)^\eta \quad (8)$$

Nusselt<sup>19</sup> suggested that the dimensionless ratio  $\frac{T_s}{T_b}$  be included in the above correlation for gases, i.e.

$$Nu = a Re^b Pr^c \left(\frac{T_s}{T_b}\right)^m \quad (9)$$

where  $m$  is a constant that has to be determined theoretically or experimentally. This permits the evaluation of  $Re$ ,  $Pr$ , and  $Nu$  at either  $T_b$  or  $T_s$  since the results can be converted from one temperature to the other by multiplying or dividing by  $f(T_s/T_b)$ .

From the data of Jordan, Babcock and Wilcox, and Groeber, as well as from fluid flow theory, Nusselt<sup>21</sup> proposed that for heat extraction,  $f(T_s/T_b)$  should be  $(T_b/T_s)^{1/3}$ . A very definitive work on the heat transfer coefficient outside tubes for high gas temperatures and

temperature differences has recently been done by Churchill,<sup>5</sup> in which he found that the Nusselt number varied as  $(T_b/T_s)^{0.12}$ .

Sieder and Tate<sup>26</sup> on the other hand, felt that the variable liquid properties during heat transfer could best be accounted for by including the factor  $(\mu_b/\mu_s)^n$  in equations (6) and (7). From their own and other investigators measurements, they obtained a value of 0.14 for  $n$  where  $\mu_s/\mu_b$  varied from 0.004 to 14, or a considerable range of heating and cooling since  $\mu_s/\mu_b = 1$  represents the "isothermal" case.

The case of non-isothermal laminar flow, which lends itself more easily to direct mathematical attack, was studied by Pigford<sup>23</sup> and Deissler.<sup>8</sup> Pigford's correlation, which accounts only for variations in density and viscosity, is difficult to apply in practice and depends, in part, on a correction factor that is a function of the Graetz number. Deissler's correlation is more practical since he suggests evaluating  $\mu$  and  $k$  at a specified film temperature between that of the bulk and the wall, the reference temperature being different for each property.

For the more difficult case of turbulent flow, an approach which many investigators used to account for radial temperature variations during heat transfer was to evaluate  $Re$  and  $Nu$  (which depend upon the temperature at which  $\mu$  and  $k$  are evaluated) at some reference temperature between the bulk and the wall temperatures, or to somehow obtain a mean  $\mu$  and  $k$ . This problem is made difficult by the fact that each property is a different function of temperature,  $\phi_i(t)$ , so that a single reference temperature does not necessarily give the mean value of all properties. Nusselt<sup>19</sup> proposed the use of the integrated mean values of the properties, namely



$$\phi_{i_m} = \frac{\int_{t_s}^{t_b} \phi_i dt}{t_b - t_s} \quad (10)$$

Because the evaluation of this integral is so time consuming, a reference temperature of  $t_r = (t_b + t_s)/2$  is often used for evaluating the "average" properties and it is called the average film temperature. However, the above values of the integral or the reference temperature do not take into account the difference in temperature and velocity profiles between heating and cooling, since they give the same result for both.

Groeber, et al.<sup>13</sup> mention that Hofmann, from experimental investigations, suggests

$$t_r = t_b - \left( \frac{0.1 \text{ Pr} + 40}{\text{Pr} + 72} \right) (t_b - t_s) \quad (11)$$

as the reference temperature.

Deissler<sup>7</sup> and Deissler and Eian,<sup>10</sup> in an analytic and experimental investigation of turbulent flow in smooth tubes with heat transfer and variable fluid properties, predicted velocity distributions and Nusselt number variations for heating and cooling of gases. Using their own and other investigators' data, they suggested using a reference temperature

$$t_r = t_b + z (t_s - t_b) \quad (12)$$

and determined the optimum values for  $z$  under the following conditions:

	<u>z</u>
Turbulent flow, heating gases	0.4
Turbulent flow, cooling gases	0.6
Turbulent flow, heating and cooling	0.5

From theory alone, Deissler predicted that using the latter value of 0.5 for both heating and cooling would cause a maximum deviation of nine percent in the predicted values of the Nusselt number when compared to those rigorously computed at the average film temperature.

For heat transfer from a flat plate to a gas stream, Rubesin and Johnson<sup>25</sup> proposed

$$T_r = T_b [ 1 + 0.32 M^2 + 0.58 (T_s/T_b - 1) ]. \quad (13)$$

The little high temperature experimental work that has been done for circular tubes will now be described. Ramey, et al.<sup>24</sup> conducted experiments with superheated steam and air up to 1200°F, but unfortunately for this present investigation, their work was primarily concerned with accounting for the effect of gas radiation on the heat transfer coefficient. They did, however, notice that a ten percent increase in the heat transfer coefficient for air was observed at 1000°F over that obtained at lower temperatures when  $h$  was plotted versus  $G$ , the mass flow rate.

The most definitive work on the effect of large wall to gas temperature differences inside tubes to date is that of Humble, et al.<sup>16</sup> Their work is primarily concerned with the heating of gases, though a few heat extraction runs were taken for inlet air temperatures up to a maximum of 1040°F. For a large range of Reynolds numbers, they passed air through electrically heated inconel and platinum tubes of various length to diameter ratios, the wall temperatures going up to as high as 2600°F and the temperature differences across the film up to 2000°F. Only average coefficients were measured, and an integrated average wall temperature was used in evaluating the mean temperature difference

between the gas and the wall. (This in itself leads to inaccuracies since  $T_s/T_b$  varies over the whole length of the tube.) As was expected, a decrease in the heat transfer coefficient was observed as the ratio  $T_s/T_b$  was increased. A constant Reynolds number cross plot of the Nusselt number evaluated at the bulk temperature vs.  $T_s/T_b$  showed a variation of Nu as  $(T_s/T_b)^{-0.55}$ . This effect of temperature level was explicitly eliminated in their final correlation, however, by using a modified Reynolds number with the density and viscosity evaluated at the surface temperature and the velocity at bulk conditions. The thermal conductivity in the Nusselt number also was referred to  $t_s$ .

The few cooling runs that were taken by the above experimenters were brought into line with their modified heating correlations by evaluating the properties at the average film temperature. Furthermore, the cooling data also was found to fit present low temperature correlations when the bulk Nusselt number was plotted against the bulk Reynolds number, but the authors themselves state that these data do not necessarily show that no effect of  $T_s/T_b$  exists. This is due to the present uncertainty of the variation of thermal conductivity with temperature since use of a smaller variation of  $k$  with temperature and its resultant increase of the Nusselt number would introduce an effect of  $T_s/T_b$  into the data. Moreover, the small number and temperature range of the cooling runs taken do not permit an exact evaluation of temperature level effects.

Weiland and Lowdermilk<sup>30</sup> extended Humble's high temperature work to shorter tubes to measure the effect of tube length, but found no appreciable difference in the results for Re above 10,000 if properties were evaluated at the average film temperature.

Local Rates of Heat Transfer with Special Emphasis on the Entrance Section of Circular Tubes

Since all of the work on the variation of local heat transfer coefficients has been done at low temperatures, a review of the experimental results and methods of correlation can only present an indication or trend of what is to be expected at higher temperature levels and heat fluxes.

The variation of heat transfer coefficients in the entrance section is intimately connected with the fluid dynamics problem, and is directly dependent upon the initial velocity and temperature distributions. Theoretically, at the entrance of the tube, the heat transfer coefficient is infinite since the incipient boundary layer is of zero thickness. At some distance downstream, both the velocity and temperature gradients will assume some finite value as the boundary layer becomes fully developed. Due to the dissimilarity of the temperature and velocity profiles, a distinction is made between the thermal and velocity boundary layers, and each of these requires a different characteristic distance from the entrance until fully developed flow prevails.

The case of laminar flow lends itself more readily to direct mathematical attack and has been extensively studied by investigators such as Graetz, Nusselt, Leveque, von Karman, and others. A good review of the practical aspects of their work may be found in Groeber, Erk, and Grigull.<sup>13</sup>

As usual, the case of turbulent flow is much more complicated from the theoretical viewpoint. Only little experimental work has been done, the most definitive of which is that of Boelter, Young, and Iversen.<sup>3</sup> An excellent review of the previous theoretical and

experimental work of Latzko, Martinelli, and others may also be found in this paper. For a variety of inlet configurations, Boelter, et al. passed air through a doubly steam jacketed 1.785 inch I.D. tube. Every inch, and later every two inches downstream, a partition was put into the middle steam jacket and the condensate formed in each of these sections due to losing heat to the air was collected from each section. This gave them a measure of the heat transferred and the heat transfer coefficient for each section. They compared their point data with correlations previously derived by other investigators, and suggested which ones were most reliable for application to certain specific inlet conditions. Since the local coefficient for tubes varies so greatly in the inlet section, the average coefficient also is affected by tube length. From their experimental data, Boelter, et al. recommend the relation

$$h_{av} = h_{min} \left( 1 + K \frac{D}{L} \right) \quad (14)$$

for values of  $\frac{L}{D} > 5$ , where K is a constant which depends on the inlet configuration and conditions. A table of values for K is provided by the authors, a value of 1.4, for instance, being recommended for fully developed flow and uniform temperature distribution at the inlet.

Cholette<sup>4</sup> measured his local rates by approximately the same method as Boelter, et al. but used a multitubular exchanger. His apparatus consisted of separate sections, each about 10.5 tube diameters long, which could be coupled together. He noticed that the average coefficient in the first section was about 30 percent higher than that for the second section, and correlated his data as  $St_{av} \propto \left( \frac{L}{D} \right)^{-0.1}$ . His work has really little bearing to the present investigation since the

increments of tube length used were too great to permit a really accurate evaluation of the local rates in the initial entrance section of a tube.

In a very thorough analytic investigation, Deissler<sup>9</sup> studied turbulent heat transfer and flow in the entrance regions of smooth passages. A variety of initial temperature and velocity distributions were considered, under the assumption of both variable and constant fluid properties. Curves for the variation of  $Nu$  and  $h_{local}/h_{final}$  versus tube length at various Reynolds numbers were presented, as well as graphs indicating the hydraulic and thermal entrance lengths required to obtain a fully developed boundary layer as a function of  $Re$ . The theoretically predicted curves of  $Nu$  vs.  $\frac{L}{D}$  for air were checked against Boelter, et al.'s and Latzko's data and agreed very well with the experimental values. An interesting result of the above study is that the thermal boundary layer, and hence heat transfer coefficient, comes to within two percent of its limiting value in half the distance it takes for the velocity distribution to develop fully. For most cases this is within nine tube diameters of the entrance, and changes in the heat flux do not appreciably alter this value. Consequently, a local heat transfer coefficient measured at an  $\frac{L}{D}$  of 10 can safely be taken as equal to that for steady state conditions.

#### High Temperature Experimental Techniques for Local Coefficients

No measurement of actual local rates at high temperatures has ever been done for the case of the inside of circular tubes. The closest to this would be the heating data of Humble, et al.<sup>16</sup> and Weiland and Lowdermilk,<sup>30</sup> obtained at high wall temperatures and heat fluxes which has previously been mentioned and which covers a range of tube  $\frac{L}{D}$ 's from 15 to 100. Only the variation of the average coefficient with tube

length was considered and the experimental technique has already been described elsewhere in this report. Since the smallest increment was 15 tube diameters, no real evaluation of the local heat transfer coefficient in the critical entrance section could be obtained.

For a different geometry, that of gas flow outside and transverse to a circular tube, Churchill<sup>5</sup> developed an ingenious method of measuring local rates at high gas temperatures and fluxes by measuring the flux induced in a thermally isolated sector of the tube wall. This method is very useful since it is also applicable to the case under consideration in the present investigation. Churchill's technique was to thermally insulate a radial annular sector of the tube, and into this he inserted thermocouples at three different radial distances. With the temperature gradients obtained, the flux in the annular sector could be computed, and from it and the wall and gas temperature the local heat transfer coefficient over the sector was obtained. This technique proved to be very accurate and reliable, and is the only one known to the author to have been used for measuring local rates at high gas temperatures.

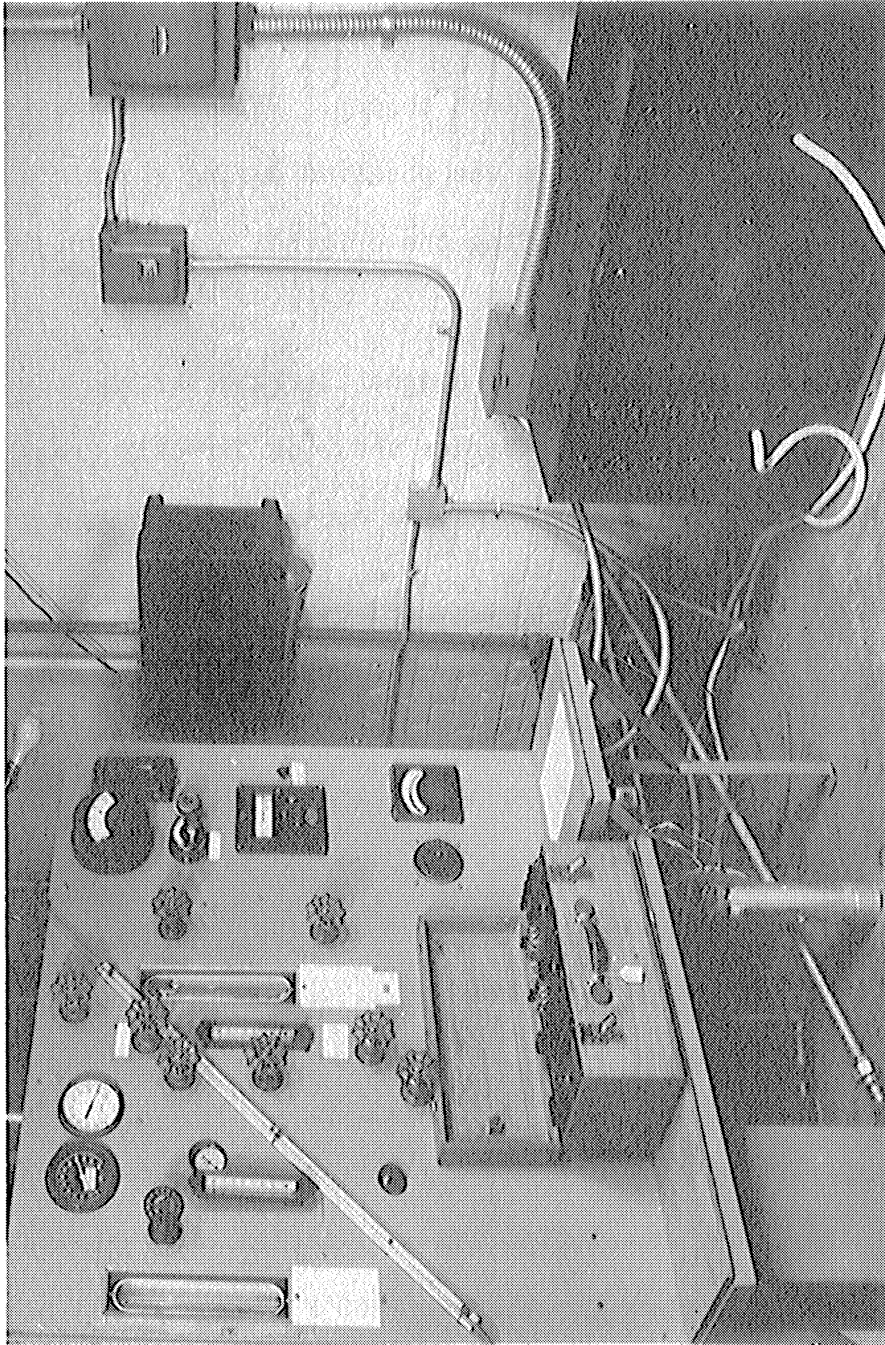
## APPARATUS

The apparatus used was designed specifically for the measurement of local rates of heat transfer inside the entrance section of a circular tube at high gas temperatures and large heat fluxes through the film and wall. Gas rates of up to 25 SCFM and temperatures of 2500°F can be obtained with this equipment.

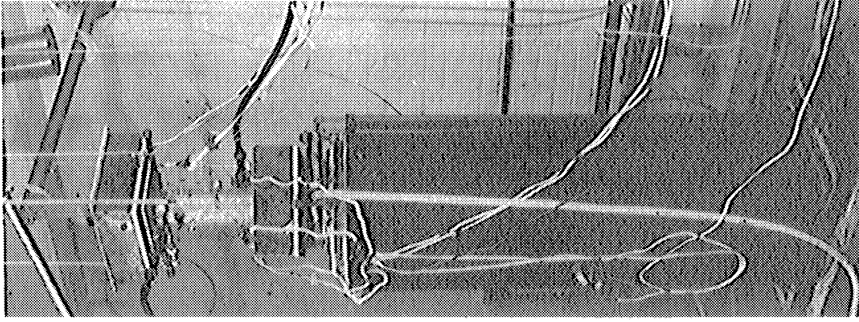
The main parts of the equipment are a furnace with auxiliaries, adiabatic sections to measure gas temperatures, a gas (compressed air) supply system, a water supply system, a heat transfer unit specifically designed for measuring the local and overall coefficients, and appropriate instrumentation and accessories. A detailed description of the above components of the equipment will follow in subsequent sub-sections, but first a brief description of the functional relationships between the major items of equipment will be given.

General views of the apparatus can be seen in Figures 1a and 1b, and a schematic flow diagram is given in Figure 5. Compressed air from the 90 psig building supply system passes through a cleaner and dehumidifier, and is then passed through a pressure regulator and rotometer for gas flow measurement. The air then is heated inside the furnace as it passes through a packed inconel tube inside a silicon carbide (Globar) electric resistance heating element. The heated gas then passes through an "adiabatic" section which consists of a packed tube surrounded by high temperature insulation, where its temperature is measured. After passing through a series of three screens for smoothing of the velocity profile and turbulence control, it enters the heat transfer test unit





a) Panel and Transformer



b) Furnace, Test Object,  
and Adiabatic Sections

Figure 1. General Views of Apparatus

which is a small heat exchanger with thermocouples imbedded in the wall for a measurement of the radial temperature profiles inside four thermally isolated annular sectors. On the exit side of the test unit, another adiabatic section is located for the measurement of the exit gas temperature. Knowing the inlet and exit temperatures give a heat balance check on the local heat transfer coefficients computed from the radial temperature profiles in the test unit. Before being vented up the stack, the hot gas passes through an inconel orifice meter for measurement of the flow rate through the test object. This was necessitated due to the fact that gas leakage was observed during the air's passage through the furnace, thus voiding the original measurement in the rotameter.

Cooling water is circulated at a constant rate through the test unit either by being pumped from the storage tanks or directly from the building supply system. All thermocouples are connected to a rotary selector switch, and the emf's are read from a semi-precision portable potentiometer.

The instrumentation and controls are all mounted on one panel so that the overall operation of the equipment can be carried out from one centralized location.

The experimental operating procedure will be treated in a separate section.

#### Electric Resistance Furnace and Adiabatic Sections

The air is heated by means of an electric resistance type furnace with the necessary instrumentation and auxiliaries. It was designed to heat 25 SCFM of air to temperatures above 2200°F, and to still higher

temperatures for lower flow rates. The maximum gas temperature is limited by the maximum safe temperature to which the silicon carbide heating element can be brought, which is in the neighborhood of 3100°F.

The furnace was built by the Harry W. Dietert Company of Detroit, Michigan. In the following description, reference will be made to the sectional drawings of the furnace and the adiabatic sections shown in Figures 2 and 4.

Power is supplied to the furnace from a 20 KVA transformer operating on a 220 volt, 60 cycle a-c power line. The output of the transformer can be varied from 0 to 256 volts in 4 volt increments, where flexible connecting cables with jacks are used to vary the impressed voltage on the furnace by plugging them into the appropriate outlets on the transformer panel. The voltage and amperage on the primary side of the transformer are measured, from which the total power to the furnace can be calculated, as well as the secondary current. The ammeter across the primary is not directly connected but is used in conjunction with a current transformer inserted in the primary circuit.

The main heating element of the furnace is a 3 inch O.D. by 2 inch I.D., 54 inch long tubular Globar (silicon carbide) resistance element. Graphite terminal blocks and water-cooled brass connections are located at either end of the element, as can be seen in the drawing. The top block is kept in tight contact by the compression plate which is tightly screwed on. At the bottom, the compression plate is held tight by means of spring action, so that the element is free to expand at one end to compensate for the thermal expansion of the element at high temperatures. The Globar element is surrounded by refractory

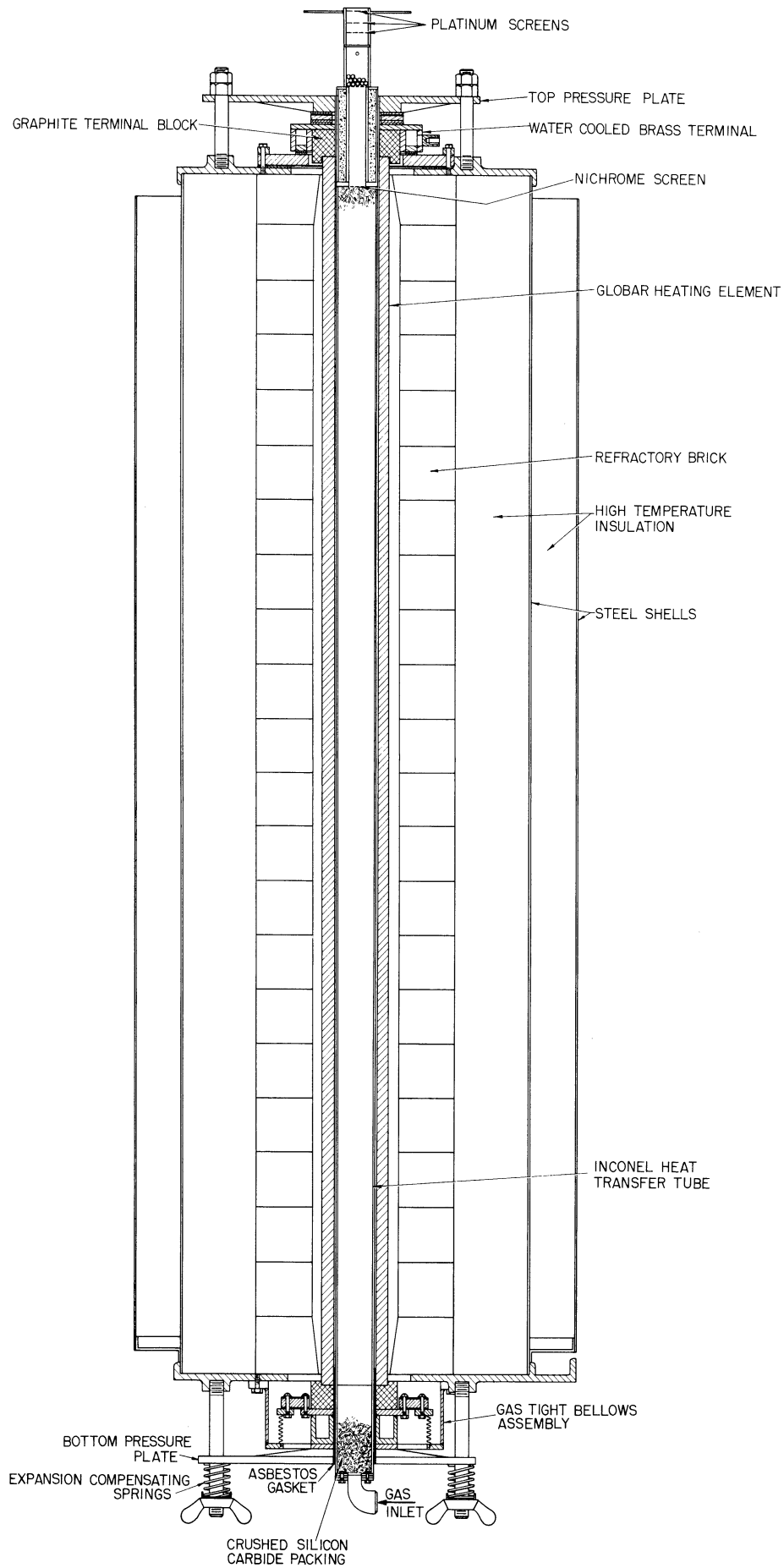


Figure 2. Furnace Detail

brick insulation and two layers of lower temperature insulation. all enclosed in a double shell metal casing.

The original furnace design differed from standard gas heating furnace design in that no protective tube was placed inside the element. In this design, crushed silicon carbide packing was directly inserted into the Globar element, and gas passed directly through the glowing packed bed. This design was much more efficient than one with a protective tube because there were no heat losses through the tube wall, there was a greater heat transfer area, and the pressure drop through the furnace was minimized because of the greater cross-sectional area exposed to flow. Also, the crushed silicon carbide packing itself acted as a source of heat, contributing to the overall efficiency of heat transfer. However, there did exist one drawback, namely, that the whole furnace had to be built gas-tight since the silicon carbide element is porous and gas could otherwise escape through it. It was for this purpose that the bottom bellows assembly seen in Figure 2 was built. Even though this furnace design appeared gas-tight, it was found that leakage occurred nevertheless, and for this reason an orifice meter was installed at the end of the exit adiabatic section to measure the quantity of gas which had actually passed through the test unit.

Because of leakage and the fact that internal pressure caused the lower compression plate to drop somewhat and interrupt contact between the element and the lower graphite block, it was found necessary to go to the more conventional design of inserting a packed inconel tube inside the globar element. Details of this tube can be seen in Figure 2. Near the top of the large tube, as shown in Figure 4, an insulated throat can be seen, which was constructed to prevent excessive temperature

losses while the hot gases pass in the proximity of the water cooling ring and graphite block. The tube is prevented from coming in contact with the Globar element by shims made of matted asbestos.

The furnace (i.e.. exit gas) temperature is automatically controlled by an oil-immersed off-on contactor in the transformer primary, actuated through an electronic relay circuit, by a 24 gauge platinum and platinum-10 percent rhodium thermocouple located 1/8" outside the Globar element at the midpoint of the furnace. It had originally been desired to have this control thermocouple located nearer to the top of the element for more sensitive control, but due to some misunderstanding, it was located at the middle. Since the temperature indicated by the control thermocouple has relative significance only, an alternate scheme for more accurate control was developed. Leads from a chromel-alumel thermocouple in the adiabatic section mounted on top of the furnace were led through a variable resistance to the electronic relay box in place of the leads from the platinum-10 percent platinum rhodium couple mounted in the furnace body. The variable resistance is of such a value that at its maximum setting it reduces the emf from the chromel-alumel couple to about that which a Pt-Pt 10 percent Rh couple would produce at the same temperature, thus indicating approximately the true temperature at which the gas is being controlled. In the low temperature range (below 1500°F), the variable resistance can be reduced. This causes the control of the gas temperature to be much more accurate and sensitive since a chromel-alumel thermocouple produces about five times the emf change for a given change in temperature than a Pt-Pt 10 percent Rh couple at the same base temperature.

Good secondary control of the exit gas temperature is also obtained from the fast temperature response of the Globar element, and the large heat capacity of the furnace and the packed tube. In order to obtain optimum control, the impressed voltage should be such that the current is on most of the time, and hence this voltage will be one adjusted to a value slightly above the minimum required for that temperature and duty. Control of the gas temperature becomes more stable at the higher flow rates, but even under the worst conditions, temperature control within about a 3°F range is possible by this procedure.

The crushed silicon carbide packing is held in place at the bottom by a nichrome screen. Since at the high temperatures, the fluidization threshold is exceeded in the high range of operating velocities, a nichrome retaining screen is placed at the top of the main section of the tube. This causes the bed to remain tightly packed and prevents bed motion and consequent spalling.

The size of packing employed was the optimum for the maximum heat transfer per unit length combined with the minimum pressure drop through the tube. In order to assure that the packing was of this approximate size, the crushed particles were screened and only those with the approximate dimensions were used for the packing.

From the heat transfer tube, the hot gas passes through a short insulated section into a 1-1/4 inch O.D. by 1.05 inch I.D. inconel tube that is 5-1/2 inches long. This tube is at the center of a large volume of insulation, so that it is essentially adiabatic, hence the term - adiabatic section. The purpose of this adiabatic section is to provide a means of accurate gas temperature measurement and to control the velocity profile and turbulence level of the gas stream before it enters the

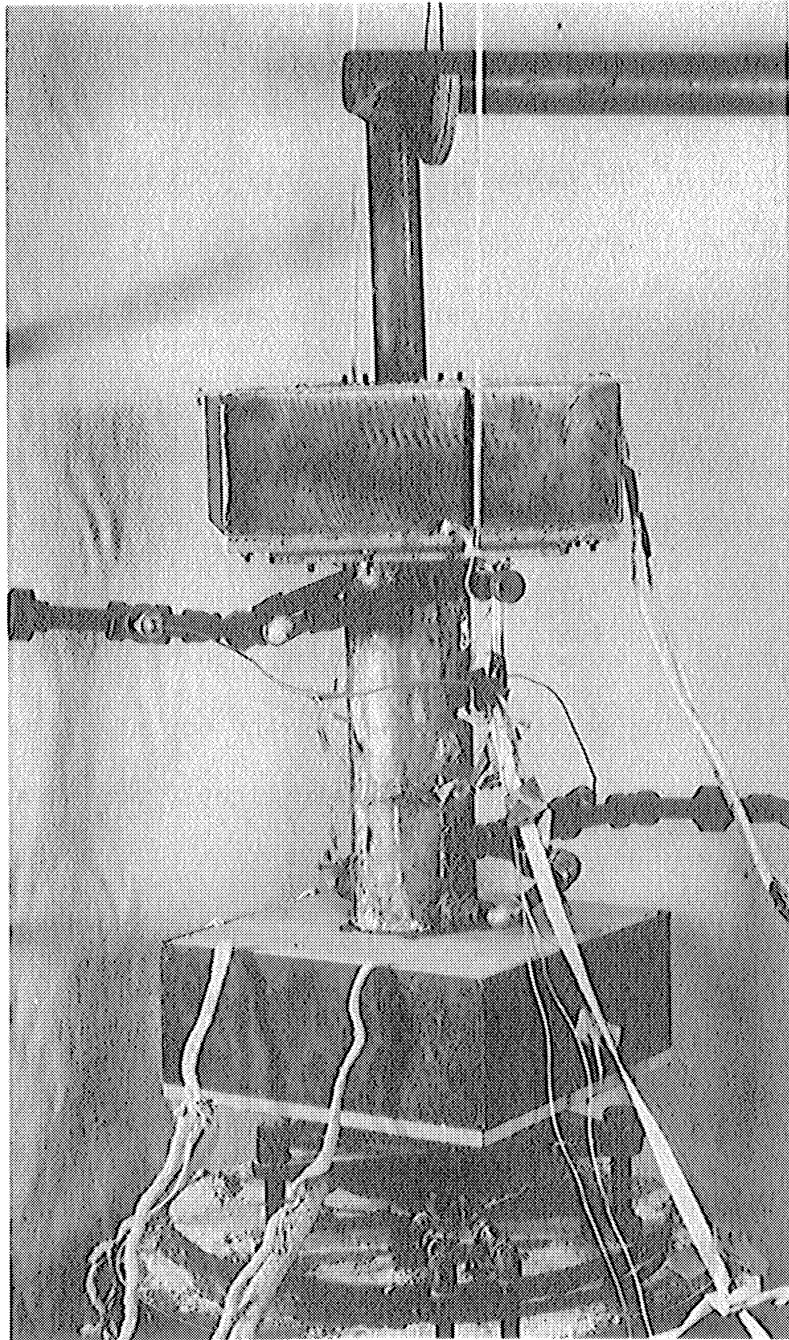


Figure 3. View of Test Object and Adiabatic Sections



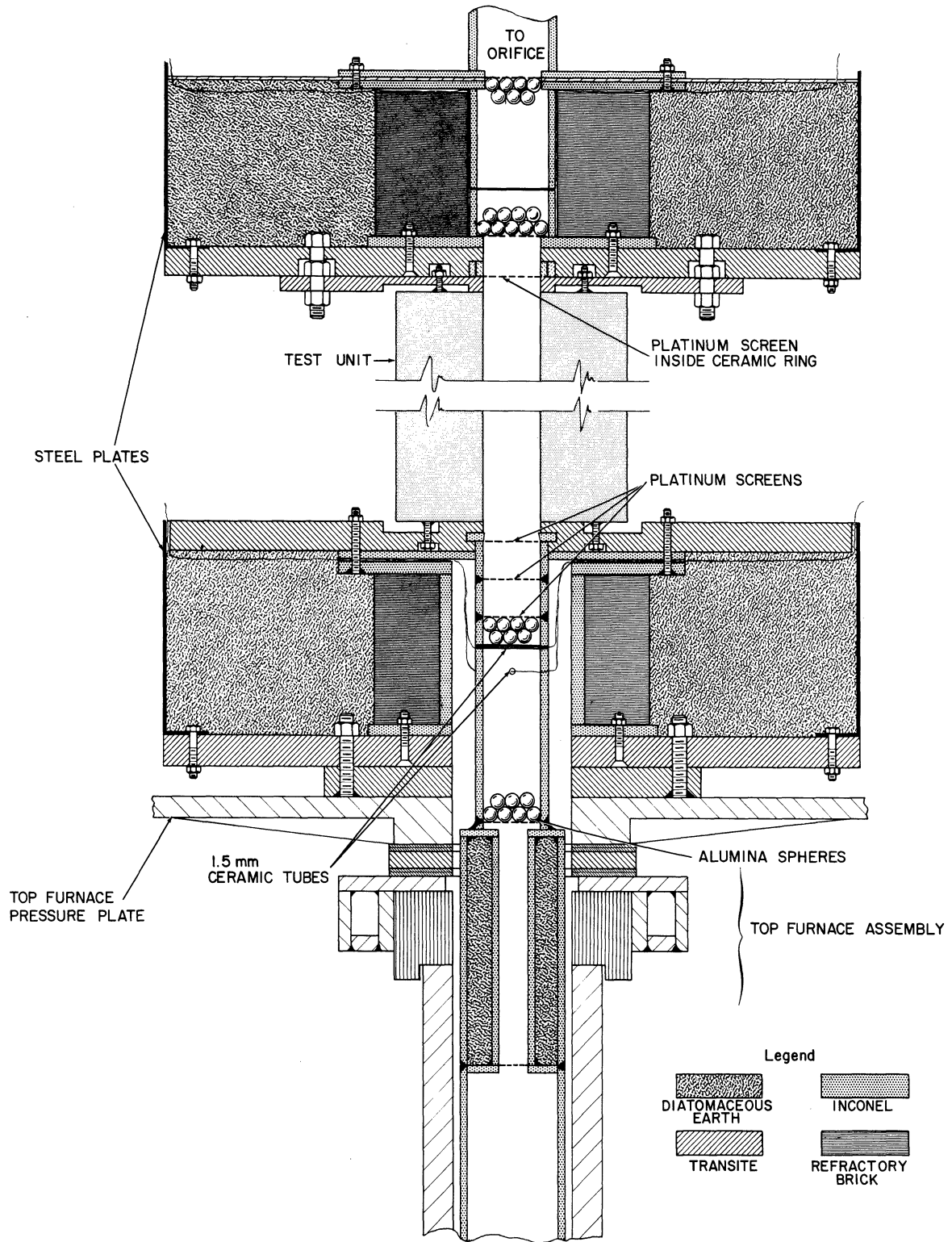


Figure 4. Detail of Adiabatic Sections and Top Furnace Assembly

heat transfer test unit. The details of the adiabatic sections can be seen in Figure 4, and a photographic view is shown in Figure 3.

The inconel tube of the adiabatic section fits through the top graphite block of the furnace. The lower 4-1/2 inches of the tube are filled with 1/4 inch spherical alumina packing, retained at the bottom by a welded on nichrome screen and at the top by a 52 mesh platinum screen. Two more platinum screens, each 5/8 inch apart, are located above the packed bed, welded in place. These screens reduce the turbulence level and establish a flat velocity profile, and have been located at optimum spacing. A theoretical discussion of this may be found elsewhere in the report. A further function of these screens is to reduce the effect of radiation on the measured amount of heat transferred in the test unit.

The temperature of the packing and that of the gas are assumed to be equal near the top of the adiabatic section. In order to measure this common temperature, a singly-perforated 0.9 mm I.E. by 1.5 mm O.D. ceramic thermocouple protection tube was located 1/2 inch below the top of the packing, in a transverse direction. A butt-welded 28 gauge chromel-alumel thermocouple made from matched wires was placed at the center of this tube (corresponding to a point at the center of the packed tube) and the leads come out on opposite sides of the protective tube. Within the tube the thermocouple wires are bare, but are sheathed with asbestos tubing elsewhere. The lead wires then go through a multiple rotary selector switch to a semi-precision potentiometer which is accurate to 10 microvolts (or 0.4°F when used with chromel-alumel thermocouples). The wiring scheme of the thermocouples is discussed in more detail in

the section of the test object, in which section a detailed wiring diagram is also presented.

A second bare 28 gauge chromel alumel thermocouple is located about 1/2 inch beneath the other one and is also in the protective tube. This thermocouple is connected to a direct reading pyrometer on the instrument panel so that gross temperature fluctuations during the course of an experimental run can be instantly noted. The holes through which both thermocouples are led out of the adiabatic tube are covered with alumina cement to prevent leakage. The emf of this latter thermocouple is also used as the actuator for the temperature control relay of the furnace.

The inconel tube of the adiabatic section comes out through the top graphite block of the furnace and rises through a hole in the top triangular pressure plate of the furnace. Six stainless steel bolts are welded on to the top pressure plate, and these are used to hold down two 1/2 inch thick sheets of transite, separated by asbestos gaskets, which form the base of the insulation holder for the adiabatic section. For structural purposes and to prevent any possible leakage in the adiabatic section, a second inconel tube with flanges on either end girdles the inner inconel tube. On the top flange of this inconel tube there are six stainless steel screw studs which hold tight the top sheet of transite to which the test unit is attached. The thermocouple wires are led out between the two upper flanges and asbestos gasketing as seen in Figure 4. Surrounding the large inconel tube is a circle of high temperature brick, surrounded by the bulk of the insulation which is diatomaceous earth. The brick is used to give some structural support to the inconel when operating in the high temperature range. The space between the outer

and inner inconel tubes is partially filled with asbestos strips which are primarily used as shims to keep the inconel tube from touching the graphite terminal block. The present design of the adiabatic section permits the test unit to be removed comparatively easily and still insures a tight seal.

The top adiabatic section for measuring the gas stream temperature after passage through the test object is very similar in construction to the lower one, the major difference being the absence of screens at the top (since no further velocity smoothing is required). The 1/3 inch I.D. inconel tube is packed with 1/4 inch tabular alumina spheres of a special composition so that they have about the same coefficient of expansion as inconel. The packing is held in on either end by nichrome screens and the thermocouple protective tube is mounted about 1-1/4 inches from the bottom (entrance) of the tube. A single 52 mesh platinum screen held between two concentric alumina rings is mounted in the transite just below the entrance to reduce back-radiation to the test object. The top adiabatic section is mounted in such a way as to permit easy removal for access to the test object for cleaning purposes.

#### Gas Supply and Measuring System

The gas used in this investigation was air, and the 90 psig building supply system was tapped for use. Since clean, dry air was required for the purposes of this work, a cleaner and dehumidifier was installed in the line before the air went to the furnace and test unit. The cleaner was a metal box made of 1/4 inch steel plate, 1 foot square, and 1-1/2 feet high. Air was led into it at the bottom at two inlets diametrically opposite to each other so that channeling was reduced,

and was taken off at the top. The bottom six inches were filled with a small cylindrical ring packing resembling Raschig rings, each ring being about  $3/16$  inch in diameter. On top of this, sandwiched in between two wire grids, was a 1 inch thick compressed layer of glass wool. The purpose of the packing and glass wool was to filter out any entrained oil and dirt particles. Above the glass wool layer was 11 inches (35 pounds) of anhydrous 4 mesh calcium chloride of dessicant quality to dry the air. Since the air was already at a high pressure, its water content, even assuming saturation, was very low. Furthermore, since the building air compressor was three floors below the location of the experimental equipment, most of the oil and dirt had already been entrained during its passage, thus making the overall duty on the cleaner and dehumidifier very light, and ensuring that the air coming from the cleaner was exceedingly dry and pure. Since the overall air velocity through the cleaner, even for maximum flow, was less than 1 foot per second, the pressure drop through this piece of equipment was negligible.

From the air cleaner, the air passed through a pressure regulator to a rotameter capable of measuring 0 to 27 SCFM at the calibration pressure of 60 psia or 45.3 psig. The regulator had a capacity of 37 SCFM and kept a constant output as long as the inlet pressure was 20 pounds above the output setting. On the outlet side of the rotameter was a needle valve which controlled the flow to the furnace and test object. Bourdon type pressure gauges were used to measure the supply pressure, the rotameter pressure, and the pressure drop through the equipment by tapping the system before and after the pressure regulator and after the needle valve, respectively. The air temperature was measured

by inserting a thermometer in the line just prior to the entrance of the rotameter.

The calibration curves for the rotameter were supplied by the manufacturer for service at 60 psia and 70°F. The temperature did not vary appreciably from this value and the calibration pressure was precisely maintained by the regulator. The instrumentation for this system was located on the left side of the panel shown in Figure 1a. No visible fluctuation in the gas rate were noted at any needle valve setting, thus indicating the good control obtained.

Because it was found that there was leakage in the air's passage through the furnace proper, an inconel orifice was installed to measure the flow coming out of the top adiabatic section. Inconel was used because ordinary steels cannot be used at such high temperatures in an oxidizing atmosphere. This orifice meter consisted of a 0.7498 inch inconel orifice mounted in a 1.9 inch O.D. and 1.6 inch I.D. inconel tube, the tubes being directly welded onto the orifice plate. The entrance section was 44 inches long, the exit section 12 inches, or about 27 and 7-1/2 pipe diameters respectively. Vena contracta taps, made of 3/16 inch inconel tubing, were located 1-5/8 inch upstream and 9/16 inch downstream from the orifice plate. These dimensions were all in accordance with orifice measurement theory, which will be treated in a later section.

At the outlet of the orifice meter, a thermocouple holder made of a short piece of 3/16 inch inconel tubing mounted at the center of a nichrome screen was welded on. The small inconel tubing was at the center line and coaxial with the large exit tube from the orifice. Through the hole of the small piece of tubing, a 30 gauge chromel-alumel

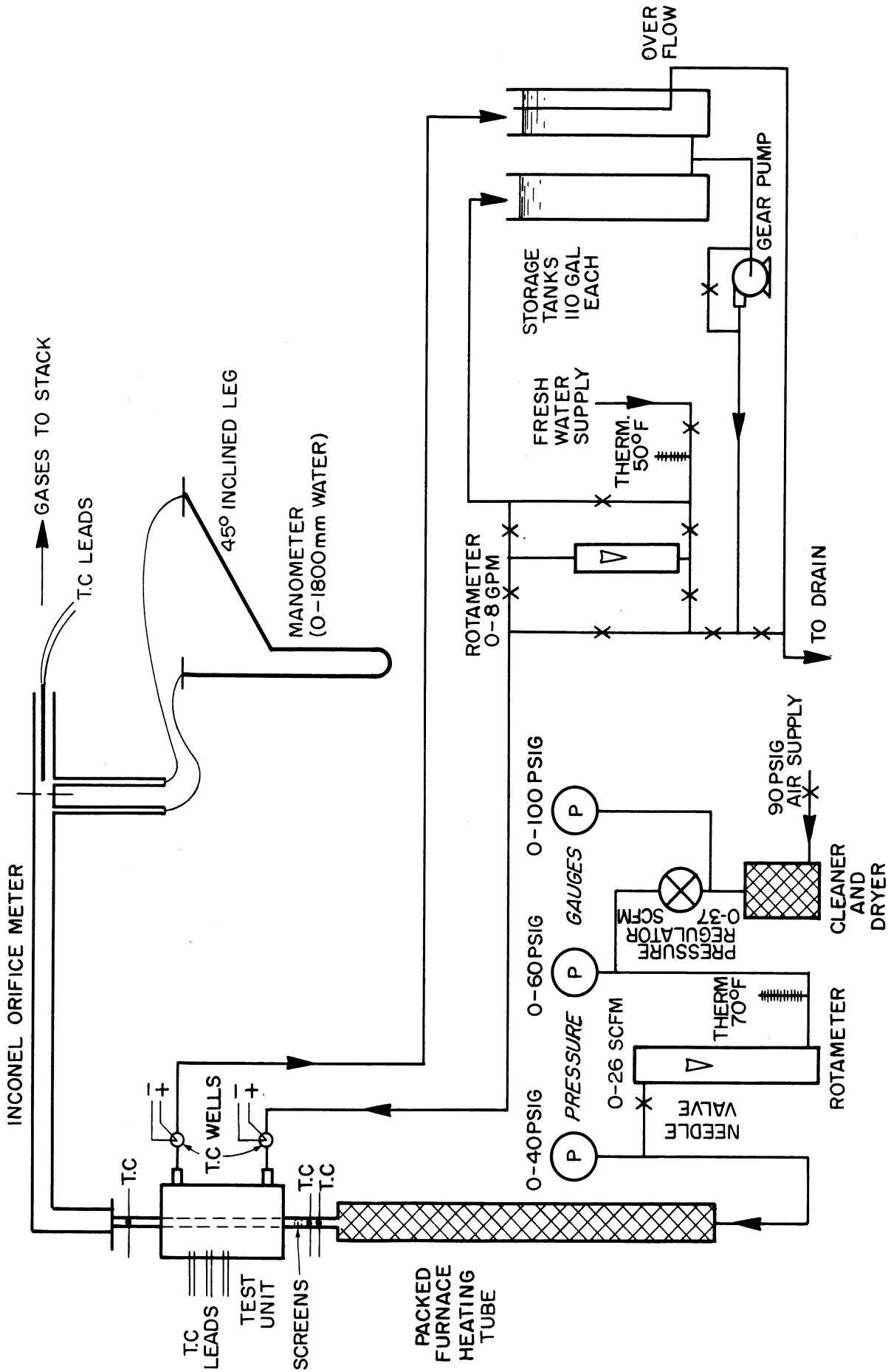


Figure 5. Schematic Diagram of Flow Systems

thermocouple whose leads run through a 10 inch long 2 mm two hole ceramic protective tube was inserted.

Water was used as the manometer fluid. Calculations showed that the total head to be expected would vary from 7 to about 1800 mm of water. Since this was a very wide range, the manometer was constructed so that only the top half of one leg is visible on the panel, and that leg was inclined on a  $45^\circ$  angle to permit greater reading accuracy. The orifice was calibrated directly against the rotameter, the orifice coefficients obtained varying from 0.74 to 0.685 for the Reynolds numbers expected during the course of the experiment. The calibration data are found in Appendix D.

#### Cooling Water System

As a safeguard against any gross variations in the service water supply temperature and pressure, a circulation system was installed, a flow diagram of which may be found in Figure 5. A gear pump was used to circulate the water from two 110 gallon storage tanks through a rotameter to the heat transfer test unit and then back to storage. The storage tanks were constructed by welding together two 55 gallon drums, and then coating the inside with "Glyptal", a rust-proof paint, for corrosion protection. Make-up water was fed to one tank and an equivalent amount overflows from the other tank. Electric relays which actuate a bell were mounted on top of each of the tanks to give warning of an overflow in case the overflow tube became clogged.

The service water supply can also be fed directly through the rotameter and to the test object. This method was used predominantly since it was found that temperature variations during a run usually did not exceed  $0.2^\circ\text{F}$  and pressure fluctuations usually did not change the



flow rate by more than 5 percent during any one run. Whenever service supply conditions became more unstable than this figure, the circulation system was turned on. The temperature of the service water was measured just before its inlet to the rotameter. The valves and instrumentation of this system may be seen at the center of the panel shown in Figure 1a.

#### Heat Transfer Test Unit

The heat transfer test unit was actually a small heat exchanger, with thermocouples located in four thermally isolated annular sectors for measurement of the local heat transfer rates. On the inside was the hot gas, and in the outside annulus flows cooling water. Since the length of the exchanger was about 11 tube diameters, this length was sufficient to study and simulate the thermal entrance section of a longer heat exchanger. Photographs of the actual test object are shown in Figure 4 and details may be found in Figure 6.

The inside heat transfer tube of the object was machined out of hot rolled inconel bar stock. The 11.25 inch long tube had an I.D. of 1 inch and an O.D. of 1.8 inches. The inside was carefully lapped to give an extremely smooth heat transfer surface. Twenty mil longitudinal grooves and chordal slots were cut to within 20 mils of the inside surface, thus producing four isolated sectors along the length of the tube, as can be seen in Figure 6. At each sector, the longitudinal grooves were 60° apart while the chordal slots were 1 inch from each other. The midpoints of these sectors were located at 1-1/2, 4, 7, and 10 inches from the front of the tube respectively, the first and third sector being located on one side of the tube and the second and fourth on the diametrically opposite side. Into each sector, three 20 mil

holes were drilled, one of which went to within 30 mils of the inside surface, one to within 30 mils of the outer surface, and one to approximately the midpoint between the two others. The holes to the top and bottom started from opposite sides of the sector, while the middle hole was drilled from the rear. The location and orientation of these holes can most easily be seen from a perusal of Figure 6. The exact depths to which these holes penetrated and the exact thermocouple locations were determined after the experiments by slicing open the unit and X-raying parts of the test sectors.

Into each hole, a 36 gauge, quadruple teflon enamel coated, butt welded chromel constantan thermocouple was inserted and fastened to the bottom by induction welding. Chromel-constantan thermocouples were used because they produce the largest emf for a given temperature, thus enabling more accurate results to be obtained. It was necessary to utilize insulated thermocouples since it was imperative that the wires did not at any time come in contact with each other or the metal wall of the hole into which they had been inserted. Because the insulation had to be thin (since both the thermocouple wires and the insulation had to fit into a 20 mil hole), strong, flexible, and stand temperatures up to a few hundred degrees F, teflon enamel coating was decided upon.

After insertion of the thermocouples, the holes and the grooves were filled with a water resistant, high temperature silicone insulating resin, and the whole test object was baked at 500°F to cure the resin. The resin had an extremely low thermal conductivity and hence thermally isolated each sector from the balance of the heat transfer tube. The whole heat transfer tube was then enclosed in a cylindrical 1/16 inch thick brass shell which was silver soldered onto two 4 inch diameter.

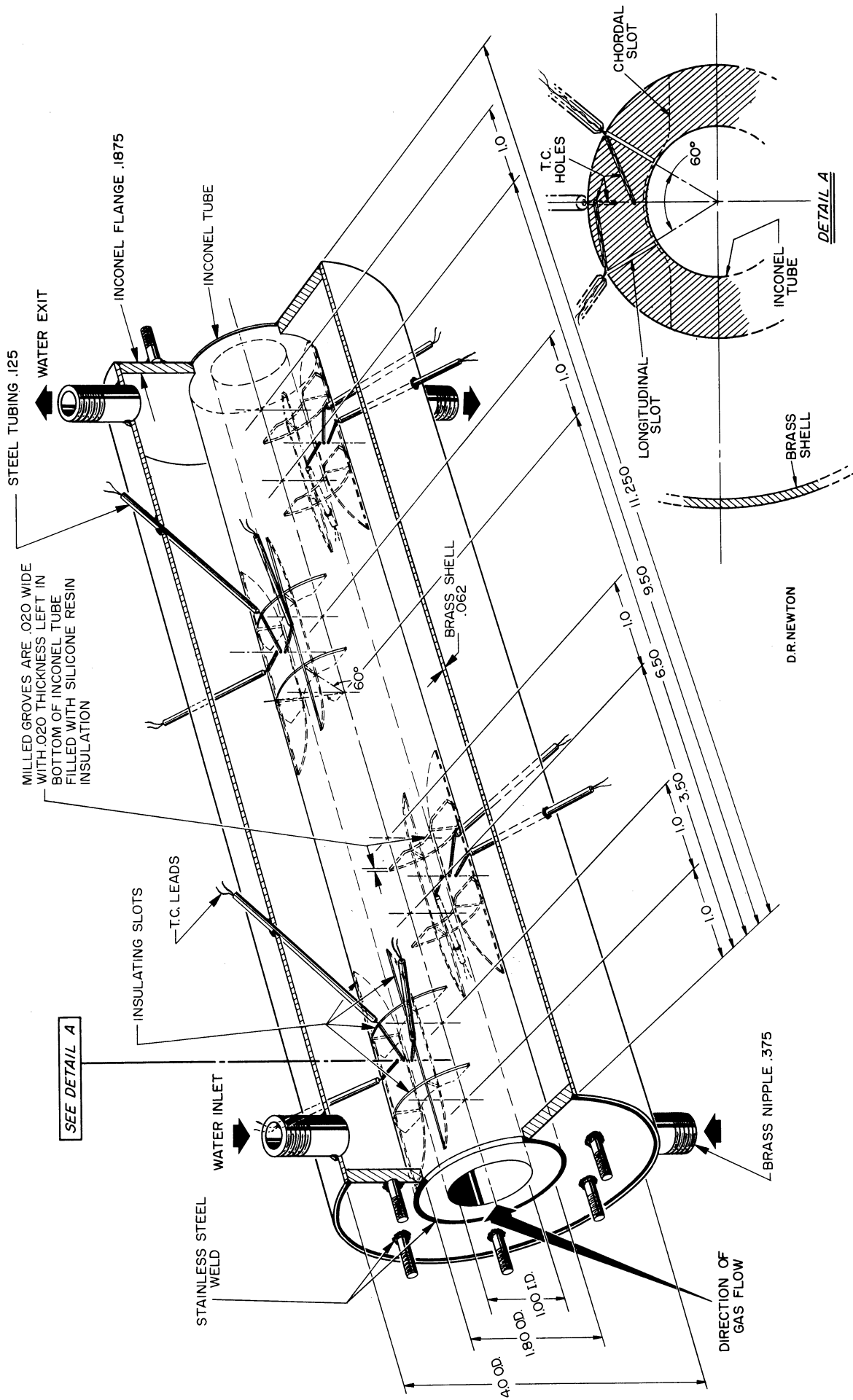


Figure 6. Detail of Test Object

3/16 inch thick, inconel flanges which had been previously welded onto the ends of the inconel tube. The brass shell was put on in two halves, the seam later being soldered closed. The thermocouples were led out of the heat transfer tube through the annulus inside of 2 inch long pieces of 1/8 inch steel tubing, which pierced the brass shell in appropriately located holes. At the point of extrusion from the brass shell, the steel protective tubes were soldered tight and the tubes were filled with silicone resin, and the whole test object was again baked for curing purposes. In this manner, tight seals were effected in leading the thermocouples out of the heat transfer tube. In order to further insure a tight seal, some Duco cement was put on the ends of the steel tubes. Threaded 3/16 inch diameter studs which had been previously welded onto the two end flanges were used to fasten the test object to transite sheets and the adiabatic sections. Water inlet and outlet nipples were provided on diametrically opposed sides of the brass shell at the top and at the bottom of the object, and thermocouple wells were put into the piping leading to and from the test object, each thermocouple well containing a 30 gauge chromel-constantan couple. These were used to measure the inlet and exit water temperatures in order to make a heat balance on the water side.

The leads from the thermocouples imbedded in the wall of the heat transfer tube extended for about five feet, after which they were carefully soldered onto 30 gauge chromel and constantan leads which went to a multiple point, low resistance rotary selector switch. The leads from all the other thermocouples, after having been suitably insulated with asbestos or tygon tubing, were led directly to the rotary selector switch. A complete wiring diagram may be found in Figure 7.

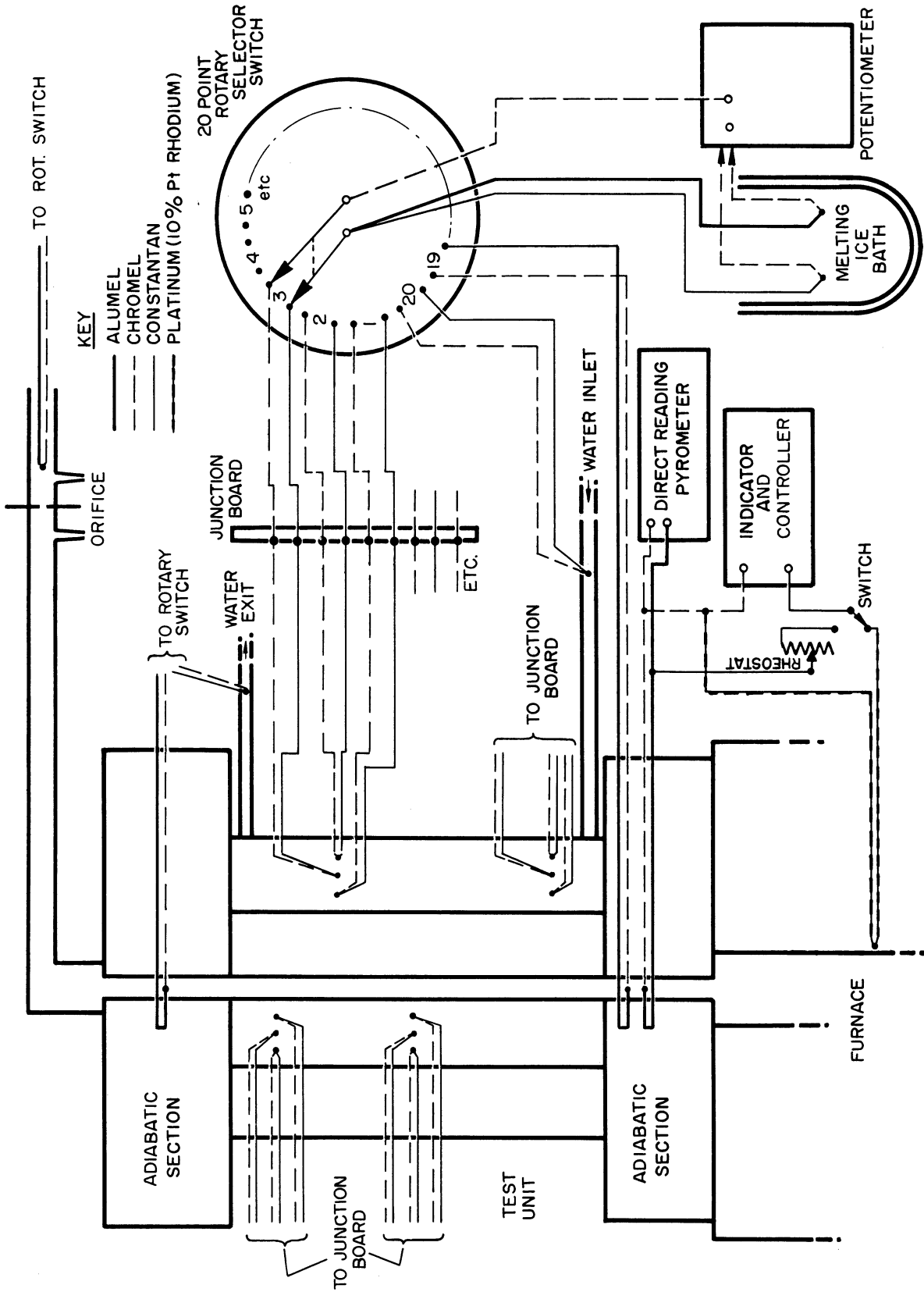


Figure 7. Thermocouple Wiring Diagram

From the rotary selector switch, an insulated 30 gauge chromel lead went directly to the positive terminal of a potentiometer. From the negative terminal of the rotary selector switch, a 30 gauge constantan and a 28 gauge alumel wire were led to a cold junction in a melting ice bath, appropriate matched chromel wires being used to make the cold reference junction in the ice bath, and the chromel leads from the cold junction were led to the negative terminal of the potentiometer. Thus, when reading the emf from the chromel-constantan thermocouples, the appropriate lead from the cold junction was connected to the potentiometer terminal, and vice-versa.

The standard cell of the potentiometer, as well as the stud dial and slide wires, were calibrated before the experiments. The thermocouples were calibrated after completion of the runs by immersion of the test object in a constant temperature bath. Thermometers and Standard cells recently calibrated by the National Bureau of Standards were used as references.

Accuracy of readings to within 2 microvolts was possible with the potentiometer used. During an average run, reproducibility varied from 2 to 15 microvolts (approximately 0.05 to 0.4°F).

## MATERIALS

The selection and source of some of the more relevant materials pertinent to the investigation are discussed below. A complete listing of the major items used in the construction of the equipment is presented in Table IV of Appendix E.

### Gas

Air was selected for use in these experiments because of its ready availability from the building compressed air system and its low radiation beam length. After passage through the air cleaner and dryer, the air, as fed to the test unit, had a negligible amount of impurities, thus being ideal for heat transfer measurements.

### Test Object

Inconel was selected for the heat transfer tube of the test object because of its resistance to oxidation at high temperatures. The pertinent physical properties of Inconel are given in Table III of Appendix D. The bar stock was supplied by Steel Sales Company in Detroit.

### Thermocouples in Test Object

The 36 gauge quadruple teflon enamel coated chromel-constantan thermocouples used in the test object were specially manufactured by the Thermo-Electric Company. Chromel-constantan was used rather than chromel-alumel because of the 50 percent greater emf at any temperature that is produced by the chromel-constantan thermocouples, thus permitting a more accurate reading of small temperature differences. Teflon enamel was used because of its flexibility and ability to withstand temperatures up to 500°F.

## EXPERIMENTAL THEORY

The equipment used in this experiment was designed to measure local heat transfer coefficients in the entrance section of a circular tube for the inlet conditions of a flat velocity profile and an initially flat temperature profile. In this section, a description of how these inlet conditions are realized, as well as the theory of how the heat transfer rates may be computed from the experimental measurements, is described, and the inherent assumptions are analyzed. The theory behind the inconel orifice meter is also presented to show how thermal expansion of the orifice at elevated temperatures was accounted for.

### Measurement of Rate of Heat Transfer

The heat conduction equation for an isotropic solid can be written as

$$\rho c_p \frac{\partial T}{\partial \theta} = \text{div} (k \text{ grad } T) \quad (15)$$

which in cylindrical coordinates becomes

$$\rho c_p \frac{\partial T}{\partial \theta} = \frac{1}{r} \left[ \frac{\partial}{\partial r} (kr \frac{\partial T}{\partial r}) + \frac{\partial}{\partial \theta} \left( \frac{k}{r} \frac{\partial T}{\partial \theta} \right) + \frac{\partial}{\partial z} (kr \frac{\partial T}{\partial z}) \right]. \quad (16)$$

In the geometry used in this experiment, the following assumptions can be made:

$$\frac{\partial T}{\partial \theta} = 0, \quad \frac{\partial T}{\partial z} = 0, \quad \text{and} \quad \frac{\partial T}{\partial \theta} = 0.$$

The validity of the above will be discussed in more detail later. For convenience, an isotropic wall with a constant thermal conductivity of  $k_{av}$  will be assumed, and this assumption will also be reviewed elsewhere.



The previous equations then reduce to the following total differential equation,

$$\frac{d^2T}{dr^2} + \frac{1}{r} \frac{dT}{dr} = 0 \quad (17)$$

which has the general solution

$$T = C_1 \ln r + C_2 \quad (18)$$

$C_1$  and  $C_2$  can be evaluated from the known temperatures at any two points,  $(T_1, r_1)$  and  $(T_2, r_2)$ , from which

$$C_1 = \frac{T_2 - T_1}{\ln r_2/r_1} \ln r_1 \quad \text{and} \quad C_2 = T_1 \frac{T_2 - T_1}{\ln r_2/r_1} \ln r_1.$$

Substituting the above into equation (18) and simplifying, the following result is obtained:

$$\frac{T - T_1}{T_2 - T_1} = \frac{\ln \frac{r}{r_1}}{\ln \frac{r_2}{r_1}} \quad (19)$$

The inside and outside surface temperatures thus can be rigorously calculated from the above or found graphically by an extrapolation of a straight line through the known points on a plot of  $T$  vs.  $\ln r$ .

The case at hand being of cylindrical geometry, the radial flux varies throughout. The flux that is of interest here is the one at the inside surface, namely

$$(q/A)_s = k_{av} \left( \frac{dT}{dr} \right)_s = \frac{k_{av}}{r_s} \frac{T_2 - T_1}{\ln \frac{r_2}{r_1}} \quad (20)$$

Since in this experiment there are four separate measuring stations, each with thermocouples at different locations, it simplifies the general procedure to work directly with the extrapolated inside and outside surface temperature,  $T_s$  and  $T_o$  at  $r_s$  and  $r_o$  respectively. Then equation (20) becomes

$$(q/A)_s = \frac{k_{av}}{r_s} \frac{T_s - T_o}{\ln \frac{r_o}{r_s}} \quad (21)$$

The flux at the inner surface also can be expressed in terms of the total heat transfer coefficient  $h_t$  so that at each measuring station

$$(q/A)_{s_t} = h_t (t_b - t_s) = \frac{k_{av}}{r_s} \frac{(t_s - t_o)}{\ln \frac{r_o}{r_s}} \quad (22)$$

where the subscript t denotes the total quantity and  $t_b$  is the local bulk gas temperature. Also,

$$h_t = h_c + h_r \quad (23)$$

and

$$(q/A)_{s_t} = (q/A)_{s_r} + (q/A)_{s_c} \quad (24)$$

In the above, the subscripts c and r stand for convection and radiation, respectively. From the above relations, it is evident that

$$(q/A)_{s_c} = h_c (t_b - t_s) = (q/A)_{s_t} - (q/A)_{s_r} = \frac{k_{av}}{r_s} \frac{(t_s - t_o)}{\ln \frac{r_o}{r_s}} - (q/A)_{s_r} \quad (25)$$

or

$$h_c = \frac{\frac{k_{av}}{r_s} \frac{(t_s - t_o)}{\ln \frac{r_o}{r_s}} - (q/A)_{s_r}}{(t_b - t_s)} \quad (26)$$

In the previous equations,  $t_b$  is the average local gas temperature extant above the particular measuring station in the test object. For all practical purposes, this will be assumed to be equal to the gas temperature at the midpoint of the measuring station. This temperature can be rigorously computed from a heat balance based on either the inlet or exit gas temperature. Since the fluxes due to convection alone can be computed directly from the data for each measuring station, a plot of  $(q/A)_c$  versus either area or  $L/D$  can be constructed and used for purposes of graphical integration to find the amount of heat transferred, and hence the temperature change, by the time the gas has reached the midpoint of any given measuring station. Since

$$q_c = W_g c_{p_g} (t_i - t_b) = \int_0^{A_i} (q/A)_c dA \quad (27)$$

where  $A_i$  is the inside area of the tube traversed up to the midpoint of the measuring station in question

$$t_b = t_i - \frac{\int_0^{A_i} (q/A)_c dA}{W_g c_{p_g}} \quad (28)$$

For all practical purposes,  $c_{p_g}$  may be considered a constant during any single run at a given temperature level.

Alternately, if the exit gas temperature,  $t_e$ , is taken as determinative, a similar procedure leads to the equation

$$t_b = t_e + \frac{\int_{A_i}^{A_{total}} (q/A)_c dA}{W_g c_{p_g}} \quad (29)$$

However, in practice, neither of the two rigorous methods presented previously was used in the computation of the local gas temperatures because of the uncertainty as to the true inlet and exit gas temperatures. Due to this uncertainty, (which manifested itself by giving gas temperature differences not in accord with the heat balances), a great error might be introduced by taking either the entrance or the exit gas temperature as determinative, causing a cumulative error down the length of the tube. In order to avoid such a cumulative error, a linear relationship with respect to the actual measured temperatures,

$$t_b = t_i - \frac{A_i}{A_{total}} (t_i - t_e) , \quad (30)$$

was assumed to hold. It is evident that this minimizes the error caused by a faulty thermocouple reading on either the measured inlet or exit gas temperature by distributing the error between the two extremes. It should be noted that in the computation of the heat transfer coefficient from equation (26) the result is not very sensitive to a small change (or error) in the group  $(t_b - t_s)$ . This will be treated in more detail in the next section of the report.

As a check on the data for internal consistency, heat balance may be made in three independent ways, namely:

$$q = W_g c_p (t_i - t_e) = W_w c_p \Delta t_{w_{net}} = \int_0^{A_{total}} (q/A)_c dA , \quad (31)$$

where  $\Delta t_w$  is the net difference between the inlet and exit water temperatures after the effect of conduction from the adiabatic sections and room effects have been subtracted from the total.

The evaluation of  $(q/A)_r$  in equation (26) will be treated subsequently and is itself predominantly a function of  $t_i$ ,  $t_e$ , and  $L/D$ . Hence it has been shown that a local  $h_c$  at each of the four measuring stations can be obtained by knowing two radial temperatures, the inlet and exit gas temperatures,  $L/D$ , and the thermal conductivity of the metal. Knowing the thermal conductivity and specific heat of the gas and the mass flow rate, the Nusselt or Stanton numbers,  $h D/k$  or  $h/c_p G$  respectively, can easily be obtained from the above.

#### Discussion of Assumptions

The following assumptions were made during the above analysis:

- 1)  $\partial T/\partial \theta = 0$  (Steady state conditions prevail)
- 2)  $\partial T/\partial Z = 0$  (Absence of longitudinal gradients)
- 3)  $\partial T/\partial \phi = 0$  (Absence of angular gradients)
- 4) The average thermal conductivity of the solid,  $k_{av}$ , evaluated at  $T_{av}$ , may be used in lieu of integrating with point values of  $k$ .
- 5) The solid wall of the test sector of the test object may be considered isotropic.

Assumption (1) is extremely valid since during the course of an experimental run, care is taken to control the inlet gas temperature at a constant value and a run is rejected if the variation of the wall temperatures is greater than about  $0.3^\circ\text{F}$  between the beginning and end of data taking.

The absence of angular and longitudinal gradients is assured by the silicone resin insulation of extremely low thermal conductivity,  $0.381 \times 10^{-3}$  cal/cm  $^\circ\text{C}$  sec,<sup>11</sup> that has been put into the chordal and longitudinal slots which isolate each measuring station from the rest of the wall. Angular gradients should not be appreciable even without the insulation since for the geometry involved, the flow of heat should

be equal at all angles. Without the insulated chordal slots there might have been a slight longitudinal gradient within the measuring section since the heat transfer coefficient varies down the length of the test unit and a temperature gradient of the order of magnitude of a few degrees does exist between the entrance and exit of the test object. However, the addition of insulation certainly makes these effects negligible over a short length of the tube, and hence the assumption of the absence of longitudinal gradients over any one measuring section appears sound.

If it is assumed that the thermal conductivity of the wall varies linearly with temperature, there is absolutely no error induced by using  $k_{av}$  in the calculations. The derivation of this may be found in Appendix C. Furthermore, Churchill<sup>5</sup> has shown for a similar case that even if a rigorous calculation of integrating point values of  $k$  rather than using  $k_{av}$  is performed over the whole thickness of the wall, only an extremely negligible error is caused. Hence assumption (4) is valid.

Due to the presence of the thermocouple holes, the geometry of each section is not isotropic throughout; however, it is shown in Appendix C that the maximum error in flux measurement caused by the presence of these holes is less than two percent, and probably much less since this value represents an upper bound. In view of this, the assumption of considering the whole wall to be isotropic is a reasonable one which approaches the ideal case rather closely.

It is evident that all of the aforementioned assumptions are reasonable and applicable to the case at hand.

Analysis of Radiation Effects

In equation (26) of the previous section, the term  $(q/A)_r$ , or the amount of radiant flux contributed to the total flux, appears. This section will be devoted to the evaluation of this quantity.

The well known Stefan-Boltzmann radiation law is

$$q = \sigma \epsilon F_{21} A_2 (T_2^4 - T_1^4) \quad (32)$$

where F is a geometrical factor representing the amount of radiation intercepted by the area in question from the source. In the present experiment, radiation from the platinum screens located at either end of the test object is intercepted by the wall of the tube, the amount intercepted by surface under each measuring station varying down the length of the tube. Platinum screens are used because of their low emissivity, thus reducing radiation effects, but even so, at  $L/D = 1.5$ , radiation at the 2000°F level can contribute up to 8 percent of the total flux, thus making it imperative that a radiation correction be applied. In these calculations, the platinum screens are assumed to be at the bulk gas temperature.

Hamilton and Morgan<sup>14</sup> have made a study of radiant interchange configuration factors, and by inversion of a similar case presented by them an expression was derived for the interchange factor over any one measuring station,

$$F_{21} = \frac{1}{6} \frac{(L/r)_2}{(L/r)_1} \left[ (L/r) [ (L/r)^2 + 4 ]^{1/2} - (L/r)^2 \right], \quad (33)$$

where the term is to be evaluated between the limits of  $L/r$  of each measuring station. Naturally, the limits of  $L/r$  are different when evaluated from each end of the tube. The derivation of the above, plus a curve showing the total amount of radiation intercepted by the inside tube wall for any distance down from the end may be found in Appendix C.

Equation (33) presents the interchange factor based on the area  $A_2$  of the circular platinum screen. This factor, however, still has to be corrected for the emissivity of the platinum and the inconel wall. According to Hottel, as stated in McAdams,<sup>18</sup> the average factor will then be

$$\overline{F}_{21} = 1 / [ 1/F_{21} + (1/\epsilon_p - 1) + A_1/A_2 (1/\epsilon_{inc} - 1) ] \quad (34)$$

where  $A_1$  is the area subtended under each measuring station and  $F_{21}$  the percent radiation intercepted as calculated from equation (33). Since the  $\overline{F}_{21}$  calculated above is the equivalent of the term  $\epsilon F$  in equation (32), substitution of  $\overline{F}_{21}$  into equation (32), and division of the same by  $A_1$  yields the desired result,

$$(q/A_1)_r = \sigma \overline{F}_{21} (A_2/A_1) (T_g^4 - T_s^4) . \quad (35)$$

Naturally, for each measuring station, the contribution to the radiant flux contributed by either end must be evaluated and added up, the gas temperature extant at either end,  $t_i$  or  $t_e$  in absolute units, being appropriately substituted into equation (35).

Radiation also takes place between the inner and outer inconel tubes of the lower adiabatic section; however, the temperature difference between the two walls is negligible due to the low heat fluxes in the



adiabatic section and also the high radiant heat transfer coefficient at high temperatures, so that radiant effects are not an important factor here.

### Turbulence Level and Velocity Profiles

As mentioned in the review of theory and prior work, it has recently come to light that turbulence level may be an important variable in the interpretation of heat transfer data. Much theoretical work has been done in the field of predicting the turbulence level of a fluid issuing from a screen, and for the purposes of this experiment, the work of Baines and Peterson,<sup>1</sup> who obtained correlations for the turbulence level and velocity profile corrections over a wide range of screen variables, was relied upon. According to them, for screens of solidity ratios of less than 0.5 and screen Reynolds numbers greater than 100, the turbulence level is less than 4 percent after 100 bar lengths downstream and less than 2 percent after 240 bar lengths. The 52 mesh platinum screens used in this experiment have a bar width of 0.004 inches and a solidity ratio of 0.353, thus giving the predicted 4 percent turbulence level in about  $3/8$  inch and the 2 percent level by the time the beginning of the first measuring station is reached.

The screens present in the adiabatic section also serve the additional purpose of velocity profile correction. The profile of the gas stream is exceedingly erratic close to the bed and is therefore unsuitable for precise heat transfer measurements. Baines and Peterson state that for the elimination of these fluctuations or disturbances, a screen whose mesh dimensions are less than the width of the disturbances must be used, and that best results will be obtained if a few

screens of moderate solidity are placed in series. Three screens in series usually gave an adequate representation of a flat velocity profile if the separation between them was at least 40 mesh widths. The three 52 mesh screens placed  $5/8$  inch apart used in this experiment amply fulfill the above requirements and thus should give an essentially flat velocity profile. Further experimental confirmation of this for a similar case was provided by Churchill<sup>5</sup> who made hot wire anemometer explorations above a gas stream issuing from a packed bed through two 52 mesh screens.

Thus the use of three screens at the top of the adiabatic section should not only reduce the turbulence level to below 2 percent but should also create a flat velocity profile.

#### Flow Measurement with Inconel Orifice Meter

The inconel orifice meter built for this experiment was designed to measure flow rates of up to 30 SCFM air at an air temperature of 2500°F. The major difficulty in interpreting readings from such an orifice is to account for the effect of the thermal expansion of the orifice itself at the elevated temperatures. The orifice was designed according to the specification set forth by Sterns, et al.,<sup>27</sup> who state that an entry length of about 15 pipe diameters and an exit section of 4 diameters will suffice for the present case. Vena contracta taps were placed according to their specifications, and the sharpness and bevel of the orifice plate itself was machined in accordance with their instructions. However, since the minimum inside pipe diameter for which standard correlations of the orifice coefficient hold is 2 inches and the present pipe is only about 1-1/2 inches, the present orifice

was calibrated against the rotameter, and the resulting curve is shown in Appendix D.

The orifice equation is:

$$W = C_o A_o \sqrt{\frac{2g_c \rho (-\Delta p)}{1 - (D_o/D_p)^4}} \quad (36)$$

In the above,  $A_o$  (i.e.,  $D_o$ ) is a function of temperature, but the ratio  $D_o/D_p$  remains a constant since both are the same functions of temperature. Hence for simplicity, the term  $1 - (D_o/D_p)^4$  will be grouped together with  $C_o$  to give a modified orifice coefficient

$$\beta = C_o / \sqrt{1 - (D_o/D_p)^4} \quad (37)$$

where  $\beta$  is actually the quantity obtained from the calibration curve.

$$A_o = c_1 D_o^2 = c_1 (\alpha_T D_{o20})^2 \quad (38)$$

where  $c_1$  is merely the conversion factor from diameter to area,  $\alpha_T$  is the total enlargement or elongation factor based on the original diameter at 20°C,  $D_{o20}$ . In other words,  $\alpha_T = \text{length at temperature } T / \text{length at } 20^\circ\text{C}$ .

Based on information in Perry<sup>22</sup> and assuming that each major constituent of inconel contributes an expansion effect relative to its proportion in the alloy, an estimate of  $\alpha_T$  was obtained. The thus derived formulae are:

$$\alpha_T = 1 + 0.1162 \times 10^{-4} (T - 20) + 0.0066 \times 10^{-6} (T - 20)^2 \quad (39)$$

(to 500°C)

$$\alpha_T = 1 + 0.1249 \times 10^{-4} (T - 20) + 0.0033 \times 10^{-6} (T - 20)^2 \quad (40)$$

(above 500°C)

where T is in degrees C. From the above equations,  $\alpha_T$  varies from unity at 20°C to 1.0214 at 1300°C (3272°F).

The orifice coefficient for which this meter was calibrated was based on the mean density of the gas at the orifice. This is naturally also a function of pressure as well as temperature. Assuming the ideal gas law to hold (which is an extremely accurate approximation for low pressures and high temperatures),

$$\rho_m = \frac{P_m}{RT} \quad . \quad (41)$$

Substituting the above as well as equations (37) and (38) into equation (36), and letting

$$c_2 = \sqrt{2g_c/R} \quad , \quad (42)$$

then

$$W = \beta c_1 c_2 (\alpha_T D_{o20})^2 \sqrt{\frac{P_m (-\Delta P)}{T}} \quad . \quad (43)$$

Since  $\alpha_T$  is itself a function of temperature, it seems logical to put it under the radical with the T term. Furthermore, since  $D_{o20}^2$  is a constant, it can be lumped together with the other two, creating

$$c_3 = c_1 c_2 D_{o20}^2 \quad . \quad (44)$$

Carrying out the above yields

$$W = \beta c_3 \sqrt{P_m (-\Delta P) \frac{\alpha_T^4}{T}} \quad . \quad (45)$$

Now, let

$$T' = (T/\alpha_T^4) \quad (46)$$

and

$$H' = P_m (-\Delta P) \quad . \quad (47)$$

Then

$$W = c_3 \beta \sqrt{H'} / \sqrt{T'} \quad (48)$$

For this orifice,  $c_3 = 331$ . A consistent system of units was used in all the above derivation. Since  $P_m$  is itself a function of  $(-\Delta P)$ , it was very easy to construct a graph of  $\sqrt{H'}$  versus the orifice manometer reading, under the assumption that the outlet pressure was essentially atmospheric. Similarly, a plot of  $\sqrt{T'}$  versus  $T$  was constructed, so that from a given orifice reading and gas temperature,  $W$  could rapidly be computed accurately.

Calculations also showed that the error in orifice thermocouple reading due to radiation losses to the wall (which was lagged with asbestos) would be negligible for gas temperatures of up to well over a  $1000^\circ\text{F}$  since it is the square root of the absolute temperature which appears in equation (48). Since no gas temperatures greater than about  $1200^\circ\text{F}$  were ever encountered at the orifice, no correction for radiation was made.

## EXPERIMENTAL PROCEDURE

The general procedure followed was one to obtain the most accurate results possible with the present equipment. The following description of the procedure will be divided into five parts, each representing a facet of the overall procedure. These parts will cover the following material:

- 1) Preliminary Experimental Work
- 2) Preparations for a Run
- 3) Variables Measured During a Run and Experimental Range
- 4) Specifications for Acceptable Runs
- 5) Location of Thermocouples in Test Object and Calibration of Equipment

### Preliminary Experimental Work

Prior to starting taking experimental data, the whole apparatus was checked for the proper working of its component parts. Before the test object was enclosed in the brass shell, each of the thermocouples in it was checked to make sure the junction was still in working condition. Preliminary runs were taken to ascertain whether the thermocouple readings were in reasonable accord with their approximate locations. The orifice meter readings were checked against the rotameter to determine the percent leakage present and to make sure that a possible subsequent increase in leakage could be spotted immediately. Furthermore, the air supply was hooked up directly to the bottom of the test unit so that the leakage through the flanges of the upper adiabatic section could be measured. This turned out to be approximately 1 percent, and was subtracted out from the total leakage recorded when the air also passed through the furnace proper and lower adiabatic section. It was found that the percent leakage, usually amounting to a total of around 7 percent,

remained a constant independent of the pressure drop through the furnace. Before assembling the complete unit of adiabatic section and test object, the inside surface of the test object was thoroughly cleaned to give a bright surface polish so that the only resistance present would be that of the gas film.

#### Preparations for a Run

The actual physical preparations for a run were comparatively few. The input voltage from the transformer was adjusted to such a level that the furnace was drawing current for about 90 percent of the time that the inlet gas temperature was kept at a given level. At the higher temperature levels (above 1000°F) the on-off controller did not respond properly and it was found most advantageous to let the gas come to an equilibrium temperature with the current on full time. Care was always taken that the furnace element temperature indicator never exceeded a reading of about 2100°F in order to protect the inconel heat transfer tube inside the element. The water and gas rates were adjusted to a constant setting, and readings were taken when equilibrium was reached. For most runs, the water flow rate was 4 gpm. When going from one temperature level to another higher one, the gas rate was always turned to a low setting until the furnace temperature approximated the desired gas temperature, at which point the flow rate was then adjusted to the desired setting and the voltage adjusted to keep steady state conditions at the desired settings. Steady state conditions were usually obtained in anywhere from a half to two hours. After steady state conditions had been reached, data taking was commenced.

Variables Measured During an Experimental Run and Experimental Range

The variables measured during any run can be divided into primary and secondary variables, the primary ones being those used directly in the subsequent computation of the heat transfer coefficients and heat balances, and the secondary ones merely relating to the general operation of the equipment. The primary variables recorded were:

1) Readings of the nine operable chromel-constantan thermocouples imbedded in the wall of the test object at the four heat transfer measuring stations.

2) The inlet and exit gas temperatures as given by the chromel-alumel thermocouples in the inlet and exit adiabatic sections.

3) The inlet and exit water temperatures given by two chromel-constantan thermocouples. Periodically at each temperature level, the gas rate was turned off completely, and the temperature rise of the water due to conduction in from the adiabatic sections and room effects was noted. This was then applied as a correction to the total temperature drop to give the net effect of heat transfer from the gas alone.

4) The water flow rate.

5) The gas flow rate, both as indicated by the rotameter and the orifice. In order to evaluate the meaning of the orifice reading, the chromel-alumel couple reading indicating the gas temperature at the orifice was also taken. The temperature of the air entering the rotameter was also recorded.

The secondary variables recorded were:

1) Pressure drop through the system.

2) Primary voltage, current in the primary, and the secondary voltage setting of the transformer.



Besides the above recorded variables, during any experimental run, a visual check was always made on the supply air pressure and the pressure of the gas entering the rotameter, which had to be kept at the calibration setting of 45.3 psig to insure accuracy. A direct reading pyrometer on the panel indicated if there were any gross inlet gas temperature variations while data was being taken. The accuracy of the variables which was required for a successful run will be treated in the next subsection.

Runs were taken over a wide temperature and moderate Reynolds number range. The inlet gas temperatures used were approximately 500, 1000, 1500, and 1900 to 2000 °F, and at each temperature level, runs were carried out at flow rates corresponding to Reynolds numbers of approximately 5000, 7500, 10,000, 12,000, and 15,000. In addition, at the lower temperature levels, additional runs at Re of about 20,000 were taken, while at the 2000°F level it was not possible to take the Re = 15,000 runs due to the high gas flow rates required at that high temperature to produce this Reynolds number.

#### Specifications for Acceptable Runs

Not all the runs taken met the stringent requirements set up below. In the following paragraphs, the reasons for the rejection of certain runs will be given, as well as probable explanation and remedy of certain effects that caused rejection of runs.

Runs were rejected because of:

- 1) Gross variations in the measured inlet gas temperature.

Any variation greater than about 0.5 percent of the absolute temperature between the beginning and end of the run caused it to be rejected. Thus

at the 1500°F level, this amounted to a change in excess of about 10 degrees. At the 1500°F level there is about a 1000°F drop across the film, so that a variation of 10°F causes a negligible effect on the heat transfer. In most cases, however, a variation of less than 3°F was obtained.

2) Variation in the thermocouple readings of the wall temperatures that amounted to more than about 1 percent of the difference in emf between two thermocouples located at any one measuring station. In general, this amounted to less than a 10 microvolt (0.3°F) deviation between the beginning and end of the run. (During all runs, the thermocouples were read at least twice to insure steady state conditions.)

3) Screens partially plugged by chips from the globar packing of the furnace heat transfer tube. This manifested itself in unusually high or low readings at the various stations, especially the first and last ones. Disassembly of the test unit from the lower adiabatic section and subsequent cleaning of the screens remedied this situation.

4) Excessive leakage or gross variation in gas flow rates. This was primarily attributable to the creation of flaws and subsequent cracking of the upper transite sheet of the lower adiabatic section, which had to be replaced three times during the course of the experiments. This leakage was easily noticed because for a constant rotameter and gas temperature setting the height of the orifice manometer slowly fell to a lower setting that indicated a greater leakage.

5) The inlet water rate varying by more than  $\pm 0.2$  gpm from the usual indicated setting of 4.0 gpm. These temporary fluctuations were usually caused by a momentary change in the water supply pressure. A run was also rejected if the inlet water temperature varied by more than 0.1°F before and after the run.

6) Indications of fouling at any one of the stations. This effect could be noticed when the deviation of the computed coefficient differed more from the expected value as the absolute value of the coefficient increased. In this case, the test object would be disassembled from the lower adiabatic section and cleaned with a xylene moistened cloth. As a precaution against fouling, the inside surface of the test object was periodically cleaned.

7) Gross inequities in the heat balance on the water side as compared to the calculated integration of the fluxes occurring in the wall. (The gas side heat balances were not given much credence, as is explained in the discussion of the results.)

It is evident that with the criteria set up above, the best accuracy possible within the limits of the equipment should be obtained.

#### Location of Thermocouples in Test Object and Calibration of Equipment

The thermocouples in the test object were located by two separate methods which, however, were not wholly independent of each other. A preliminary estimate of the probable thermocouple locations was obtained by taking a series of low temperature (180-190°F inlet temperature) runs and computing the fluxes required at each station in order to reproduce the shape of Boelter, et al.'s<sup>3</sup> curves for the variation of  $h$  vs.  $\frac{L}{D}$  which were obtained for low temperature differences across the film. For the limiting value at  $\frac{L}{D} = 10$ , McAdams equation was assumed to hold, and using this value of  $h$  as a base, a profile proportioned after Boelter, et al.'s data for the Reynolds number range in question was calculated. This "in situ" calibration gave the most probable value of  $\ln(r_2/r_1)$  in equation (20) at which the thermocouples must be located

to yield the required flux from the known temperature drop across the film that was present at each measuring station and the known temperature differences between the thermocouples in question.

Following the end of the experimental runs, the test object was sliced open and about 1/8 inch thick annular slices were cut out transverse to the axis of the inconel tube of the test object, the thermocouple holes being located within the slices. Actual grinding until the holes were exposed was not thought feasible since grinding could have destroyed the thermocouple junction welds and would have left no trace of prior location during the experiment. Therefore, each slice was X-rayed and the resulting negative was put into a photographic enlarger and the radial distances of the thermocouple junctions were measured from the projected enlargement. Since in most holes there were a number of junctions visible which were the results of unsuccessful attempts at insertion and fastening of the wires, the ratios of  $r_2/r_1$  obtained from the "in situ" calibration were relied upon to give an indication of which were the true thermocouple locations. A more detailed discussion of possible errors in this may be found in a subsequent section of this report. It is hence seen that the location of the thermocouples is an essentially independent determination whose only comparison with known data is to have used the known data as a reference guide in the selection of the most plausibly operable junctions.

The standard cell of the potentiometer was calibrated against a standard cell recently calibrated by the National Bureau of Standards. The stud dials and slide wires were also checked against the K-2 potentiometer.

Calibration curves for the gas rotameter were supplied by the manufacturer and may be found in Appendix D.

Difficulty was encountered in the calibration of the chromel-constantan thermocouples located in the test object since no primary standards for the 60-140°F range were available. However, a thermometer that had been calibrated for the room temperature range against a thermometer calibrated by the National Bureau of Standards was used to obtain one reference temperature check. Eight of the nine operable thermocouples in the test object gave the same reading, but the ninth, TC-7, was slightly off. In the absence of any other means of accurate reference, the eight remaining couples were assumed to be correct and this "stray" thermocouple was calibrated against the other eight in a constant temperature bath. The resulting calibration curve may be found in Appendix D.

Calibration of the chromel-alumel thermocouples was not attempted since, according to Thomassen,<sup>28</sup> calibration of these 28 gauge couples does not have any meaning. A discussion of this may be found in a subsequent section of the report.

The orifice meter was calibrated directly against the air rotameter by connecting it directly to the exit of the rotameter. In Appendix D, the resulting curve of the variation of orifice coefficient with Reynolds number may be found.

## DISCUSSION OF FACTORS AFFECTING ACCURACY OF EXPERIMENTAL RESULTS

There are many factors which may affect the accuracy of the data presented in this report, some of which are fixed, that is, can cause a permanent shift in the evaluation of the experimental quantities, and others which are variable and hence can cause variations from run to run. These will all be discussed in detail below, where an estimate of the errors entailed will also be made. Naturally, every effort at minimization of these errors was attempted.

### Location of Thermocouples in Test Object

This is a very important item since the fluxes calculated at each measuring station are directly dependent upon where the thermocouples are assumed to be located. As mentioned previously, a preliminary calibration "in situ" was undertaken by taking low temperature runs and computing the values of  $\ln r_2/r_1$  that would be necessary to reproduce the shape of Boelter, et al.'s  $\frac{1}{3}$  curve for the variation of  $h$  vs.  $L/D$  and produce a Nusselt number in accord with McAdams recommended equation at  $L/D = 10$ . These preliminary values of  $\ln r_2/r_1$  were reproducible to  $\pm 1$  percent, the deviations for most measuring stations being much less. These values of  $r_2/r_1$  served as a guide in the selection of the proper thermocouple locations from those visible in an X-ray negative of a cross sectional slice of the test object. The X-rays in themselves could not provide the precise calibration desired since in most of the holes two or even three junctions were visible. This was due to the fact that great difficulty was encountered in the insertion and induction welding of the thermocouples to the bottom of the holes.

In many cases, also, each wire had to be inserted and fastened separately, and often a wire came out or even broke off repeatedly before ultimately being fastened tight. This is what caused the presence of the multiple junctions or thermocouple welds visible in any one hole of the X-ray negatives. It was therefore felt not to be unreasonable to use the values of  $r_2/r_1$  required to produce the low temperature difference data as an indication of which were the good junctions. In one case it was felt that the two thermocouple wires had become fastened at different levels in the hole, and it is shown in Appendix C that for this case the temperature read would correspond to that indicated by a simple junction fastened to the wall at a radial distance that is the geometric mean of the two actual positions.

In all cases, the other visible thermocouple welds present in any one hole were sufficiently separated from the chosen junction so that the assumption that these were the operable junctions would have led up to a 50 percent disagreement with the values reported in the literature and would have caused an extremely erratic and non-monotonic variation of Nu with L/D.

A table of the thermocouple locations obtained from the X-ray negatives which correspond to those giving the best value of  $\ln r_2/r_1$  when compared with the "in situ" calibration follows.

L/D Test Object	Location of Operable Junctions in	$\ln (r_2/r_1)$ Obtained from "in situ" Calibration	Possible Positions from X-ray (mils)	$\ln (r_2/r_1)$ for the Couples Located by X-ray	% Dev. of the $\ln (r_2/r_1)$ by X-ray from "in situ"
1.5	Surface Center*	0.303	905 <sup>a</sup>	0.301	0.5%
	Bottom		$\frac{650, 693^b}{(\sqrt{650 \times 693} = 670)}$		
4	Top	0.231	872	0.231	0%
	Bottom		693		
7	Surface Center	0.226	900 <sup>c</sup> 917	0.226	0%
10	Top		842		
	Bottom	0.3565	590	0.3565	0%

\* Center hole thermocouple location could not be verified by X-ray but was 736 mils from the "in situ" calibration.

<sup>a</sup> Thermocouple was welded right onto surface. Since there was a slight hump at the junction's location, a radial distance of 905 mils was assumed.

<sup>b</sup> The two wires of the couple appear to be at the indicated radii. The geometric mean radius gives virtual position which indicated temperature would correspond to.

<sup>c</sup> Same as footnote a, except since junction seemed fused right onto the surface, the radius of the surface, 900 mils, was assumed as its location.

It can be seen how accurately the locations chosen from the X-rays correspond to the "in situ" calibration values of  $\ln (r_2/r_1)$ . However, the location of the thermocouples from the X-ray negative can really only be considered accurate to within  $\pm 4$  mils, which in no case



would cause an error of more than  $\pm 3$  percent in the values of  $\ln (r_2/r_1)$  listed in the table. This would result in a maximum possible fixed error of  $\pm 3$  percent in the computation of the flux at any given measuring station, but it is felt that the error is much more minimal due to the excellent agreement between the "in situ" and X-ray calibration values. Further verification that the values used must approach the correct ones very closely is the good agreement between the heat transferred calculated from the integration of the fluxes computed with the present values of  $\ln (r_2/r_1)$  and the water side heat balances.

A change in the location of the thermocouple positions would also affect the extrapolated inside wall temperature but this effect is so small that it is completely negligible.

#### Gas Temperature Measurement

Gas temperatures are probably accurate to within  $\pm 4$  percent of the Fahrenheit temperature, the possible absolute error hence increasing with increasing temperature. The reason for the possibility of such a large error is due to the fact that for such a small thermocouple wire as 28 gauge, the surface reactions and corrosive film formation on the wires when exposed to an oxidizing atmosphere cause the film thickness to be preponderantly large in comparison to the cross section of the wire, thus creating the effect of another set of junctions in series with the main junction. Since this corrosive film is located in a section of severe temperature gradients a quite appreciable additional emf may be produced causing the thermocouple to indicate a lower temperature. According to Thomassen<sup>28</sup> there is also the possibility of a reverse reaction in the neighborhood of the main junction which is enclosed inside the ceramic tube if the tube is airtight and the oxygen has all been

used up. These competing reactions could thus cause both positive and negative errors, change with time and temperature level in a random fashion, and could give absolute errors of 70-80°F or more at 2000°F. In order to minimize the error caused by estimating the wrong  $t_0$  at each station, a linear relationship between the indicated inlet and exit gas temperatures was assumed to hold. In almost all cases, the gas side heat balance was from 15 to 35 percent low, indicating that in all probability the inlet thermocouple was at a higher temperature than indicated by the emf read at the potentiometer. This is because the general tendency for chromel-alumel couples is to read low, and hence more credence was given to the exit thermocouple reading, the heat balance error being attributed mainly to the low reading of the entrance thermocouple. A comparison of various possible methods of computing  $t_0$  will be shown below and compared with the straight line method. A typical run, Run No. 46, for which the graphical integration of the fluxes may be found in Appendix B, will be used as an example. Case 1 represents equation (29) where the exit gas temperature is taken as determinative and the gas temperatures are calculated from a heat balance obtained from an integration of the thermal fluxes induced in the wall. Case 3 is for equation (28) and is hence the same as case 1 except that the inlet temperature has been assumed to be the correct one. In case 2, the error in heat balance has been evenly distributed between the inlet and exit temperatures. A summarizing tabulation as well as a graphical presentation of the temperature variation curves is presented in the following table and summarized graphically in Figure 8.

L/D	Straight Line Method			Case 1		
	t <sub>b</sub> <sup>'</sup> , (°F)	t <sub>s</sub> (°F)	t <sub>b</sub> -t <sub>s</sub> (°F)	Exit Fixed		Percent Error*
				t <sub>b1</sub> (°F)	t <sub>b1</sub> -t <sub>b</sub> <sup>'</sup> (°F)	
Inlet	1003			1031		
1.5	979	108	871	992	13	-1.5
4	940	100	840	940	0	0
7	893	104	789	890	-3	.3
10	847	101	746	845	-2	.2
Exit	827			827		

L/D	Case 2			Case 3		
	Error Split		Percent Error*	Entrance Fixed		Percent Error*
	t <sub>b2</sub> (°F)	t <sub>b2</sub> -t <sub>b</sub> <sup>'</sup> (°F)		t <sub>b3</sub> (°F)	t <sub>b3</sub> -t <sub>b</sub> <sup>'</sup> (°F)	
Inlet	1017			1003		
1.5	978	-1	.1	964	-15	1.7
4	926	-14	1.6	912	-28	3.2
7	876	-17	1.9	862	-31	3.6
10	831	-16	1.8	817	-30	3.4
Exit	813			799		

\* Percent error column denotes error that would be caused in the evaluation of h from equation (26) and is equal to  $-(100)(t_{b_i} - t_b') / (t_b - t_s)$ .

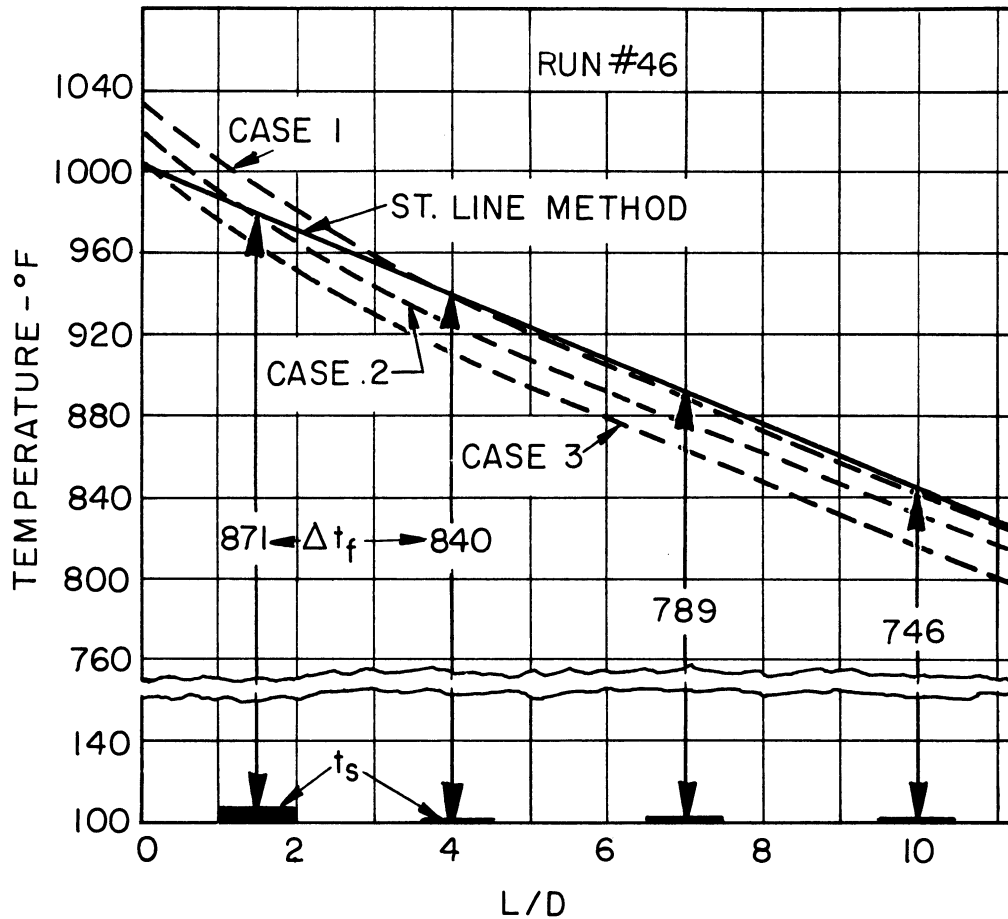


Figure 8. Comparison Between Methods of Estimating Local Bulk Temperature

It can be seen that the errors caused by assuming the straight line relationship are minimal for cases 1 and 2 and are somewhat more significant though still not very appreciable for case 3, which is the most unlikely one. It can be argued that case 1 or case 2 should have been used consistently in the computation of the heat transfer coefficients instead of the straight line relationship; however, it is seen that use of either of these methods causes a constant error in the estimation of  $t_b$  down the whole length of the tube (except in the extremely fortuitous case when the inlet temperature assumed is the absolutely correct one), while with the straight line method the odds of estimating the correct temperature at any one of the measuring stations

are greatly enhanced. Since the errors of the thermocouple reading can vary from run to run, on an overall basis the straight line relationship will most nearly give the lowest percentage error in estimation of  $t_b$ , for even though only some of the points on the line will approach the true  $t_b$ , use of curves 1 and 2 will always yield an error. It can also be seen that except for the very unlikely case 3, the straight line is bound to hit some points correctly. Furthermore, it should be noted how closely the straight line follows the major portion of the curve of case 1, the most probable condition.

It is therefore seen that on an overall basis, use of the straight line method yields the least probable error in local bulk temperature estimation and that errors caused by the faulty thermocouple readings are hence minimized and affect the computation of the overall coefficient by less than 2 percent. For the higher temperature runs, even though the possible absolute error in  $t_b$  may be greater, the error relative to the temperature drop across the film,  $t_b - t_s$ , does not increase. Naturally, not much accuracy can be expected in the gas side heat balances which are directly proportional to the difference between the inlet and exit temperatures, but since there are two remaining heat balances which can be used as a check on the internal consistency of the data, this third balance is not of paramount importance.

#### Minor Clogging of Screens

Since the screens in the adiabatic sections were not visible at any time except when the test object assembly was dismantled from the lower adiabatic section, the effect of partial clogging by small fragments of the silicon carbide packing could only be noticed by gross irregularities in the variation of the heat transfer coefficient down the

length of the tube. Periodic cleaning of the screens was done to minimize this effect; however, it is entirely reasonable to suppose that minor screen clogging could effect a change in the heat transfer coefficients of up to 5 percent without being explicitly noticeable. This variation in the coefficient is due to the fact that clogging of some of the screen holes causes a change in the apparent mass velocity extant at each section. This mass velocity change can be either an increase or a defect over the average mass velocity at each measuring station, and hence can cause both positive and negative deviations in the measured heat transfer coefficients. It thus can be seen that even though this effect is a contributing factor to the scatter of the data, under the assumption that the minor clogging of the screens is in a random fashion for a whole series of runs, the effect on the mean value will be negligible.

#### Gas Flow Rate

The orifice meter used in this experiment is accurate to within  $\pm 1$  percent for readings over 50 mm. Since it was calibrated against the air rotameter which also has a reproducibility of 1 percent, the total possible error in flow rate is  $\pm 2$  percent. Thus, the maximum error in  $Re^{.8}$  due to an error in flow readings is about  $\pm 1.5$  percent.

#### Net Temperature Differences on the Water Side

Measuring the net water temperature difference due to the heat transferred by the gas alone meant measuring the overall temperature difference during a run and then shutting off the gas flow and measuring the temperature rise due to conduction and room effects alone. Each individual temperature (i.e., thermocouple emf) reading is accurate to

2 microvolts. Therefore, the possible maximum error in reading the overall temperature difference is 4 microvolts, and the same limit of accuracy is also present when the blank reading with no gas glow is taken. Hence, the possible maximum error in the measurement of the net water temperature difference is 8 microvolts, which is equal to 0.25°F. This corresponds to 480 Btu/hr at a flow rate of 4 gpm; however, in all likelihood the errors in reading are compensating, so that little or no error should be present.

#### Thermal Properties of Air

The accuracy of the Nusselt and Reynolds numbers is a function of the accuracy of the values used for the thermal conductivity and viscosity of air. For low temperatures these are known to a high degree of accuracy, but for temperatures higher than about 700°F there is some disagreement as to what the correct values are, especially for the thermal conductivity. Both Keenan and Kaye<sup>17</sup> and Hilsenrath<sup>15</sup> give values for the high temperature properties of air, but only Keenan and Kaye give values of the thermal conductivity up to 2000°F. Therefore, to use a consistent set of values, both the viscosity and thermal conductivity values reported in Keenan and Kaye were used. The viscosities tabulated in Hilsenrath are in excellent agreement with Keenan and Kaye's for temperatures up to 800°F, above which Hilsenrath's tend to be slightly lower until at 2000°F his values are about 2 percent below those in Keenan and Kaye. Thus, use of Hilsenrath's viscosity data would cause a maximum increase of about 1.5 percent in the computation of  $Re^{.8}$  at high temperatures, which is a comparatively small deviation. The values of  $Pr^{1/3}$  reported in Hilsenrath vary from 0.879 to 0.891 for the whole

temperature range of these experiments, so for computational purposes, a constant value of 0.885 was assumed to hold, which causes a negligible error.



## EXPERIMENTAL RESULTS

The results obtained from the present set of experiments are presented in the form of standard dimensionless groups, which permits a much greater generalization of the results even though these values have been obtained for only a single gas and a limited range of Reynolds numbers. The local heat transfer coefficients for each of the measuring stations were arrived at from the theory of the calculations that has already been discussed, and a sample calculation is presented in Appendix B. The original data as well as the relevant associated dimensionless groups are presented in Tables 1 and 2 of Appendix A. In these tables, the local Nusselt and Reynolds numbers and values of  $T_b/T_s$  are listed, each of these taking into account the temperature variation down the length of the tube and the resultant effect of the change in the temperature dependent thermal properties. The thermal conductivity and viscosity data of Keenan and Kaye<sup>17</sup> were used, and these values are included in Table 1.

Representation of the data in terms of  $h_c$  or Nu profiles down the length of the tube for each individual run was not felt to be desirable because:

a) The objective of this study is to ascertain the effect of temperature level on heat transfer down the length of the tube; this effect could not be evaluated from a series of plots of  $h_c$  or Nu versus  $L/D$  for each run, especially if the effect of temperature level were to vary with position.

b) The temperature level and  $T_b/T_s$  vary down the length of the tube.

c) A plot of  $h_c$  or Nu versus  $L/D$  is a poor form of correlation where the temperature varies appreciably down the length of the tube, and this will be discussed in the next section of this report,

d) The scatter of the data points in any one run due to factors mentioned in a previous section of this report will cause inaccuracies in the profiles for a single run; however, the data points for any given measuring station will accurately describe the mean tendency of that station when evaluated for a whole series of runs.

Instead, the results obtained at each value of  $L/D$  were treated as completely separate entities, comparisons between all the stations being made only for the ultimate correlations derived at each measuring station.

The results obtained at each measuring station were assumed to fit an equation of the form predicted by dimensional analysis, namely

$$\text{Nu} = a \text{Re}^{0.8} \text{Pr}^{1/3} \left( \frac{T_b}{T_s} \right)^m \quad (49)$$

where the dimensionless groups are to be evaluated at some given reference temperature, and  $a$  and  $m$  are constants to be evaluated from the experimental data. A Reynolds number exponent of 0.8 and a Prandtl number exponent of  $1/3$  were assumed on the basis of the extensive prior work in the field of heat transfer. The assumption of these exponents in no way hinders the validity of this present work since the main objective of these experiments is to evaluate the effect of temperature level and distance from the tube entrance on the local heat transfer coefficients, and these effects are connected with the evaluation of  $a$  and  $m$ . Rearrangement of equation (49) into the form

$$\frac{\text{Nu}}{\text{Re}^{0.8} \text{Pr}^{1/3}} = a \left( \frac{T_b}{T_s} \right)^m \quad (50)$$

permits an easy evaluation of  $\underline{a}$  and  $\underline{m}$ . Values of  $Nu/Re^{0.8}Pr^{1/3}$  were plotted against  $T_b/T_s$  on logarithmic coordinates, and the method of least mean squares was used to find the best line through the data. On such a plot, the slope of the line is equal to  $\underline{m}$  and the intercept denotes the value of  $\underline{a}$ . Correlations based on evaluating the dimensionless groups at the bulk, film, and surface temperatures were tried, the best results being obtained when all the properties were referred to the bulk temperature. The values of  $\underline{a}$  and  $\underline{m}$  were determined for three different cases, namely:

1) Best Free Fit. This is the best line that could be drawn through all the data points and gives the optimum values for  $\underline{a}$  and  $\underline{m}$ .

2) Fixed Intercept. The intercept  $\underline{a}$  was fixed at a value in accord with the variation of heat transfer coefficient down the length of the tube as reported for low temperatures by Boelter, et al.<sup>3</sup> for the present Re range, with McAdams' value of  $a = 0.023$  used at  $L/D = 10$ . These fixed values are as follows:

L/D	(Nu/Nu <sub>10</sub> ) from Boelter	a <sub>F</sub>
1.5	1.26	0.0290
4	1.09	0.0251
7	1.03	0.0236
10	1.00	0.0230

Using these fixed values of  $a_F$ , the exponent of  $T_b/T_s$  for the best fit of the data was determined. This method thus forces the data to extrapolate down to the present correlations for low temperatures.

3) Mean Value for No Temperature Effect. The best line of zero slope through the data was found, thus giving the optimum value of  $\underline{a}$  for  $\underline{m} = 0$ .

In order to test and compare the relative reliability of these three methods in representing the data, a statistical analysis was relied upon. The standard deviations of the data points from the best line drawn in accordance to the stipulations of case 1, 2, or 3 was calculated. This standard deviation was in terms of the percentage deviation of the points from the calculated line. It should be mentioned here that the "best line" through the data mentioned above represents the line with the minimum percent deviation rather than the minimum absolute deviation since percent deviation gives a much more reliable estimate of accuracy for the whole range of values of the parameter that is being varied.

For the evaluation of all the properties at the bulk temperature, the following values of  $\underline{a}$  and  $\underline{m}$  in equation (49) were obtained. The standard deviations, S. D., listed in the table are accurate to  $\pm 1\%$ .

Values of Constants in Equation (49) with Properties Referred to Local Bulk Temperature

L/D	Case 1			Case 2			Case 3		
	Best Free Fit			Intercept Fixed			No Effect of Temp.		
	a	m	S.D.	$a_F$	m	S.D.	a	m	S.D.
1.5	.0295	+ .007	6.3%	.0290	+ .027	7.8%	.0297	0	7.8%
4	.0264	- .026	7.8%	.0251	+ .026	10.2%	.0257	0	7.8%
7	.0237	- .003	7.2%	.0236	+ .002	7.8%	.02365	0	7.2%
10	.0223	+ .042	6.3%	.0230	+ .005	6.8%	.0231	0	7.8%

Since standard deviations are greater than the mean deviation or the probable error, it is not surprising to find the comparatively high values listed above. In fact, assuming a normal distribution, the probable error is only  $0.6745 \times \text{S.D.}$  It should also be remembered that the values of S.D. listed above are only accurate to  $\pm 1$  percent. What is really significant in the above tabulation is that when all of the properties are referred to the local bulk temperature, there is no significant difference between the standard deviations of all the three cases and hence use of the simplest case, Case 3, where no effect of temperature level is assumed, causes no serious errors. A further corroboration of the fact that temperature level is not a significant factor is that for Case 1, the best free fit of the data, two of the  $T_b/T_s$  exponents are slightly positive and two are slightly negative. It is also seen that there is no significant variation of the effect of temperature level down the length of the tube, and a further more detailed discussion and analysis of these results will be given in the next section.

Since use of the fit for  $m = 0$  is the simplest to apply in practice and yet entails no significant loss of accuracy in representing the data, the data has all been correlated conveniently in terms of

$$\text{Nu}_b/\text{Pr}_b^{1/3} = a \text{Re}_b^{0.8} \quad (51)$$

where a is the best value obtained from a least mean square fit for Case 3 and has been tabulated on the preceding page. Plots of the data for  $L/D = 1.5, 4, 7,$  and  $10,$  in terms of  $\text{Nu}_b/\text{Pr}_b^{1/3}$  versus  $\text{Re}_b$  on logarithmic coordinates, representing equation (51), may be found in Figures 9a - d, in which the best line of 0.8 slope has been drawn through the data. Beneath each of the main plots in these figures is an auxiliary log-log

plot of the data expressed as  $\log \text{Nu}_b / \text{Re}_b^{0.8} \text{Pr}_b^{1/3}$  versus  $\log (T_b/T_s)$ , representing equation (50). These plots show the exact effect of temperature level as evaluated for Cases 1 and 2, and in each case support the fact that the term  $T_b/T_s$  is not a significant parameter when the properties are evaluated at the bulk temperature. These latter plots are on a much larger scale than the main figure, and hence all the experimental errors are magnified. The mean deviation of the observed Nusselt numbers from the values predicted by the individual correlations of the form of equation (51) vary from about 4 to 6 percent for the various measuring stations, and the individual percent deviation for each point is tabulated in Table 1 of Appendix A. Since there are so many possible factors that can cause a spread in the data (as was discussed in the previous section), it is felt that these values show the excellent agreement between the data and the proposed correlations which do not utilize  $T_b/T_s$  as a significant parameter to account for the high temperature levels attained in this study.

A comparison of the effect of evaluating the properties at reference temperatures other than the bulk, namely the film and surface temperatures, was done for the data at  $L/D = 1.5$ . The measuring station at  $L/D = 1.5$  was chosen for comparison purposes because the bulk temperature data had a low mean deviation from the predicted line and the values of  $\underline{m}$ , the  $T_b/T_s$  exponent, were very minimal for both Cases 1 and 2 when the properties were evaluated at the bulk temperature. The resultant data evaluated at the film temperature is plotted in Figure 9e in the same fashion as for Figures 9a - d, and the increased spread of the data and greater effect of  $T_b/T_s$  can be noticed. The line derived from Boelter's low temperature work has also been included in the graph, and it is

seen how all the data points lie above it, denoting the necessity of including a term to account for the temperature level. It should also be noticed that the main logarithmic plot of  $Nu_f/Pr_f^{1/3}$  versus  $Re_f$  in Figure 9e is on a smaller scale than for the previous four similar figures, and hence the increased spread of the data caused by evaluating the properties at the film temperature does not at first become quite as apparent. A tabulation of the results of these computations for various reference temperatures is given below for Cases 1 and 2 only, since Case 3, in which it is assumed that there is no effect of temperature level, is evidently nonsensical when applied to the evaluation of the properties at the film and surface temperatures.

Values for the Constants in Equation (49) for  $L/D = 1.5$

Reference Temperature for Properties	Case 1		Case 2	
	Best Free Fit		Intercept Fixed	
	a	m	$a_F$	m
Bulk	.0295	.007	.0290	.027
Film	.0315	.065	.0290	.149
Surface	.0288	.337	.0290	.332

It should be noticed how much of an increase the effect of temperature level has as the properties are evaluated at successively lower temperatures. The free fit through the data evaluated at the film temperature gives an unnaturally high value of the intercept  $a$ , while if the intercept is fixed at the literature value, the effect of the parameter  $T_b/T_s$  increases tremendously. Also, the calculated standard deviation for this case is about 15 percent, an unusually high value. The

reason for this is analyzed and explained in the next section of this report. It also is seen from the table that with the properties evaluated at the surface temperature, a very similar fit is obtained for either Case 1 or Case 2, the extrapolated value of  $\underline{a}$  from Case 1 almost coinciding with the fixed value,  $a_F$ , and the  $T_b/T_s$  exponents being almost identical. This leads to the supposition that evaluating the properties at the surface temperature and including the factor  $(T_b/T_s)^{0.33}$  in equation (49) would correlate the data very well; however, evaluation of the properties at the bulk temperature, which is usually explicitly available, is more convenient and makes the temperature dependence negligible, thus simplifying the correlating procedure and the subsequent evaluation of heat transfer coefficients from the correlation.

One more computation was done as a check against Deissler's<sup>9</sup> analysis in which he assumed a constant Prandtl number of 0.73 and a thermal conductivity variation proportional to  $T^{0.68}$  rather than the true reported values which vary approximately as  $T^{0.85}$ . This computation was performed only for  $L/D = 7$ , which was chosen because it was some distance away from the inlet and had a very small scattering of the data. The viscosity was evaluated as usual at the bulk temperature, and the thermal conductivity was also referred to the bulk temperature except that it was assumed to be equal to  $0.0140 (T_b/492)^{0.68}$ . The results were that for the best free fit,  $\underline{a}$  was equal to 0.0242 and  $\underline{m}$  was 0.174, while for the intercept fixed at 0.0236, the exponent of  $T_b/T_s$  turned out to be 0.201. A further discussion of this will follow in the next section.

In Figure 10, a plot of  $h_c$  versus  $G$ , the mass flow rate, is given for  $L/D = 10$ . Arithmetic coordinates have been chosen because they more clearly show the spread between the various temperature levels, even



though absolute errors are magnified. This plot was included merely to demonstrate that  $h_c$  itself does increase with temperature when the data is not reduced to the appropriate dimensionless groups and corroborates the findings of previous investigators who did not correlate their data dimensionlessly.

Figure 11 is a summary of the heat balances obtained from the water side as compared to the heat transferred as calculated from an integration of the thermal fluxes induced in the wall from the heat given up by the flowing gas stream. The mean deviations of the water side values from those calculated by a rigorous integration of fluxes is about 5 percent. This indicates an excellent agreement since the water side heat balances are subject to some error as discussed in the previous section. This good check on the internal consistency of the data also is further evidence that the thermocouples in the test object are in approximately the observed locations since an error in thermocouple location would cause severe errors in the computed fluxes.

A comparison of the present data with the variation of  $Nu_b/Re_b^{0.8} Pr_b^{1/3}$  versus  $L/D$  derived from Boelter, et al.<sup>3</sup> is presented in Figure 12. The mean value of the 30 points obtained at each measuring station is plotted on the figure, and from either side of these points extend lines which correspond to the magnitude of the limits of probable error as obtained from a statistical analysis of the data. It will be seen that the points obtained in this study are very slightly above Boelter's curve for  $L/D = 1.5$  and  $L/D = 4$ , thus indicating a slightly steeper variation, but the difference, practically speaking, is negligible. Furthermore, Boelter's curve still goes through the limits of probable error of these points, so any definite conclusion as to whether

the present points represent the true situation any better than Boelter's is impossible. However, it should also be noted in what excellent agreement the present high temperature data are in comparison with Boelter's data obtained at low temperatures.

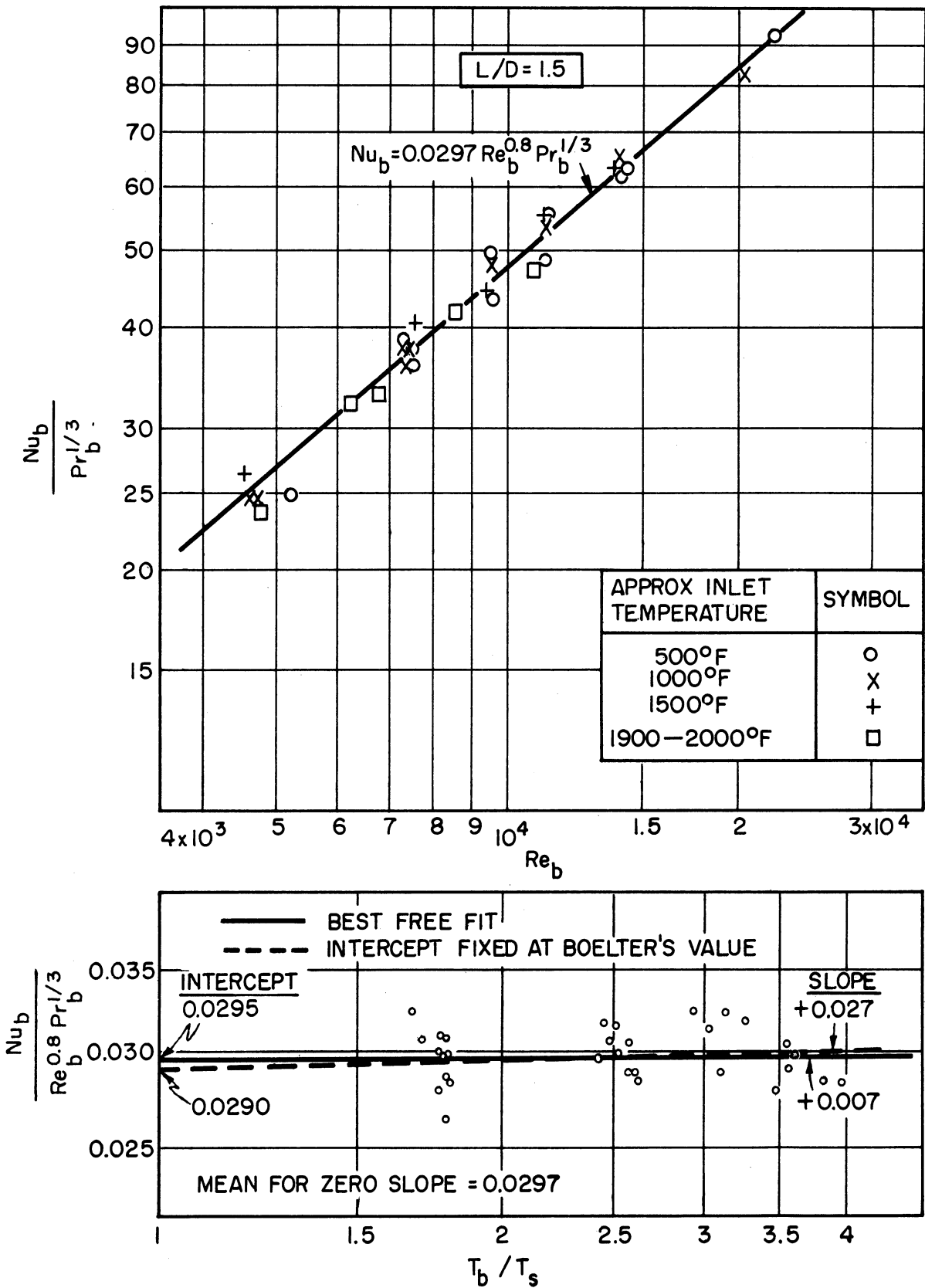


Figure 9a. Correlation of Local Heat Transfer Data and Determination of Effect of Temperature Level for  $L/D = 1.5$ , Properties Evaluated at Bulk Temperature

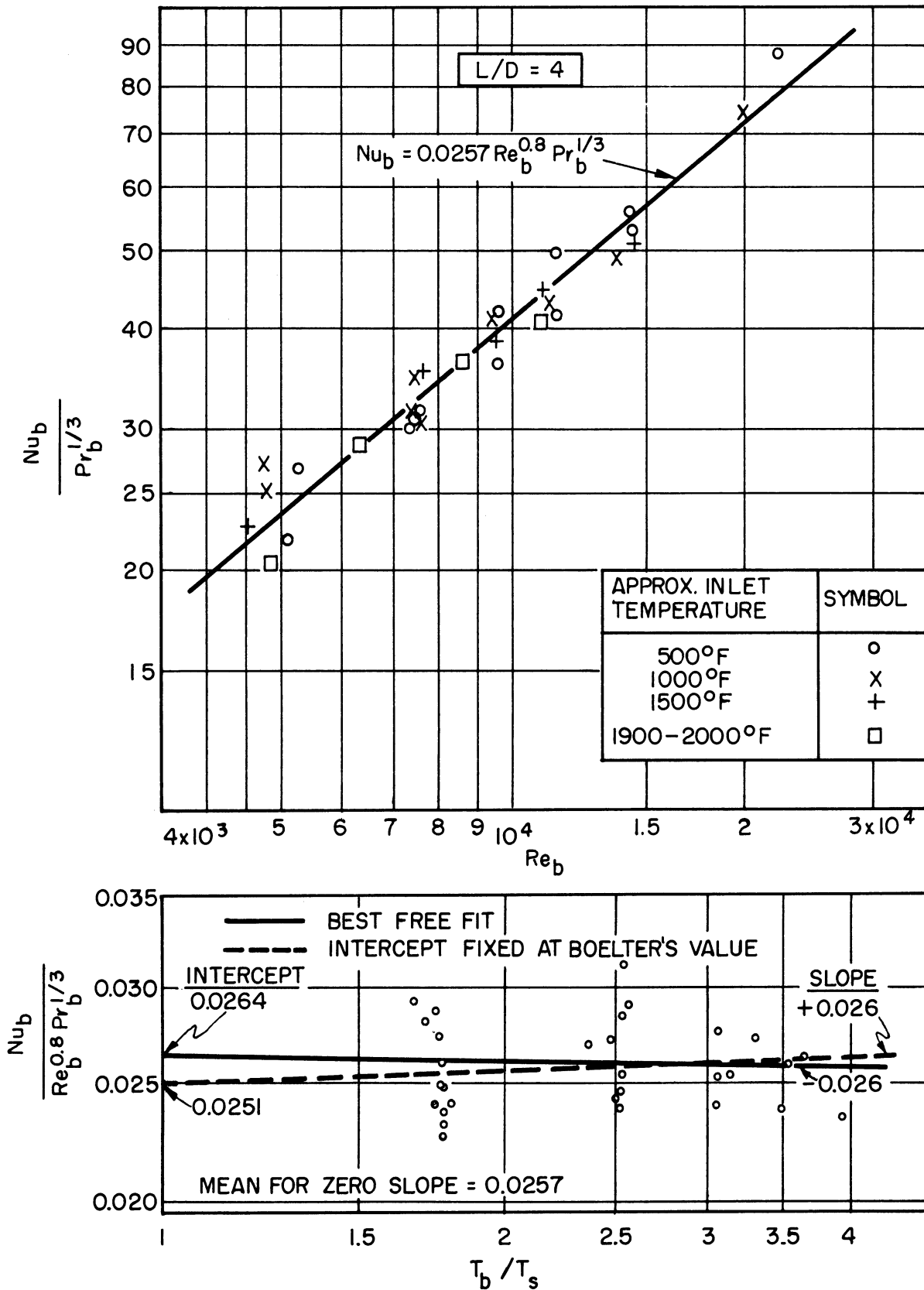


Figure 9b. Correlation of Local Heat Transfer Data and Determination of Effect of Temperature Level for  $L/D = 4$ , Properties Evaluated at Bulk Temperature

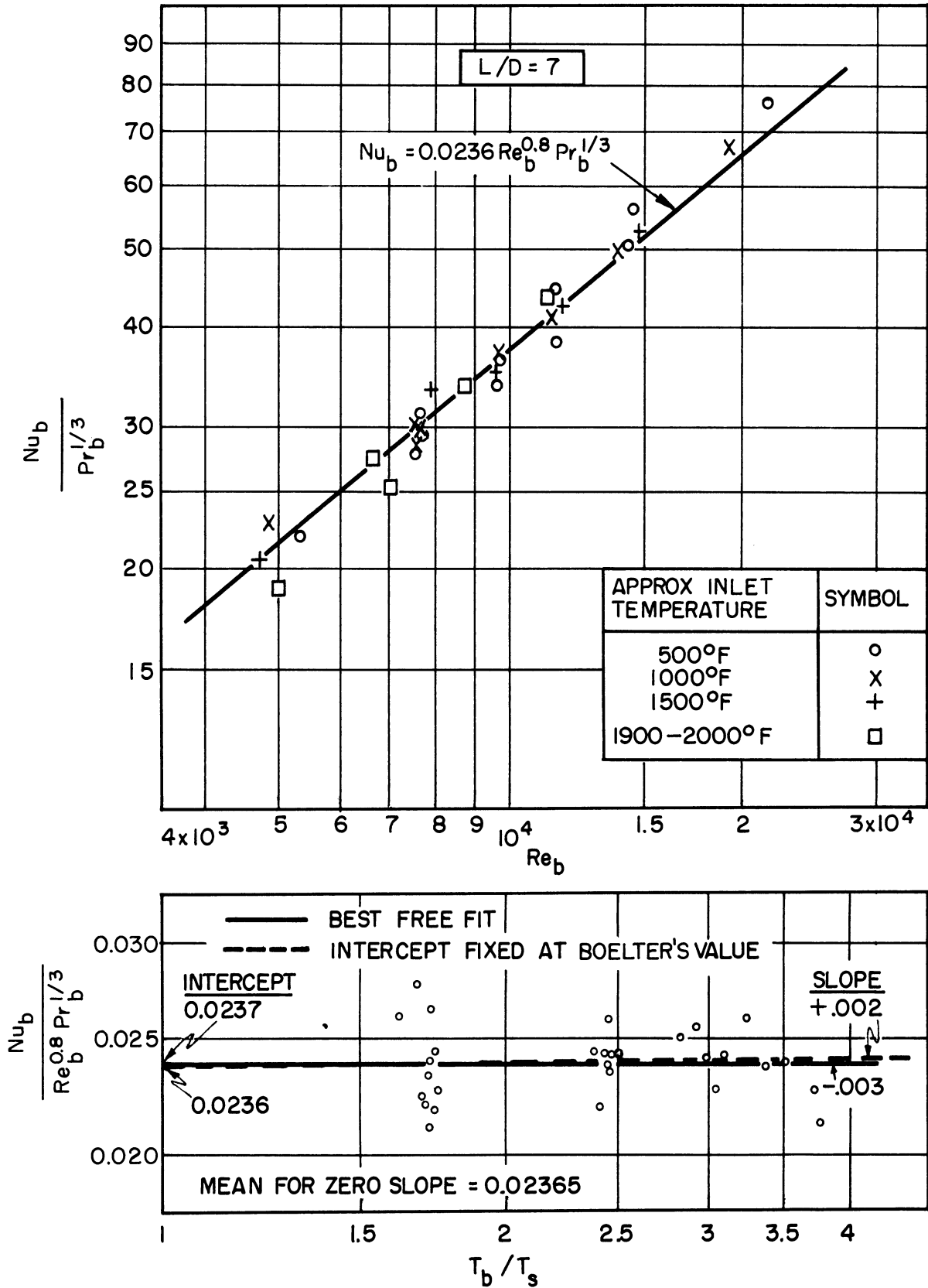


Figure 9c. Correlation of Local Heat Transfer Data and Determination of Effect of Temperature Level for  $L/D = 7$ , Properties Evaluated at Bulk Temperature

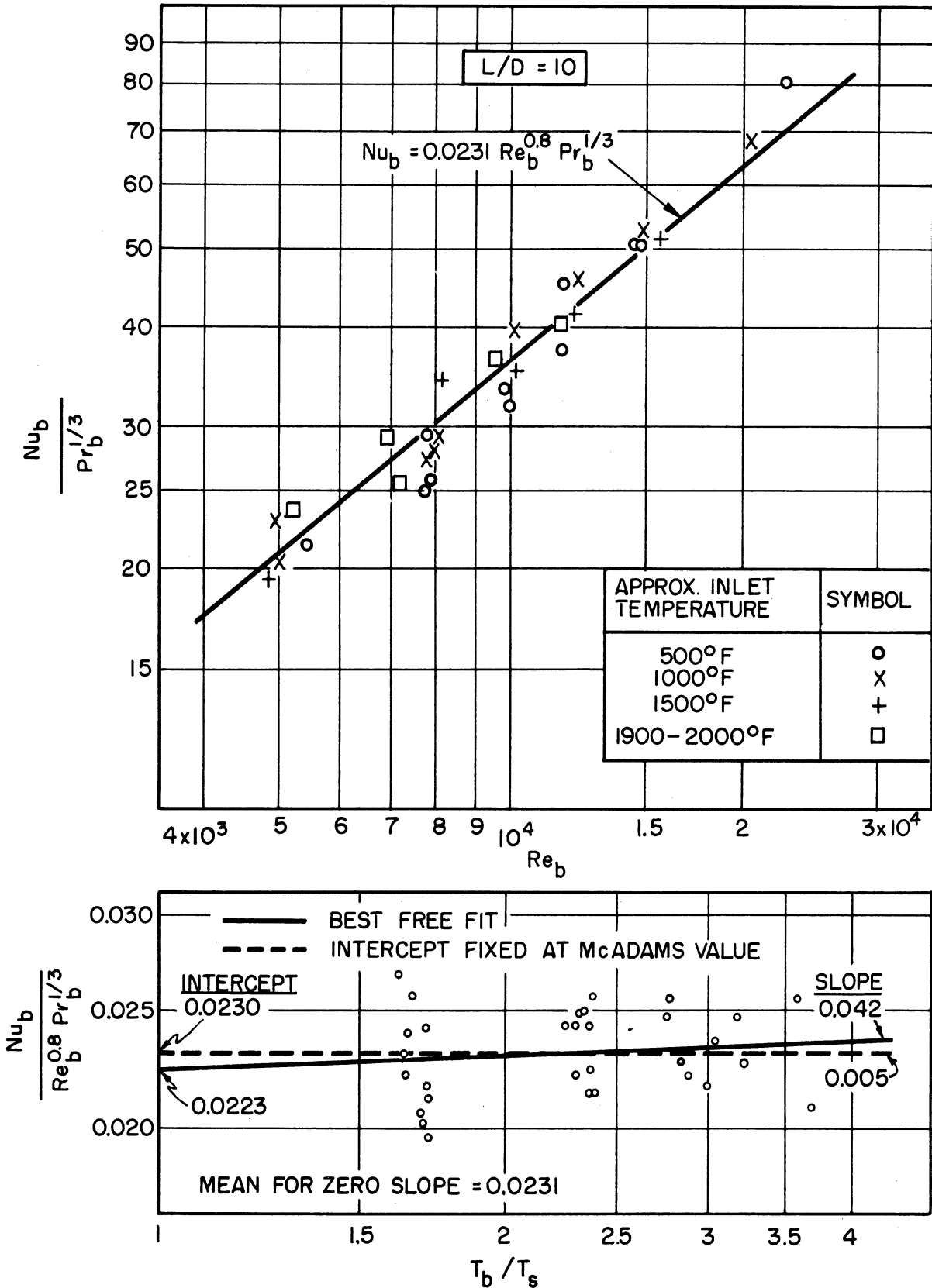


Figure 9d. Correlation of Local Heat Transfer Data and Determination of Effect of Temperature Level for  $L/D = 10$ , Properties Evaluated at Bulk Temperature

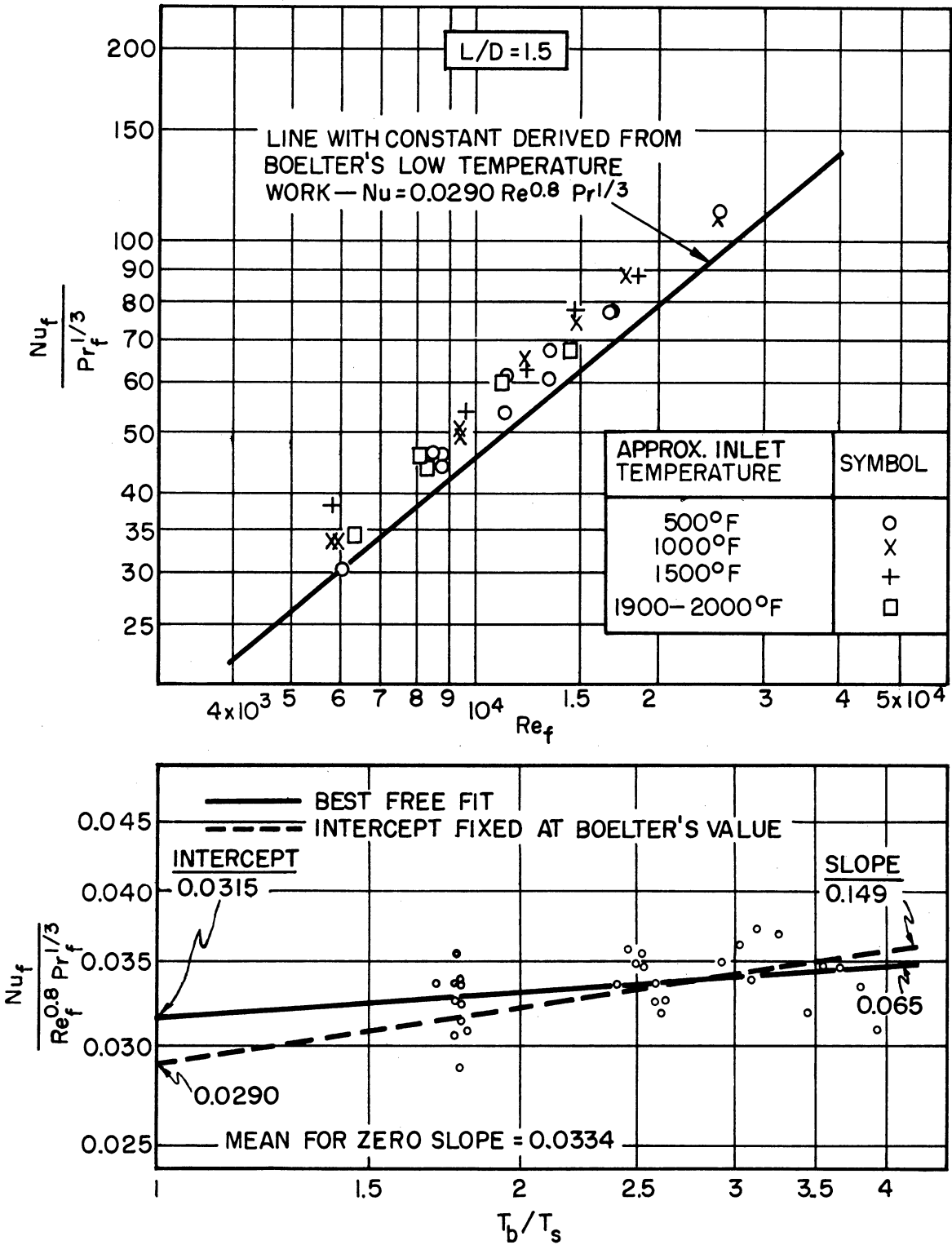


Figure 9e. Correlation of Local Heat Transfer Data and Determination of Effect of Temperature Level for  $L/D = 1.5$ , Properties Evaluated at Film Temperature

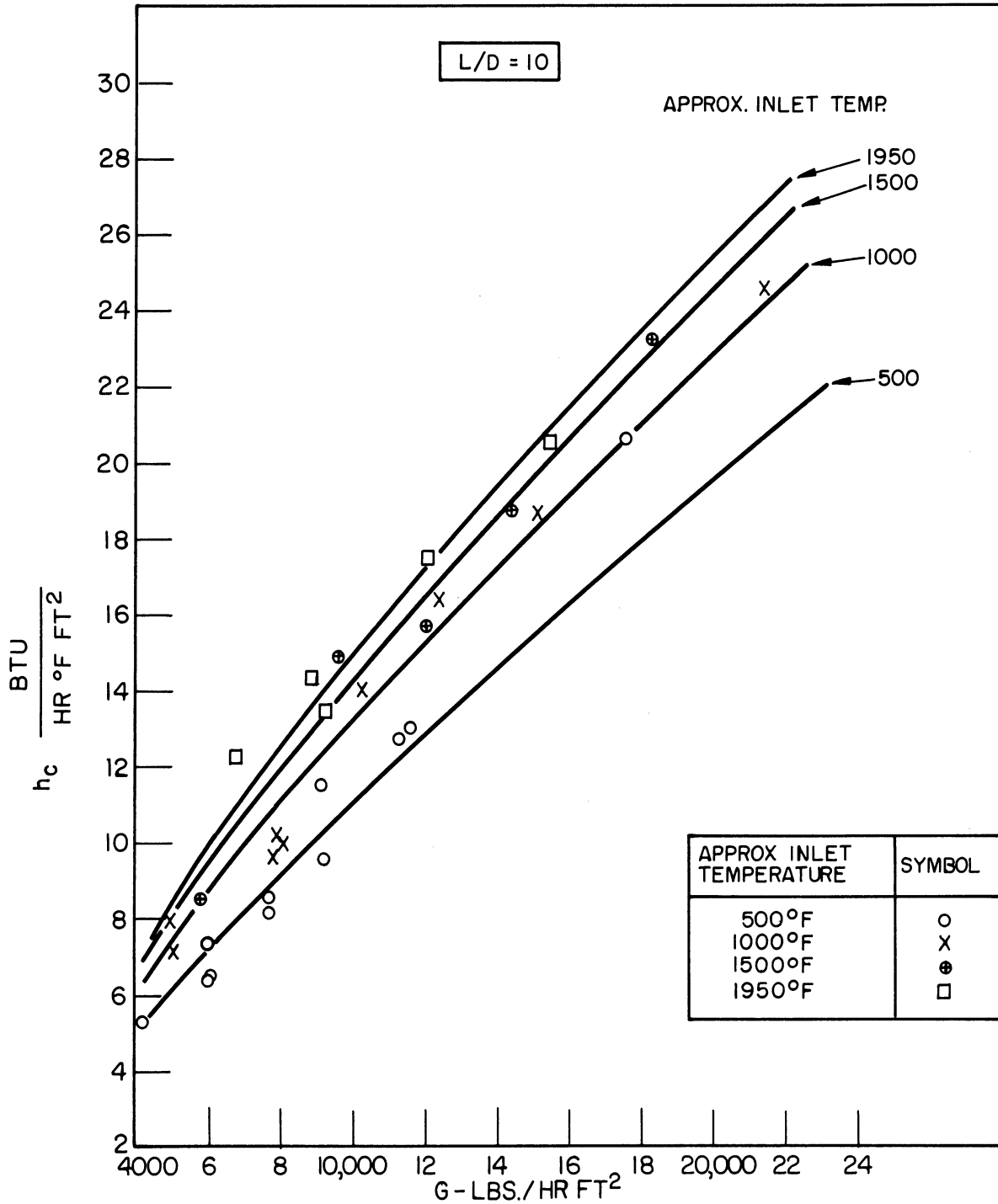


Figure 10. Correlation of Local Heat Transfer Coefficients at L/D = 10 as a Function of Mass Velocity



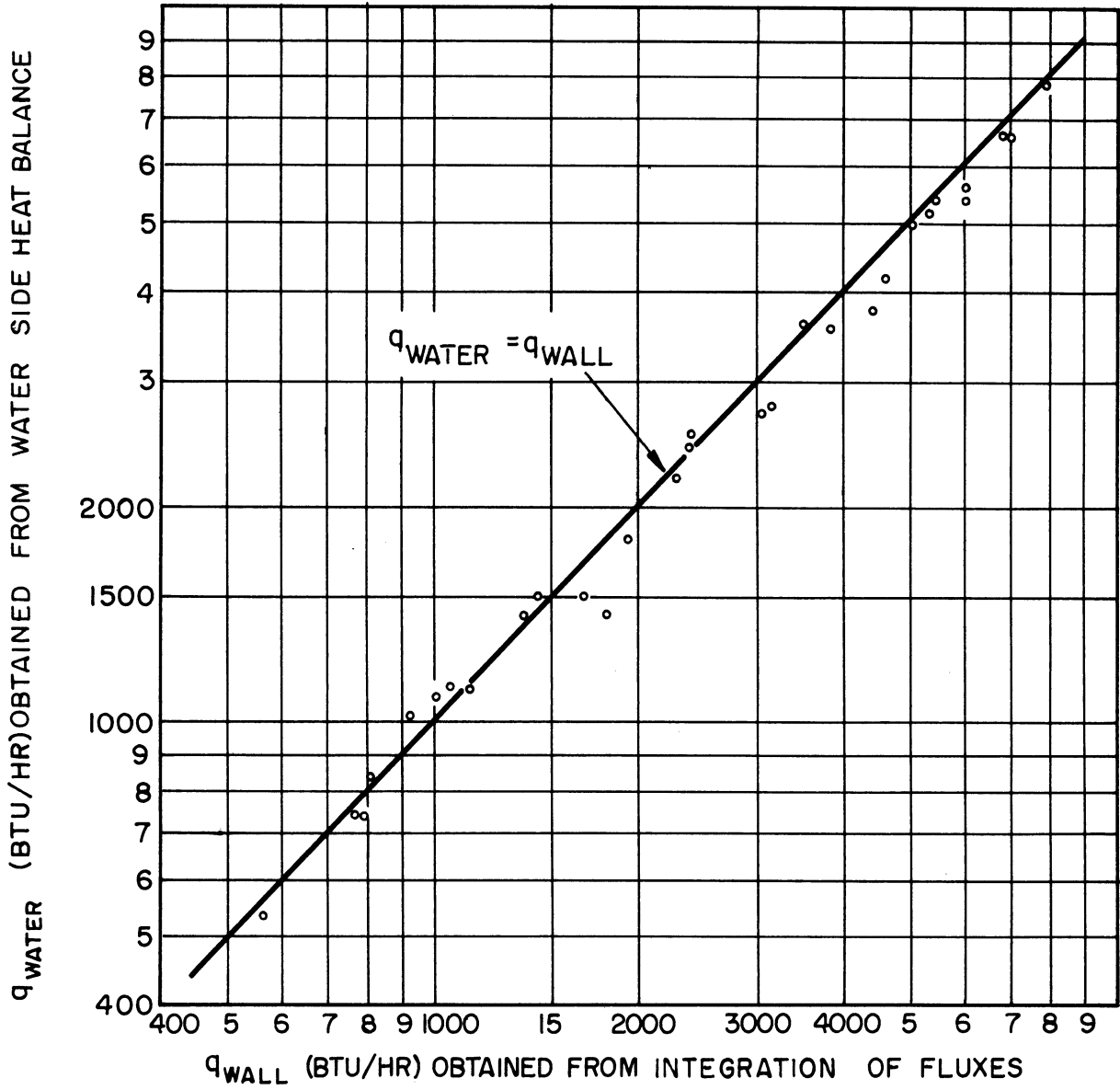


Figure 11. Summary of Heat Balances

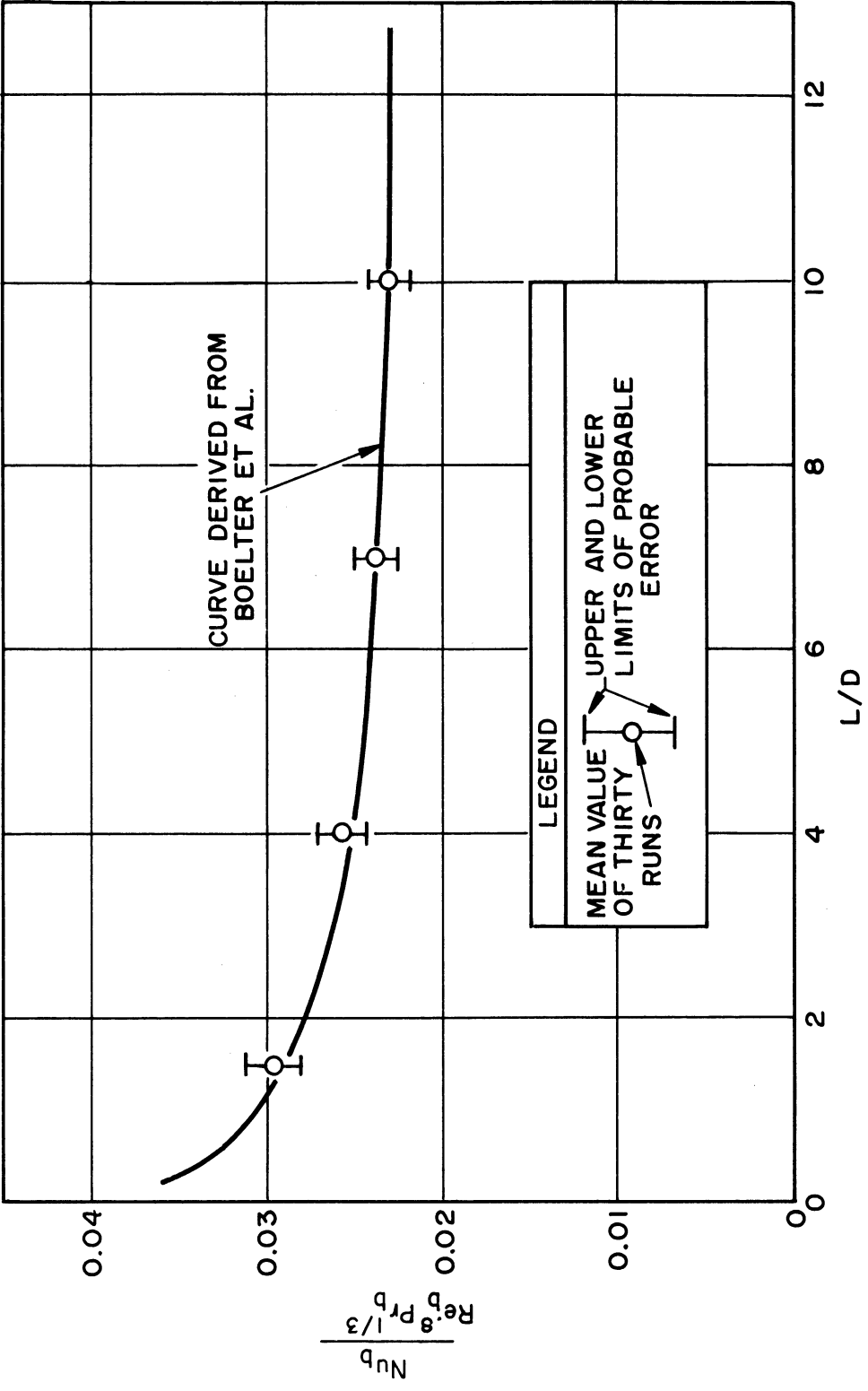


Figure 12. Comparison of Present Data with Curve Derived from Boelter, et al.

## DISCUSSION AND INTERPRETATION OF RESULTS

In the following section, the experimental results described in the previous section will be analyzed and interpreted, the conclusions these results lead to will be critically examined, and comparisons with previous work in the field will be made.

### Correlations Based on Use of Bulk Temperature for Evaluation of Properties

The experimental measurements obtained in this study extend to a higher temperature level than has previously been attained for the case of heat extraction from a gas flowing inside a circular tube. These measurements have the further advantage that they are for local rates, and in this manner, any significant variation in the effect of temperature level down the length of the tube could be noted.

From the auxiliary plots of  $\ln (Nu_b/Re_b^{0.8} Pr_b^{1/3})$  versus  $\ln (T_b/T_s)$  at the bottom of Figures 9a - d, it can be seen that the effect of temperature level is very minimal. These plots are on a much larger scale than the main figure and hence all experimental errors and irreproducibilities are magnified. Inspection of these plots shows that there is no significant difference between the effect of temperature level for any of the four measuring stations. As a test for the significance of any locally obtained exponent of  $T_b/T_s$ , the following criterion was chosen, namely, that no exponent obtained was significant if at a temperature level corresponding to  $T_b/T_s = 4$ , which is the approximate upper limit of the data obtained, it did not predict a percentage change in Nusselt number over  $Nu$  at  $T_b/T_s = 1$  that was greater than the

standard deviation of the "best free fit" case for its station. It is only at  $L/D = 10$  that the calculated exponent of 0.042 causes a 6.2 percent increase in  $Nu_b$  at  $T_b/T_s = 4$  over that at  $T_b/T_s = 1$  and hence closely approaches the standard deviation of 6.3 percent. However, this comparatively high exponent is probably due to the accidental and random series of low lying 500°F level data points that can be found in the main plot of Figure 9d at  $Re_b$  of about 8000 and 10,000. That this result is an unreal representation of actual fact is evidenced by the fact that the extrapolated intercept  $\underline{a}$  for the "best free fit" case falls below McAdams value of 0.023, which is really a lower bound to all the values that  $\underline{a}$  should assume at any point in the tube. Hence, the value of 0.005 of the exponent for  $\underline{a}$  fixed at the literature value of 0.023 must be a better indication of the true temperature level dependence of the bulk Nusselt number at  $L/D = 10$ .

The next largest absolute value of  $\underline{m}$  for either the "best free fit" or "fixed intercept" case was 0.027. Such a value merely predicts that  $Nu_b$  at  $T_b/T_s = 4$  will deviate by about 3 percent from the value obtained at  $T_b/T_s = 1$ . This variation of 3 percent is less than half the standard deviation for any of the stations and also much lower than the lowest local mean deviation of the data correlated by assuming no temperature effect. Furthermore, for two of the measuring stations,  $\underline{m}$  for the "best free fit" case was slightly positive and for two stations it was slightly negative, thus showing the randomness of the slight temperature variation and indicating that the true effect must be in the neighborhood of zero. With the present scatter of data, under absolutely no circumstances can the minimally different values of  $\underline{m}$  obtained for

each of the measuring stations be construed as an indication that a longitudinal variation of the effect of temperature level on the bulk Nusselt number actually exists. Because of all the above reasons for assuming that the true value of  $\underline{m}$  for all stations must be approximately equal to zero, as well as because of the all important fact that the standard deviations for all the three types of data fits did not differ significantly, the simplest form of correlation, namely the one in which the parameter  $T_b/T_s$  is depressed completely, i.e., equation (51), was chosen to correlate the data for all stations.

In the foregoing discussion, even though it was shown that temperature level had a negligible effect on heat transfer when the correlations were referred to the bulk temperature, it was tacitly assumed that if any adjustment for temperature level had been necessary, it could have been represented by a function of the form  $(T_b/T_s)^m$ . That the term  $(T_b/T_s)^m$  can successfully account for the dynamic dissimilarities introduced by large temperature differences has been demonstrated by Churchill,<sup>5</sup> though for a different geometry. Also, as will be discussed in the next subsection, inclusion of the factor  $(T_b/T_s)^m$  for the case of properties referred to the surface temperature, for which case  $\underline{m}$  is appreciable, caused the correlation to extrapolate directly back to the present low temperature form for  $T_b/T_s = 1$ . This, in addition to the theoretical justification for the inclusion of such a parameter, lends credence to the implicit assumption that use of a parameter of the form  $(T_b/T_s)^m$  is valid, even though perhaps arbitrary. However, some limitations to the applicability of the factor  $T_b/T_s$  do exist, and these will be analyzed in the next subsection.

Considering all the factors which can cause a scatter of the data, as discussed in a previous section, the mean deviations of the actual data points from the proposed correlations is very small, and the agreement between these proposed correlations and the previously obtained ones for low temperatures is remarkable. This provides further proof that no additional parameter need be included to account for the extreme ranges of temperature attained in this study if the properties are referred to  $T_b$ . Since these experiments also show that there is no significant variation of the effect of temperature level down the length of the tube, a wide sweeping generalization can be made, namely: all the data obtained at low temperatures for the variation of local heat transfer coefficients down the length of the tube can be applied to high temperature levels if these are reduced to dimensionless correlations with properties referred to the bulk temperature. The same applies to all low temperature correlations which have been obtained for average coefficients. Hence this knowledge permits extremely accurate measurements for later high temperature application to be made at low temperatures where equipment and temperature measurement difficulties are less severe and more accurate experimental methods can be devised. Then, these results can confidently be utilized for the high temperature applications.

Inspection of the main plots in Figures 9a - d will show that a line of 0.8 slope does represent the trend of the data points extremely well, and therefore confirms the initial assumption, based on extensive prior work in the field of heat transfer, that the Reynolds number exponent may be taken as 0.8.

No attempt was made to present the experimental data for each run in terms of  $Nu_b$  or  $h_c$  profiles down the length of the tube. The reason for this will immediately become apparent. In order to show a comparison of the relative shapes these profiles would assume, and in order to compare them with the proposed invariant representation, this discussion will be made for "normalized" profiles. In the normalized form, each locally observed quantity is divided by the value of that quantity at  $L/D = 10$ , which for all practical purposes will be assumed to represent the limiting or fully developed value of the quantity in question. Such a method has been used by other investigators. Boelter, et al.,<sup>3</sup> correlated their low temperature data for variation of the average coefficient with  $L/D$  in an analogous form, and Deissler<sup>9</sup> represented the case where constant properties are assumed in the form of  $Nu/Nu_{\text{fully developed}}$  versus  $L/D$ . However, it will be shown that the only valid, generalized form of such a normalized presentation of data that retains its shape even under the presence of severe temperature gradients along the axis of the tube, as are encountered in high temperature work, is the group  $(Nu_b/Re_b^{0.8})/(Nu_b/Re_b^{0.8})_{10}$ . A hypothetical sketch is presented in Figure 13 which shows the variation of these quantities down the length of the tube for some given bulk temperature drop between the inlet and exit of the tube.

For the case where there are no axial temperature gradients, curves A, B, and C will all coincide. Absence of a temperature gradient is of course impossible if heat is transferred, but this case can theoretically be approached as a limit at high flow rates and small temperature differences across the film. For the case of heat extraction, as the temperature gradient increases, the curves will separate, curve A rising

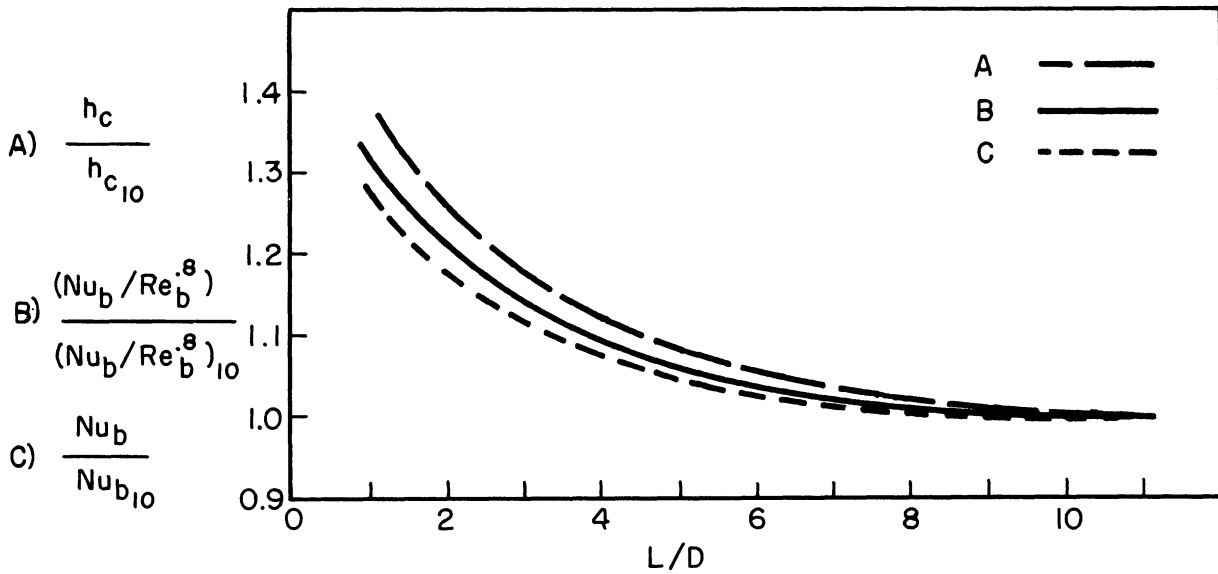


Figure 13. Sketch of Normalized Heat Transfer Rate Profiles in Inlet Region for Various Methods of Correlation

up, curve C flattening out, and only curve B remaining invariant under all conditions. That the shape of curve B should be invariant for all temperature levels can easily be derived, and is a direct consequence of the experimental result that temperature level has no effect on the proposed correlations at any and all distances down the tube. Since a correlation of the form  $Nu_b = a Re_b^{0.8} Pr_b^{1/3}$  accurately represents the data for the whole range of temperatures encountered in this study, where  $a$  is a constant whose magnitude is a function of  $L/D$ , then under the assumption of the constancy of  $Pr_b^{1/3}$ ,  $(Nu_b/Re_b^{0.8})/(Nu_b/Re_b^{0.8})_{10} = a/a_{10}$ . This latter group is a function of  $L/D$  only and hence is completely independent of temperature level and temperature gradients. In the back-calculation of  $h_c$  and  $Nu_b$  profiles by this method, the variation in fluid properties is accounted for by evaluating the properties at the local bulk temperature extant at the value of  $L/D$  in question.



Since curve B is known to be invariant, it is now easy to show that for heat extraction, curve A must always lie above it and curve C below. By a simple rearrangement of terms, it can be shown that  $(Nu_b/Nu_{b_{10}}) = (a/a_{10}) (Re_{b_{10}}/Re_b)^{0.8}$  and  $(h_c/h_{c_{10}}) = (a/a_{10})(Re_{b_{10}}/Re_b)^{0.8} (k_b/k_{b_{10}})$ , where  $(a/a_{10})$  is known to be invariant. Due to the fact that for gases, viscosity increases with temperature, the term  $(Re_{b_{10}}/Re_b)^{0.8}$  must always be less than unity so that  $(Nu_b/Nu_{b_{10}})$  must always lie below curve B. Since thermal conductivity also increases with temperature, and also because this function of temperature is much greater than the temperature dependence of the viscosity, the term  $(k_b/k_{b_{10}})$ , besides always being greater than unity, will also always be greater than the reciprocal of  $(Re_{b_{10}}/Re_b)^{0.8}$ , and hence will always cause the variation of  $(h_c/h_{c_{10}})$  to be steeper than the invariant case. The amount of deviation of these curves from the invariant one is a function of the temperature gradient, which is itself a function of the flow rate and the temperature difference across the film.

Because it is predominantly this axial temperature variation which causes the variation of the shape of the  $h_c$  and  $Nu_b$  profiles, it is evident that if the experimental data for each run had been presented in the form mentioned above, a whole series of different profiles would have been obtained. Because of the scatter of the data, many of these individual profiles would have been somewhat erratic, thus not permitting a good estimate of what the true shape at each temperature level and flow rate should be. However, since it was known that the variation of  $a/a_{10}$  results in a single invariant curve for all temperature levels, it was easy to obtain an accurate picture of what the invariant profile is by finding the mean local value of  $\underline{a}$  for a whole series of runs, as was

done in the present correlations. These values of  $a$  should approach the true value if the scatter of the data points is random. In this manner, the data was smoothed, and could be used to predict the  $h_c$  or  $Nu_b$  profiles without the necessity of evaluating individual profiles for each run. An alternate method of presenting this data, rather than in the "normalized" form, is to just plot the locally obtained values of  $a$  as a function of  $L/D$ , since the normalized form was used in this discussion only because it afforded a method of comparing the relative shapes of the various profiles.

All the present work on the variation of local heat transfer coefficients that was obtained at near room temperatures can easily be converted into the above mentioned form, and this single curve obtained will then be applicable for all temperature levels. (Actually, a very slight change in the "invariant" profile will occur over a very great range of Reynolds numbers because of the different number of tube diameters it takes for the thermal boundary layer to become fully developed, but this variation is negligible, especially for the small range of Reynolds numbers encountered in this present experiment.) Inspection of Figure 12 will show that it actually is a plot of  $a$  versus  $L/D$ , since  $a = Nu_b / Re_b^{0.8} Pr_b^{1/3}$ . Therefore, Figure 12, whose curve was derived from Boelter, et al.<sup>3</sup> and whose points were obtained in the present study, should be applicable over the whole range of temperature levels encountered in this study if the properties are referred to the local bulk temperature.

#### Effect of Evaluating Properties at Varying Reference Temperatures

The results of the calculations at  $L/D$  of 1.5 when the properties were evaluated at the bulk, film, and surface temperatures brought some interesting facts to light. For the evaluation of the properties at

either the bulk or surface temperatures, the best fit through the data showed that by inclusion of the factor  $(T_b/T_s)^m$ , the constant a obtained for equation (49) is in very close agreement with the low temperature value of 0.0290 derived from Boelter's data. This is in itself proof that the parameter  $T_b/T_s$  can successfully account for the dynamic dissimilarities introduced by the high temperature levels when the properties are evaluated at the surface or bulk temperatures. However, the best fit through the data with properties evaluated at the film temperature yields an unnaturally high value of a of 0.0315, which means that the correlation does not extrapolate back to the known low temperature values. This fact throws doubt on the assumption that the parameter  $T_b/T_s$  is appropriate for this case. Furthermore, at the film temperature, when the best exponent for  $T_b/T_s$  was obtained for the case where a was fixed at the known literature value of 0.0290, thus assuring extrapolation of the results back to present low temperature correlations at  $T_b/T_s = 1$ , the exponent m turned out to be 0.149, a great increase over the value of 0.065 obtained for the previous case of the best free fit. In addition, the standard deviation was an unnaturally high 15 percent. It was therefore felt that there must be some explanation for this anomalous result, that the factor  $T_b/T_s$  is able to excellently account for temperature effects when the properties are evaluated at the bulk or surface temperatures, and yet fails for the film temperature. The results of the calculations with properties referred to the film temperature are graphically portrayed in Figure 9e.

The following analysis was undertaken to explain the above results and to gain further insight into the failure of the parameter  $(T_b/T_s)^m$  to act as an accurate adjustment factor in high temperature

correlations when the data is correlated at any arbitrary reference temperature between the bulk and surface temperatures. It will now be demonstrated that if the effect of temperature level is represented by a factor of the form of  $(T_b/T_s)^m$ , this factor cannot accurately account for the effect of temperature level for properties evaluated at any temperature between  $T_b$  and  $T_s$ . At best, it gives an adequate correction over only a comparatively small range of  $T_b/T_s$ . A comparison between the values of a and m predicted by this analysis for the film temperature as the reference temperature and the actual rigorously calculated values will also be made.

The derivation presented below depends on three major assumptions, all of which, however, are closely realized in actuality. These assumptions are:

1) A factor of the form  $(T_b/T_s)^m$  adequately accounts for the dynamic dissimilarities due to high temperature level effects when either the bulk or the surface temperatures are used as reference temperatures. This assumption is certainly borne out by the calculations done with the present data, and hence appears valid. (It will be shown below that if this factor gives an accurate representation of the data evaluated at  $T_b$ , a factor of the same form, only having a different exponent, is bound to accurately represent the data evaluated at  $T_s$ , and vice versa. Hence it is sufficient to know, from an evaluation of experimental data, that an accurate fit is obtained for only one of the two reference temperatures,  $T_s$  or  $T_b$ , the good fit for the other being a direct consequence.)

2) The thermal conductivity and viscosity can be adequately represented over the whole range of temperatures by a straight line on a plot of  $\ln k$  or  $\ln \mu$  versus  $T$ . This implies that these properties are

proportional to a power of the absolute temperature. This assumption is valid because the true values of  $k$  and  $\mu$  can be represented quite accurately in such a manner over the whole range of temperatures encountered in this study.

3)  $Pr^{1/3}$  is a constant for all temperatures encountered in this study, and hence its value will be the same no matter at what reference level this dimensionless group is evaluated at.

For the purposes of this analysis, the basis of comparison will be the values obtained using the bulk temperature as a reference. This choice was made because the results of this study are mainly evaluated at the bulk temperature, but this choice is only for convenience, since the surface temperature could also have been used as the primary basis of comparison.

According to assumption 1), the results at bulk temperature can, for the general case, be represented by a correlation of the form of equation (49), namely

$$\frac{Nu_b}{Pr_b^{1/3} Re_b^{0.8}} = \left[ \frac{Nu}{Pr^{1/3} Re^{0.8}} \right]_b = a_b \left( \frac{T_b}{T_s} \right)^{m_b} \quad (52)$$

where the subscript  $b$  on  $\underline{a}$  and  $\underline{m}$  denotes that these were the quantities obtained from the experimental data for properties evaluated at the bulk temperature. Now, according to assumption 2), let

$$\mu_r = \mu_b (T_r/T_b)^{\nu} \quad (53a)$$

and

$$k_r = k_b (T_r/T_b)^{\xi} \quad (53b)$$

where  $\mu_r$  and  $k_r$  are the viscosity and thermal conductivity at any given reference temperature and  $\nu$  and  $\xi$  are the powers of temperature to which  $\mu$  and  $k$  are known to vary. For air,  $\nu \cong 0.68$  and  $\xi \cong 0.85$ .

Now, the group

$$\frac{\text{Nu}}{\text{Pr}^{1/3} \text{Re}^{0.8}}$$

will be evaluated for any arbitrary reference temperature  $T_r$  in terms of

$$\left[ \frac{\text{Nu}}{\text{Pr}^{1/3} \text{Re}^{0.8}} \right]_b$$

Substitution of equations (53a) and (53b) into the group

$$\left[ \frac{\text{Nu}}{\text{Pr}^{1/3} \text{Re}^{0.8}} \right]_r$$

leads to:

$$\left[ \frac{\text{Nu}}{\text{Pr}^{1/3} \text{Re}^{0.8}} \right]_r = \frac{(hD/k_r)}{\text{Pr}^{1/3} (DG/\mu_r)^{0.8}} = \frac{(hD/k_b) (T_r/T_b)^{-\nu}}{\text{Pr}^{1/3} (DG/\mu_b)^{0.8} (T_r/T_b)^{-0.8\xi}}$$

or

$$\left[ \frac{\text{Nu}}{\text{Pr}^{1/3} \text{Re}^{0.8}} \right]_r = \left[ \frac{\text{Nu}}{\text{Pr}^{1/3} \text{Re}^{0.8}} \right]_b \left( \frac{T_r}{T_b} \right)^{0.8\xi - \nu} \quad (54)$$

Now let

$$\gamma = 0.8\xi - \nu \quad (55)$$

Then

$$\left[ \frac{\text{Nu}}{\text{Pr}^{1/3} \text{Re}^{0.8}} \right]_r = \left[ \frac{\text{Nu}}{\text{Pr}^{1/3} \text{Re}^{0.8}} \right]_b \left( \frac{T_r}{T_b} \right)^\gamma \quad (56)$$

Now, if the factor  $T_b/T_s$ , raised to some power  $\underline{m}_r$ , representing the value of that exponent for that particular reference temperature, could adequately represent the effects of temperature level for the data evaluated at the given reference temperature, the correlation would also have to be of the form of equation (49), which specifically for this case would be

$$\left[ \frac{\text{Nu}}{\text{Pr}^{1/3} \text{Re}^{0.8}} \right]_r = a_r \left( \frac{T_b}{T_s} \right)^{m_r} \quad (57)$$

In the above equation,  $\underline{a}_r$  represents the value of  $\underline{a}$  that would be obtained for the given reference temperature. Substitution of equation (56) into equation (57), and additionally substituting equation (52) into equation (56), results in

$$\left[ \frac{\text{Nu}}{\text{Pr}^{1/3} \text{Re}^{0.8}} \right]_r = \left[ \frac{\text{Nu}}{\text{Pr}^{1/3} \text{Re}^{0.8}} \right]_b \left( \frac{T_r}{T_b} \right)^\gamma = \left[ a_b \left( \frac{T_b}{T_s} \right)^{m_b} \right] \left( \frac{T_r}{T_b} \right)^\gamma = a_r \left( \frac{T_b}{T_s} \right)^{m_r}$$

or

$$a_b \left( \frac{T_b}{T_s} \right)^{m_b} \left( \frac{T_r}{T_b} \right)^\gamma = a_r \left( \frac{T_b}{T_s} \right)^{m_r} \quad (58)$$

Let

$$\left( \frac{T_r}{T_b} \right)^\gamma = \Gamma_r \quad (59)$$

so that

$$a_b \left( \frac{T_b}{T_s} \right)^{m_b} \Gamma_r = a_r \left( \frac{T_b}{T_s} \right)^{m_r} \quad (60)$$

It is evident from an inspection of equation (60) that in order for the form of the left hand side to made to fit the form of the right hand side,  $\Gamma_r$  must assume the form

$$\Gamma_r = \lambda (T_b/T_s)^\delta \quad . \quad (61)$$

Equation (61) represents a straight line on a plot of  $\ln \Gamma_r$  versus  $\ln (T_b/T_s)$ , where  $\delta$  is the slope and  $\lambda$  the intercept. Now let us investigate what the  $\Gamma_r$  function defined by equation (59) actually looks like on a plot of  $\ln \Gamma_r$  versus  $\ln (T_b/T_s)$ . In order to generalize the procedure for any reference temperature, the following relationship will be used to define an arbitrary reference temperature:

$$T_r = T_b - z (T_b - T_s) \quad (62)$$

where  $z$  ranges from 0 to 1 and  $z = 0.5$  denotes the average film temperature. Substituting the above into equation (59) and simplifying, results in

$$\Gamma_r = [(1 - z) + z/(T_b/T_s)]^\gamma \quad (63)$$

As an example,  $\Gamma_r$  will now be evaluated for the average film temperature,  $z = 0.5$ , and the tabulated values are plotted in Figure 14. The curves obtained from a series of such calculations are shown in Figure 15. From equation (55),  $\gamma$ , for air, = [ 0.8 (0.68) - 0.85 ] = -0.31. The calculated values of  $\Gamma_f$  for  $z = 0.5$  are:

$T_b/T_s$	0	1.5	2	3	4
$\Gamma_f$	1	1.058	1.093	1.133	1.157



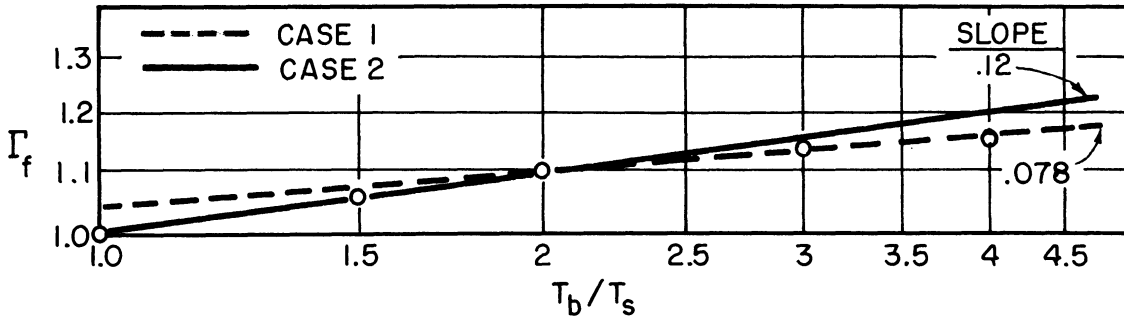


Figure 14. Plot of Reference Temperature Adjustment Function for Film Temperature

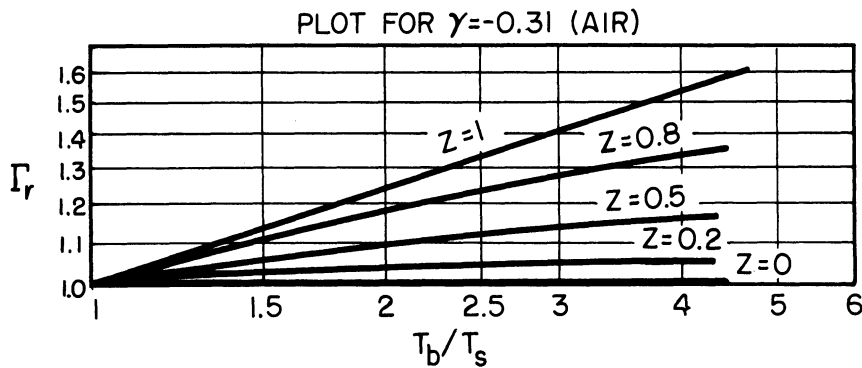


Figure 15. Diagram of Reference Temperature Adjustment Function for Various Methods of Correlation

These points, as plotted in Figure 14, will be seen to lie on a curve, and all the lines in Figure 15, except for  $z = 0$  and  $z = 1$ , are curved. In order to fit the points in Figure 14 by a straight line, as would be necessary for a solution of the type required by equation (61), it is evident that some arbitrary choice as to where to locate the best line is involved. In order to simulate the conditions of the experiment itself, where most of the data points were in the  $T_b/T_s$  range of about 1.7 to 3.5, a line through that region of the curve was drawn and is denoted by the line for Case 1. This also corresponds to the Case 1 of the treatment of the experimental results, the "best free fit" case. The "best line" in Figure 14 should of course be weighted in proportion to the location of the actual data points; however, since this is only a demonstration of how to apply this method, such rigor seems uncalled for.

For Case 1,  $\lambda = 1.04$  and  $\delta = 0.078$ . For Case 2, in which the line is forced to extrapolate to the origin, i.e.,  $\lambda = 1$ , the best fit through the points at  $T_b/T_s = 1.5, 2, \text{ and } 3$ , which closely resembles the actual data, gave a line with a slope of 0.12. Before these values can be used in predicting the constants of equation (58) for the reference temperature, equation (61), to which form these lines have been forced to fit, will be substituted into equation (60), giving,

$$a_b \left( \frac{T_b}{T_s} \right)^{m_b} \lambda \left( \frac{T_b}{T_s} \right)^{\delta} = a_r \left( \frac{T_b}{T_s} \right)^{m_r}, \quad (64)$$

from which it is evident that

$$a_r = \lambda a_b \quad (65)$$

and

$$m_r = m_b + \delta \quad (66)$$

where, it will be remembered,  $a_b$  and  $m_b$  are the experimentally determined quantities for properties evaluated at the bulk temperature. The results of this analysis for evaluation of properties at the film temperature will now be utilized in predicting what the values of  $a_r$  and  $m_r$  at the film temperature should be, and these will be compared with the actual calculated values in the table following on the next page.

It can be seen from this table how closely the results from this analysis approach the actual values. The small discrepancies in the predicted slope and intercept from the experimental values for Case 1 are easily accounted for by assuming that the line drawn for Case 1 in Figure 14 does not represent the true case and should have been weighted a little more heavily in favor of the higher values of  $T_b/T_s$ , thus reducing the slope and increasing the intercept.

	Case 1 <u>Best Free Fit</u>	Case 2 <u>Intercept Fixed</u>
$m_b$ (from data)	0.007	0.027
$a_b$	0.0295	0.0290
$\lambda$ (from Figure 14)	1.04	1.00
$\delta$	0.078	0.12
$m_f$ (predicted by equation (65))	0.085	0.147
$m_f$ (from evaluation of data at $T_f$ )	0.065	0.149
$a_f$ (predicted by equation (66))	0.0307	0.0290
$a_f$ (from evaluation of data at $T_f$ )	0.0315	0.0290

In case the instantaneous value of the  $(T_b/T_s)$  adjustment exponent  $\delta$  at any given  $T_b/T_s$  level is desired, it can be obtained from finding the value of  $d \ln \Gamma_r / d \ln (T_b/T_s)$  at the given level of  $T_b/T_s$ , which is:

$$\delta_{\text{at any given } T_b/T_s} = \left[ \frac{d \ln r}{d \ln (T_b/T_s)} \right]_{\text{at the given value of } T_b/T_s} = \frac{-z\gamma}{[(1-z)(T_b/T_s) + z]} \quad (67)$$

For the properties evaluated at the surface temperature,  $z$  in equation (62) equals unity, and hence  $\Gamma_s$  from equation (63) =  $(T_b/T_s)^{-\gamma}$ . Substituting this value into equation (60) and comparing with the form of equation (64) makes it evident that  $\delta = -\gamma$  and  $\lambda = 1$ . Hence for properties evaluated at  $T_s$ ,  $a_s = a_b$ , and  $m_s = m_b - \gamma$ . Since  $\gamma$  for air = -0.31 and  $m_b$  from the data is about 0.01,  $m_s$  should be about 0.32. This is in excellent agreement with the actually obtained value of 0.33.

It is thus seen from this analysis that the exponent on the factor  $(T_b/T_s)^m$  in equation (49) can rapidly be predicted for evaluation of the properties at either the surface or bulk temperatures once the exponent for one of the two cases has been determined experimentally. As an alternate method in obtaining the above result,  $z = 1$  can be substituted into equation (67), from which  $\delta = -\gamma$ , independent of the value of  $T_b/T_s$ . Equation (67) can also be used to predict  $\delta$  over any short range of  $T_b/T_s$  for any desired reference temperature by evaluating the equation at the midpoint of the desired  $T_b/T_s$  interval.

The case presented in Figure 14 and the curves shown in Figure 15 vividly demonstrate why the case of evaluation of the properties at any temperature between the surface and bulk temperatures cannot be adequately correlated over a wide range of temperatures by a parameter of the form  $(T_b/T_s)^m$  since this involves arbitrarily letting a straight line represent a curve. It will be seen that over any short interval of  $T_b/T_s$ , the best straight line parallel to a tangent of the midpoint of the  $T_b/T_s$  interval chosen can be drawn. This, however, will also result in a value of  $\lambda$ , the intercept, greater than unity, and thus shows why this type of approximation insures that under no circumstances will the final correlation extrapolate back to the values of  $\underline{a}$  obtained for low temperatures. Furthermore, for Case 2, where the intercept is fixed so that  $\lambda = 1$ , the best straight line drawn to approximate the  $\Gamma_r$  curves can never accurately account for all the data which lie on that curve. This method of linearization of a curve explains why such a great standard deviation was obtained in the original calculations for properties evaluated at  $T_f$  and the intercept fixed at the value derived from Boelter. (That the data would lie on a curve is assured by the fact that

for the present experiments, they lie in a straight line at the surface or bulk temperatures. Conversely, if the data for some different set of high temperature experiments, when plotted as  $\ln \left[ \frac{\text{Nu}}{\text{Pr}^{1/3} \text{Re}^b} \right]_b$  versus  $\ln (T_b/T_s)$ , were to lie on a curve whose slope was constantly increasing, i.e., curving upward, then evaluation of the properties at some film temperature and use of an adjustment factor of  $(T_b/T_s)^m$  would actually improve the correlation since this procedure will tend to straighten out the curve.)

Inspection of Figure 15 shows that the accuracy of the fit for a linearization of the curves improves as  $z$  approaches the limits of  $z = 0$  and  $z = 1$ , the fit being worst for intermediate values. It will also be seen that no serious errors are engendered over the whole range of film temperatures if a straight line relationship is assumed to hold for  $1 < (T_b/T_s) < 2$ , and that the fit would progressively get worse the larger a range of  $T_b/T_s$  was to be encompassed by the linearization. The method outlined above, however, has one distinct advantage that, if, for some reason, the values of  $\underline{a}$  and  $\underline{m}$  for a comparatively small range of  $T_b/T_s$  are desired for any other reference temperature than the one at which the data has been evaluated, or if it is desired to re-correlate some other researcher's data at a new reference temperature, the new constants can rapidly be estimated. Hence, data points need not be individually re-evaluated at the new reference temperature and the method of least mean squares applied to the re-evaluated data.

It thus has been shown why it is not good practice to apply a factor of the form  $(T_b/T_s)^m$  in order to account for temperature level if the properties are referred to any arbitrary reference temperature between  $T_b$  and  $T_s$ . By mere virtue of the fact that this parameter can

excellently account for the dynamic dissimilarities caused by high temperature differences across the film when applied to the case of properties evaluated at  $T_b$  or  $T_s$  causes it to be inadequate in representing data evaluated at other reference temperatures. It also has been shown that if the value of  $\underline{m}$  is known for either the properties referred to  $T_b$  or  $T_s$ , the value of  $\underline{m}$  at the other reference temperature can rapidly be estimated by knowing the exponents on the variation of  $\mu$  and  $k$  with temperature. The agreement between the values predicted by this analysis for the film and surface temperatures and those actually obtained is excellent and hence is an added validation for the correctness of the method of analysis used and the assumptions which were made.

This analysis also indicates that use of the surface temperature gives just as valid and accurate a correlation as the one in which the properties are referred to the bulk temperature; however, since the bulk temperature is a much easier variable to ascertain because it is usually explicitly available, and, as has been shown before, use of the bulk temperature makes the temperature dependence of the correlations negligible, it seems much more convenient to use the bulk temperature as the reference temperature.

#### Comparisons with Prior Work

One of the most important aspects of this study is that it embraces the results of all the previous work in both high and low temperature heat transfer from a hot gas stream inside circular tubes. It is an extension into a higher temperature range than has ever been studied experimentally for the case of heat extraction, and agreement between the results of this work and that of other investigators, wherever the experimental ranges overlap, is excellent.

The results of this experimental study corroborate those of the few high temperature cooling runs of Humble, et al.,<sup>16</sup> who also found that by referring their correlations to the bulk temperature, no significant effect of temperature level could be noted. This present work, though, not only extends by 1000°F the known range of validity of this fact, but also demonstrates that it is not only the average effect of temperature level over the whole tube that is negligible but also the local effect at all distances down the tube.

Since Humble, et al.'s work is mainly for heat addition, where  $T_b/T_s < 1$ , and these investigators have reported the quantitative effect of  $T_b/T_s$ , i.e., the exponent necessary, for obtaining the best correlation when properties are referred to the bulk, film, and surface temperatures, it is interesting to compare these results with those obtained in this present work for heat extraction. An overall picture of the relative effects of heating and cooling can be obtained by considering both the heat extraction and the heat addition results obtained in these two reports as a single function of  $T_b/T_s$  over a range of  $T_b/T_s$  values that covers both heating and cooling. In this manner, the effect of temperature level for the whole spectrum of  $T_b/T_s$  values from those below unity to those above unity can be observed. Figure 16 is exactly such a presentation, where Humble's results have been spliced onto the present results to give a complete picture of the whole  $T_b/T_s$  continuum.

It is apparent from the way Humble, et al. reported their results that they fixed the intercept at McAdams value of 0.023 for  $T_b/T_s = 1$ , and then only determined the best slope of the line that would fit their data evaluated at the particular reference temperature. This is exactly the same as the "fixed intercept" case used in this present

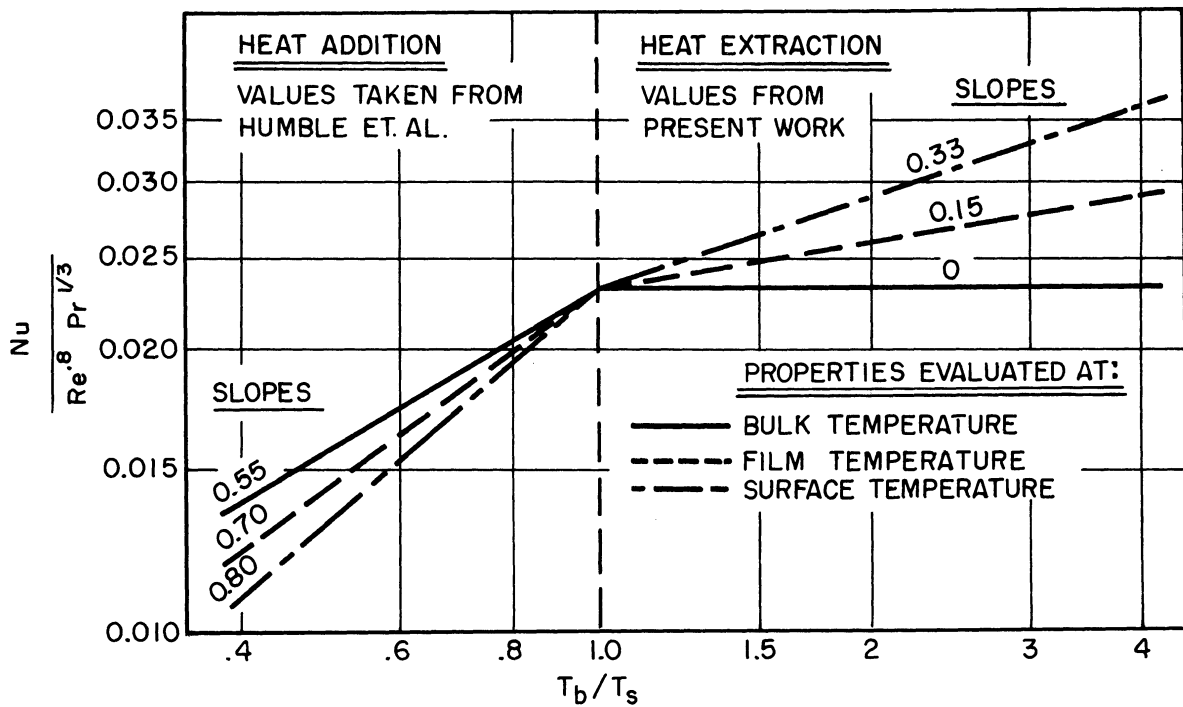


Figure 16. Effect of Temperature Level for Heating and Cooling

work, and so the comparisons in Figure 16 have all been made on this basis. From the present work, only the values from the measuring station at  $L/D = 1.5$  have been calculated for the film and surface temperature case, but since it has been shown that the variation in effect of temperature level is negligible down the length of the tube, these results have been transposed to a distance down the tube where  $a$  is equal to 0.023. This was done so that a direct comparison between this work and Humble's may be made and so that a single point will represent  $T_b/T_s = 1$  for both the present and Humble's work. (Actually, from this present work, the slope of the line for the properties referred to the bulk temperature averages about 0.01 for the "fixed intercept" case, but since this has been assumed negligible in other sections of this report, a line of zero slope has been drawn in to represent this case.)



Inspection of Figure 16 indicates that there is a sharp discontinuity of the effect of  $T_b/T_s$  at  $T_b/T_s = 1$  for all reference temperatures, and that the change in slope of the lines for all cases is approximately the same. The diagram also vividly illustrates why any single procedure for evaluating "average" properties for a proposed correlation is bound to fail to represent both the case of high temperature heating and high temperature cooling since the discontinuity of the effects is so marked. It is interesting to speculate if the effects of temperature level actually don't fall on a somewhat smoother curve, at least in the neighborhood of  $T_b/T_s = 1$ , since the author feels that the transition from heating to cooling should not be as discontinuous as Figure 16 would seem to indicate.

It was shown in the previous sub-section that use of the film temperature as a reference temperature is poor practice, providing that a good representation of the data is obtained at the bulk and surface temperatures; however, the film temperature case was also presented in Figure 16 for comparison purposes since Humble, et al. did give a value of the best slope for it. Because Humble, et al. fixed their intercept and did not show their data for the film temperature, it was impossible to check the theory whether, for heat addition also, the best fit through their data would not have given a value of  $a$ , the intercept, that differed appreciably from the fixed value. The theory presented in the last sub-section also predicts that the difference in slope between the bulk and surface temperature lines should be about 0.31 for air. This is very close to the difference obtained in the present work, but in Humble, et al.'s paper the difference is only 0.25. Since they used approximately the same values for the thermal properties as was used in the present

work, the reason for this must lie elsewhere. It leads one to suspect that possibly they only drew the best lines through their data by eye and thus misjudged, or possibly made a slight error in computing the slope, since a re-measurement of the slope of their bulk temperature line by the present author gave a slope of 0.84, in which case the difference in slopes between the bulk and surface temperature lines would be 0.29, which is much more in accord with the predicted value of 0.31.

The results of this experiment are also in excellent agreement with Nusselt's<sup>21</sup> 1930 estimate of the effect of temperature level on the heat transfer coefficient. Because the surface temperatures encountered in this study are relatively constant, especially when compared to the great variations in bulk temperature, the temperature dependence of the group  $Nu_s/Re_s^{0.8}$  should approximately be equal to the temperature dependence of  $h_c/G^{0.8}$ . For properties evaluated at the surface temperature,  $Nu/Re^{0.8}$  was found to vary as  $(T_b/T_s)^{0.33}$ . This result is, for all practical intents and purposes, exactly equal to Nusselt's prediction that  $h_c \propto (T_b/T_s)^{1/3}$ .

As mentioned in the review of prior work, Deissler<sup>9</sup> made a theoretical analysis on the variation of Nusselt number with temperature level, both for heat addition and extraction. (Actually, his results are expressed in terms of a parameter that is a function of the flux, wall temperature, and shear stress at the wall, but from which it is possible to determine the temperature level.) Deissler's result for heat extraction was that at a  $T_b/T_s$  of about 2.5, the bulk Nusselt number should be about 20 percent higher than the Nusselt number at  $T_b/T_s = 1$ ; however, in his theoretical analysis, Deissler, on the basis of his assumptions, was forced to use a thermal conductivity that was proportional to the

to the 0.68 power of the absolute temperature rather than the 0.85 power to which power the values reported in the literature actually vary. In order to check Deissler's analysis, the bulk Nusselt numbers at  $L/D = 7$  were completely re-evaluated in accordance with Deissler's assumption of the variation of  $k$ , and a least mean square fit of the "fixed intercept" case gave the result that  $Nu_b \propto (T_b/T_s)^{0.2}$ . At a  $T_b/T_s$  level of 2.5, since  $(2.5)^{0.2} = 1.202$ , an increase of approximately 20 percent is to be expected in the bulk Nusselt number on the basis of the re-evaluated data. This is in exact agreement with Deissler's prediction, and also points out what erroneous results were obtained by Deissler's analysis since by using the actual thermal conductivity data, no appreciable effect of temperature level on the bulk Nusselt number was observed in the present set of experiments. However, the result of this re-evaluation of data does show that, within the limitation of his assumptions, Deissler's analysis is absolutely correct.

As far as the shape of the profiles of the heat transfer coefficients in the inlet section of a tube are concerned, excellent agreement with Boelter, et al.'s<sup>3</sup> results for a flat velocity profile inlet condition was obtained. The comparison between the results of this study and Boelter's work was made on the basis the variation of the dimensionless group  $(Nu_b/Re_b^{0.8} Pr_b^{1/3})$  with  $L/D$ , Boelter's data also having been converted into this form. The reason for this, as was explained a few pages back, was that this particular profile will not be affected by the temperature variations along the axis of the tube. The comparison between the data obtained in this work and Boelter's profile may be found in Figure 12. It will be noticed that the mean values of the present data for each measuring station indicate a minutely steeper

variation in the shape of the curve than that obtained by Boelter, et al.; however, in every case, Boelter's curve still passes through the limits of probable error of the points in question, thus indicating that no final conclusion can be justified as to whose data represents the profile better. Furthermore, since the mean values shown in Figure 12 are a function of the thermocouple locations, and uncertainties in thermocouple location can possibly cause a  $\pm 3$  percent shift in the location of the indicated mean data points, the discrepancy between Boelter's curve and the points at  $L/D = 1.5$  and  $L/D = 4$ , which lie slightly above it, could easily be accounted for by an error in the estimation of thermocouple locations. Notwithstanding the fact that a slight error due to thermocouple location may exist, the results obtained are in excellent agreement with Boelter, et al. and indicate that Boelter, et al.'s data, if converted into the suggested form, will be applicable over the whole range of temperatures encountered in this study.

## CONCLUSIONS

The following conclusions can be drawn from this investigation of convective heat transfer from an air stream inside a circular tube, in which the inlet air temperatures varied from 480° to 2000°F over an  $Re_b$  range of 4,800 to 22,000, and the inside tube surface was kept at about 100°F:

1) Existing correlations based upon experiments with small temperature differences can adequately represent the data for large temperature differences if the thermal properties in the correlations are referred to the bulk temperature; this bulk temperature is to be taken as the local bulk temperature in correlations for the evaluation of local coefficients and the average bulk temperature should be used in correlations for the average heat transfer coefficients.

2) The effect of temperature level does not vary with distance down the tube.

3) Existing correlations can also adequately represent the present data for high temperature heat extraction if the properties are referred to the surface temperature and an additional factor  $(T_b/T_s)^{0.33}$  is included in the correlations to account for the effects of temperature level; however, a factor of the form  $(T_b/T_s)^m$  can never successfully account for the effects of temperature level in the correlations if the properties are referred to the film temperature.

APPENDIX A

ORIGINAL AND PROCESSED DATA

TABLE Ia. SUMMARY OF ORIGINAL AND PROCESSED DATA FOR L/D = 1.5

Run No.	$t_b$ (°F)	$t_s$ (°F)	$T_b/T_s$	$\mu_b$ $\frac{lb}{ft\ hr}$	$k_b$ $\frac{Btu}{hr\ ft\ ^\circ F}$	$c_{p,b}$ $\frac{Btu}{lb\ ^\circ F}$	$Re_b$	$h_c$ $\frac{Btu}{hr\ ft^2\ ^\circ F}$	$Nu_b$ original	$Nu_b^a$ comp.	$\% \text{ Dev.}^b$
1	496	77	1.78	.0669	.0251	.247	5,220	6.58	21.9	24.7	11.3
2	494	74	1.78	.0668	.0250	.247	7,520	9.55	31.8	33.1	6.9
3	496	76	1.80	.0669	.0251	.247	9,550	11.51	38.4	40.0	4.0
4	501	81	1.78	.0670	.0251	.248	11,430	14.55	48.3	46.3	4.3
5	499	83	1.76	.0669	.0250	.248	14,400	16.73	55.7	55.2	0.9
6	491	79	1.77	.0666	.0249	.247	9,620	13.25	43.9	40.3	8.9
7	494	75	1.78	.0668	.0250	.247	7,520	9.98	33.2	33.2	0.0
8	502	82	1.78	.0670	.0251	.248	14,200	16.50	54.8	54.4	0.7
9	993	89	2.64	.0891	.0358	.263	4,630	9.32	21.7	22.2	2.4
10	989	100	2.58	.0890	.0357	.263	7,430	13.62	31.8	32.6	2.4
14	989	102	2.58	.0890	.0357	.263	7,390	14.18	33.1	32.3	2.5
24	503	86	1.76	.0671	.0252	.248	11,340	13.03	43.2	46.0	6.0
25	483	98	1.70	.0664	.0247	.247	22,200	24.1	81.2	78.7	3.2
26	997	95	2.62	.0892	.0359	.263	4,700	9.28	21.6	22.3	3.1
28	998	148	2.40	.0893	.0359	.263	20,100	31.2	73.1	73.6	0.7
29	1948	149	3.95	.1217	.0528	.285	4,780	13.77	21.7	22.8	5.0
30	1957	173	3.82	.1220	.0530	.285	6,800	18.51	29.1	30.5	4.6
31	1000	125	2.49	.0894	.0360	.263	11,900	20.8	48.2	46.4	3.8
32	997	134	2.45	.0892	.0359	.263	13,800	25.0	57.9	54.6	6.0
34	1464	192	2.94	.1063	.0451	.276	14,150	30.4	56.2	55.0	1.4
35	1457	174	3.03	.1061	.0450	.276	11,300	26.4	48.9	46.3	5.6
36	1454	125	3.27	.1060	.0449	.276	4,520	12.75	23.6	22.1	6.8
38	994	118	2.52	.0891	.0358	.263	9,500	18.12	42.4	40.0	6.0
39	1456	158	3.10	.1061	.0449	.276	9,450	21.05	39.0	39.8	2.0
40	1848	167	3.68	.1187	.0514	.284	6,250	17.55	28.4	28.1	1.1
41	1859	193	3.55	.1190	.0516	.284	8,520	23.0	37.1	36.4	1.9
43	1855	208	3.46	.1189	.0515	.284	10,900	25.8	41.8	44.6	6.3
44	497	80	1.77	.0669	.0250	.247	7,350	10.18	33.8	32.4	4.3
46	979	108	2.53	.0886	.0355	.263	7,500	14.30	33.5	33.0	1.5
48	1491	150	3.14	.1059	.0448	.276	7,570	19.40	36.0	33.2	8.4
											4.1%
											Mean

<sup>a</sup> Computed from equation (51) using  $a = 0.0295$ .

<sup>b</sup> Percent Dev. =  $\frac{(|Nu_{orig} - Nu_{comp}|)}{Nu_{comp}} (100)$ .

TABLE Ib. SUMMARY OF ORIGINAL AND PROCESSED DATA FOR L/D = 4

Run No.	$t_b$ (°F)	$t_s$ (°F)	$T_b/T_s$	$\mu_b$ $\frac{lb}{ft\ hr}$	$k_b$ $\frac{Btu}{hr\ ft\ ^\circ F}$	$c_{p_b}$ $\frac{Btu}{lb\ ^\circ F}$	$Re_b$	$h_c$ $\frac{Btu}{hr\ ft^2\ ^\circ F}$	$Nu_b$ original	$Nu_b^a$ comp.	$\% \text{ Dev.}^b$
1	478	78	1.74	.0662	.0246	.247	5,260	7.03	23.7	21.3	11.2
2	482	73	1.77	.0666	.0247	.247	7,560	8.13	27.4	28.6	4.2
3	484	74	1.77	.0667	.0248	.247	9,630	9.47	31.8	34.6	8.1
4	489	78	1.76	.0668	.0249	.247	11,500	10.90	36.6	39.7	7.8
5	488	81	1.75	.0668	.0248	.247	14,500	13.80	46.4	48.0	3.3
6	478	76	1.75	.0662	.0246	.247	9,680	10.93	37.0	34.8	6.3
7	479	72	1.76	.0663	.0247	.247	7,570	8.18	27.6	28.6	3.5
8	491	82	1.75	.0669	.0250	.247	14,300	14.38	48.0	47.5	1.0
9	946	91	2.4	.0872	.0348	.262	4,720	10.00	23.9	19.6	16.8
10	957	100	2.53	.0877	.0350	.262	7,530	13.18	31.4	28.5	10.5
14	960	97	2.54	.0878	.0352	.262	7,480	11.75	27.8	28.1	1.1
24	472	86	1.70	.0661	.0247	.246	11,430	12.98	43.6	39.7	8.9
25	472	98	1.67	.0661	.0247	.246	22,400	22.8	77.5	68.4	13.3
26	960	95	2.56	.0878	.0352	.262	4,780	9.40	22.2	19.8	15.1
28	977	149	2.36	.0885	.0355	.262	20,150	27.9	65.5	62.6	4.6
29	1868	133	3.92	.1193	.0517	.284	4,880	11.10	17.9	20.0	10.5
30*	1904	147	3.89	.1203	.0522	.284	6,900	13.16	21.0	27.0	(22.2)
31	975	108	2.52	.0884	.0355	.262	11,500	16.15	37.8	39.6	4.5
32	976	115	2.51	.0884	.0356	.262	13,850	18.42	43.1	46.5	7.1
34	1423	167	3.05	.1048	.0443	.275	14,600	23.8	44.8	48.2	7.0
35	1413	146	3.04	.1045	.0440	.275	11,450	20.6	39.0	39.1	0.2
36	1393	109	3.26	.1038	.0438	.274	4,620	10.48	19.9	18.9	5.2
38	957	113	2.47	.0877	.0350	.262	9,550	15.30	36.3	34.6	4.9
39	1401	146	3.07	.1042	.0440	.274	9,640	18.08	34.2	34.8	1.7
40	1773	150	3.66	.1165	.0502	.283	6,370	15.30	25.4	25.1	1.2
41	1794	176	3.54	.1172	.0506	.283	8,650	19.51	32.1	32.1	0.0
43	1779	183	3.49	.1166	.0503	.283	11,100	21.6	35.8	38.8	7.7
44	477	77	1.74	.0662	.0246	.247	7,430	7.85	26.6	28.4	6.3
46	940	100	2.50	.0870	.0347	.262	7,650	11.33	27.2	28.8	5.5
48	1383	139	3.08	.1035	.0436	.274	7,730	16.40	31.3	29.3	6.8
23**	464	69	1.78	.0658	.0242	.246	5,140	5.60	19.30	20.8	7.2
											6.4% Mean

<sup>a</sup> Computed from equation (51) using  $a = 0.0257$ .

<sup>b</sup> Percent Dev. = 
$$\frac{(| Nu_{orig} - Nu_{comp} |)}{Nu_{comp}} (100)$$

\* Error suspected - Not included in correlations.

\*\*Additional point taken at L/D = 4 only.

TABLE Ic. SUMMARY OF ORIGINAL AND PROCESSED DATA FOR L/D = 7

Run No.	$t_b$ (°F)	$t_s$ (°F)	$T_b/T_s$	$\mu_b$ $\frac{lb}{ft\ hr}$	$k_b$ $\frac{Btu}{hr\ ft\ ^\circ F}$	$c_{p_t}$ $\frac{Btu}{lb\ ^\circ F}$	$Re_b$	$h_c$ $\frac{Btu}{hr\ ft^2\ ^\circ F}$	$Nu_b$ original	$Nu_b^a$ comp.	$\%^b$ Dev.
1	457	76	1.71	.0653	.0238	.246	5,330	5.60	19.4	19.9	2.5
2	468	73	1.74	.0660	.0244	.246	7,640	7.45	25.6	26.6	3.7
3	472	75	1.74	.0662	.0245	.246	9,700	8.70	29.7	32.0	7.2
4	474	78	1.73	.0662	.0245	.247	11,610	9.86	33.6	36.7	8.4
5	474	85	1.71	.0662	.0245	.247	14,610	14.60	49.6	44.4	11.7
6	462	76	1.72	.0656	.0243	.246	9,770	9.26	31.7	32.2	1.5
7	462	74	1.73	.0656	.0243	.246	7,670	8.00	27.4	26.7	2.6
8	477	83	1.72	.0663	.0246	.247	14,410	12.88	44.4	44.0	0.9
9	896	92	2.26	.0851	.0337	.260	4,840	8.08	20.0	18.5	8.1
10	918	100	2.46	.0861	.0342	.260	7,680	10.82	26.3	26.7	1.5
14	926	100	2.48	.0864	.0344	.261	7,600	11.12	26.8	26.5	1.2
24	459	88	1.67	.0655	.0243	.246	11,530	12.63	44.3	36.7	20.6
25	459	104	1.61	.0655	.0243	.246	22,500	19.50	66.5	63.0	5.5
26*	916	88	2.51	.0860	.0342	.260	4,880	5.96	14.52	18.50	(21.7)
28	934	132	2.36	.0868	.0346	.261	20,300	23.8	58.7	57.8	1.5
29	1772	133	3.76	.1165	.0502	.282	5,000	9.95	16.5	18.8	12.3
30	1840	161	3.70	.1185	.0513	.283	7,000	13.60	22.1	24.6	10.1
31	946	114	2.45	.0872	.0348	.261	11,650	15.10	36.2	36.5	0.8
32	946	118	2.43	.0872	.0348	.261	14,000	18.35	43.8	43.2	1.4
34	1373	188	2.82	.1031	.0434	.273	14,800	24.6	47.2	45.1	4.6
35	1361	163	2.97	.1027	.0432	.273	11,780	19.32	37.3	37.1	0.5
36	1319	112	3.10	.1013	.0425	.272	4,730	9.26	18.1	18.0	0.6
38	913	108	2.43	.0858	.0342	.260	9,800	13.45	32.7	32.1	1.9
39	1334	135	3.02	.1017	.0427	.272	9,700	16.00	31.3	31.9	2.5
40	1683	152	3.48	.1135	.0487	.281	6,640	14.00	23.9	23.5	1.7
41	1715	180	3.37	.1146	.0493	.281	8,850	17.50	29.5	29.7	0.7
43	1709	202	3.27	.1143	.0491	.281	11,320	23.2	39.3	36.4	8.0
44	452	78	1.69	.0651	.0240	.246	7,540	6.90	24.5	26.3	6.8
46	893	104	2.41	.0850	.0336	.260	7,830	10.13	25.1	26.6	5.6
48	1300	139	2.94	.1006	.0421	.272	7,950	14.88	29.4	27.3	7.2
4.9%											
Mean											

<sup>a</sup> Computed from equation (51) using  $a = 0.0236$ .

<sup>b</sup> Percent Dev. =  $\frac{(| Nu_{orig} - Nu_{comp} |)}{Nu_{comp}} (100)$

\* Error suspected - Not included in correlations.



TABLE Id. SUMMARY OF ORIGINAL AND PROCESSED DATA FOR L/D = 10

Run No.	$t_b$ (°F)	$t_s$ (°F)	$T_b/T_s$	$\mu_b$ lb ft hr	$k_b$ Btu hr ft °F	$c_p b$ Btu lb °F	$Re_b$	$h_c$ Btu hr ft <sup>2</sup> °F	$Nu_b$ original	$Nu_b^a$ comp.	$\%^b$ Dev.
1	435	77	1.63	.0643	.0237	.246	5,410	5.38	18.9	19.7	4.0
2	456	73	1.72	.0654	.0241	.246	7,700	6.37	22.0	26.0	15.4
3	459	76	1.71	.0655	.0242	.247	9,800	8.59	29.6	31.6	6.3
4	460	78	1.71	.0655	.0242	.247	11,700	9.58	33.0	36.2	8.8
5	460	84	1.69	.0655	.0242	.247	14,710	13.10	45.2	43.7	3.4
6	447	75	1.69	.0648	.0239	.246	9,880	8.07	28.2	31.8	11.3
7	445	72	1.70	.0646	.0238	.246	7,800	6.54	22.9	26.2	12.5
8	464	84	1.70	.0656	.0243	.247	14,500	12.67	43.5	43.3	0.5
9	845	89	2.38	.0830	.0327	.258	4,960	7.96	20.3	18.5	9.7
10	880	96	2.36	.0845	.0334	.259	7,820	9.74	24.3	26.3	7.6
14	889	104	2.35	.0850	.0337	.260	7,890	9.92	24.6	26.4	6.8
24	446	87	1.66	.0648	.0239	.246	11,660	11.55	40.0	36.2	9.5
25	440	98	1.62	.0645	.0238	.246	22,750	20.6	72.1	62.5	15.3
26	859	92	2.36	.0840	.0331	.259	4,990	7.15	18.0	18.5	2.7
28	900	140	2.18	.0852	.0340	.260	20,600	24.5	60.1	57.0	5.4
29	1676	138	3.58	.1132	.0487	.280	5,140	12.17	20.8	18.9	10.1
30	1777	147	3.68	.1167	.0503	.282	7,120	13.42	22.3	24.6	5.3
31	896	123	2.34	.0851	.0338	.260	12,120	16.45	40.7	37.7	8.0
32	901	132	2.30	.0852	.0339	.260	14,800	18.98	46.7	44.3	5.5
34	1323	187	2.76	.1014	.0426	.272	15,060	23.1	45.2	44.7	1.1
35	1308	164	2.83	.1009	.0427	.272	12,000	18.7	36.8	37.2	1.6
36	1246	110	2.99	.0986	.0412	.270	4,850	8.44	17.1	18.1	5.5
38	869	113	2.31	.0840	.0336	.259	10,180	14.15	35.1	32.6	0.8
39	1267	136	2.89	.0995	.0415	.271	10,140	15.45	31.0	32.3	4.0
40	1593	162	3.30	.1104	.0472	.279	6,870	14.50	25.6	24.0	6.7
41	1627	182	3.25	.1112	.0478	.280	9,000	18.36	32.0	31.1	2.8
43	1630	187	3.24	.1113	.0479	.280	11,600	20.4	35.5	35.6	0.3
44	426	77	1.65	.0633	.0234	.246	7,750	7.30	26.0	26.0	0.0
46	847	101	2.30	.0830	.0327	.258	8,000	10.10	25.8	27.0	4.4
48	1218	142	2.78	.0977	.0408	.270	8,180	14.90	30.3	27.5	10.2
											6.2% Mean

<sup>a</sup> Computed from equation (51) using  $a = 0.0231$ .

<sup>b</sup> Percent Dev. =  $\frac{(| Nu_{orig} - Nu_{comp} |)}{Nu_{comp}} (100)$

TABLE II. SUMMARY OF OPERATING CONDITIONS AND HEAT BALANCES

Run No.	W $\frac{\text{lb}}{\text{hr}}$	G $\frac{\text{lb}}{\text{hr ft}^2}$	Inlet Gas Temp. °F	Exit Gas Temp. °F	q from Integration of Fluxes Btu/hr	q from Water Heat Balance Btu/hr
1	22.8	4,170	507	426	566	540
2	33.0	6,030	501	448	806	840
3	42.9	7,700	501	454	930	1040
4	50.2	920	508	454	1070	1140
5	63.2	11,580	506	454	1440	1500
6	42.1	7,690	499	440	930	1040
7	33.0	6,030	502	438	792	740
8	62.5	11,320	509	458	1360	1400
9	27.0	4,940	1017	823	1830	1400
10	43.4	7,930	1008	864	2410	2420
14	43.8	8,020	1006	877	2410	2500
24	50.0	9,150	510	451	1145	1120
25	96.6	17,680	486	408	1940	1800
26	27.5	5,030	1019	853	1665	1500
28	116.9	21,400	1010	881	5380	5160
29	38.2	6,980	1996	1636	4480	3720
30	54.6	9,210	1989	1750	5480	5400
31	62.8	12,400	1018	881	3510	3600
32	82.6	15,110	1014	887	3860	3580
34	100.3	18,310	1489	1302	6950	6600
35	79.4	14,510	1483	1286	6070	5300
36	31.4	5,750	1491	1215	3160	2820
38	56.1	10,270	1016	850	3060	2720
39	67.2	12,020	1490	1239	5070	4980
40	48.6	8,870	1893	1555	6050	5520
41	66.5	12,170	1898	1604	7150	6620
43	85.0	15,520	1895	1597	7930	7820
44	32.1	5,890	510	417	775	740
46	43.6	7,970	1003	827	2330	2200
48	52.3	9,600	1493	1183	4670	4140

APPENDIX B

DATA PROCESSING

To illustrate the methods used in processing the data, the calculations for Run No. 46 will be outlined. The original and processed data for this run may be found in Tables I and II of Appendix A, and all references to the graphical calculations performed will refer to Figure 17.

Raw Data for Run No. 46

The raw data for the run and the wall temperatures measured at  $L/D = 1.5$  will be given.

$W_g = 43.6$  pounds per hour (from orifice reading).

Inlet gas temperature -  $1003^\circ\text{F}$

Exit gas temperature -  $827^\circ\text{F}$

Inlet water temperature -  $66.69^\circ\text{F}$

Exit water temperature -  $67.94^\circ\text{F}$

Water flow rate - 4 gpm

For the measuring station at  $L/D = 1.5$ , the temperatures and thermocouple locations were as follows:

<u>Temperature °F</u>	<u>Radius (mils)</u>
73.89	905
86.06	736
91.44	670

Calculation of Local Heat Transfer Coefficient and Nusselt Number

Since the procedure for all the measuring stations is analogous, only the one at  $L/D = 1.5$  will be treated in detail.

Assuming a linear relationship between the inlet and exit gas temperatures, the local bulk temperature at  $L/D = 1.5$  is:

$$t_b = 1003 - \left( \frac{1.5}{11.25} \right) (1003 - 827) = 979^\circ\text{F}$$

From the data of Keenan and Kaye,<sup>17</sup> at  $979^\circ\text{F}$ ,

$$\mu = 0.0886 \text{ lb/ft hr}$$

and

$$k = 0.0355 \text{ Btu/hr ft } ^\circ\text{F}$$

These values are also tabulated in Table I of Appendix A.

The reasons for assuming a linear relationship are discussed in the main body of the report, and a comparison between this and some other methods of obtaining the local gas temperature extant at each measuring station may be found in Figure 8.

In order to find the total flux at the surface as well as the temperatures at the inner and outer surfaces of the tube wall, the temperatures obtained for this measuring station are plotted as a function of  $\ln r$  at the top of Figure 17. (The lines for the other three measuring stations have also been drawn in to give an overall picture.) From the graph, the extrapolated outside temperature is  $74.1^\circ\text{F}$  and the inside surface temperature comes to  $108.2^\circ\text{F}$ . Hence  $(t_s - t_o) = 34.1^\circ\text{F}$ . For the wall, then, the average temperature is  $91.4^\circ$ , for which the thermal conductivity of inconel is  $9.09 \text{ Btu/hr ft } ^\circ\text{f}$ , which was obtained from a graphical working plot of the conductivity data given in Table III of Appendix D.

To find the total flux, equation (21) of the text is used.

$$(q/A)_s = \frac{k_{av}}{r_s} \frac{(t_s - t_o)}{\ln r_o/r_s} = \frac{9.09 (34.1)}{0.500(1/12) \ln(.900/.500)} = 12,650 \text{ Btu/hr ft}^2.$$

The previous equation is the total flux, from which the radiant effects still have to be subtracted. The only significant amount of radiation will come from the screens at the entrance, which are assumed to be at the gas temperature of 1003°F. The radiation from the exit screen is negligible.

Equation (33) from the text is used to compute  $F_{21}$ , the percent radiation emitted by the screens that is intercepted by the measuring station. The measuring station extends from  $L/r = 2$  to  $L/r = 4$ , and subtends an angle of 60° or 1/6 the circumference. From this, Figure 18 can be applied instead of evaluating the equation, so that

$$F_{21} = 1/6 (0.945 - 0.825) = 0.020.$$

Applying equation (34) to correct for emissivities, and knowing (from information in Perry<sup>22</sup>) that  $\epsilon_{inc.} = 0.67$  and  $\epsilon_{plat.} = 1.102$  at 1000°F, as well as that  $A_2/A_1 = 3/2$ , the average interchange factor,  $\overline{F}_{21}$  is equal to:

$$\overline{F}_{21} = \frac{1}{\frac{1}{0.020} + \left(\frac{1}{.102} - 1\right) + \frac{3}{2} \left(\frac{1}{.67} - 1\right)} = 0.0168$$

Substitution of the above into equation (35) of the text yields:

$$\begin{aligned} (q/A_1)_r &= \sigma (A_2/A_1) \overline{F}_{21} (T_{g_i}^4 - T_s^4) = 1730(3/2)(.0168) \left[ \left(\frac{1463}{1000}\right)^4 - \left(\frac{568}{1000}\right)^4 \right] \\ &= 175 \text{ Btu/hr ft}^2. \end{aligned}$$

The above obtained radiant flux is now subtracted from the total flux to give the net flux due to convection alone:

$$(q/A)_c = 12,650 - 175 = 12,475 \text{ Btu/hr ft}^2.$$

With the previous information,  $h_c$  can now be calculated.

$$h_c = \frac{(q/A)_c}{t_b - t_s} = \frac{12,475}{(979 - 108)} = 14.30 \text{ Btu/hr ft}^2 \text{ }^\circ\text{F}.$$

Since the tube diameter is 1 inch or 1/12 foot, the bulk Nusselt number is equal to

$$(h_c D/k_b) = \frac{14.30}{(12)(.0355)} = 33.5.$$

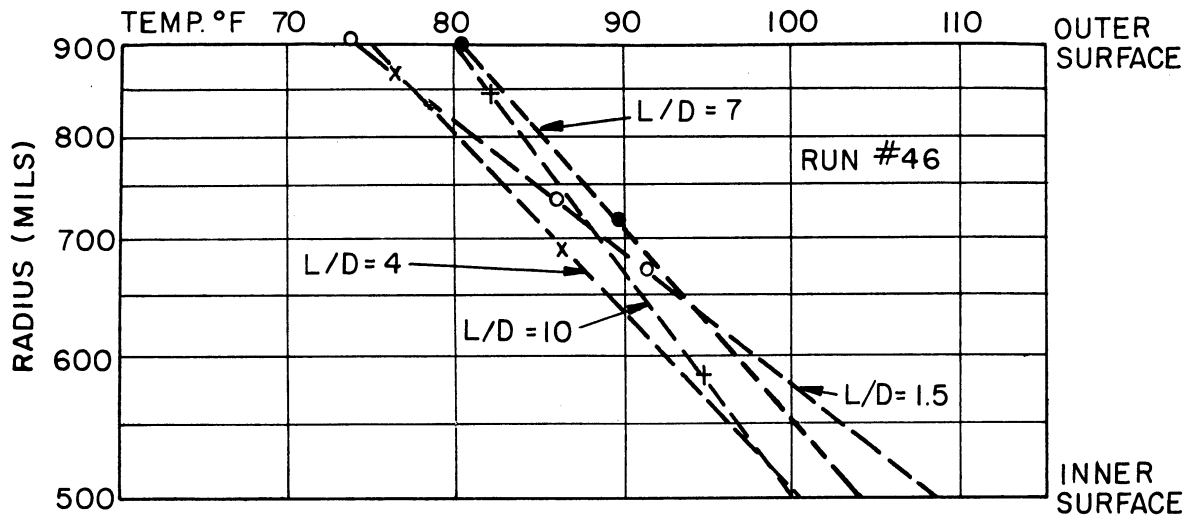
The Nusselt number evaluated for any other reference temperature is easy to obtain by merely substituting the appropriate value of the thermal conductivity into the equation.

#### Calculation of Amount of Heat Transferred

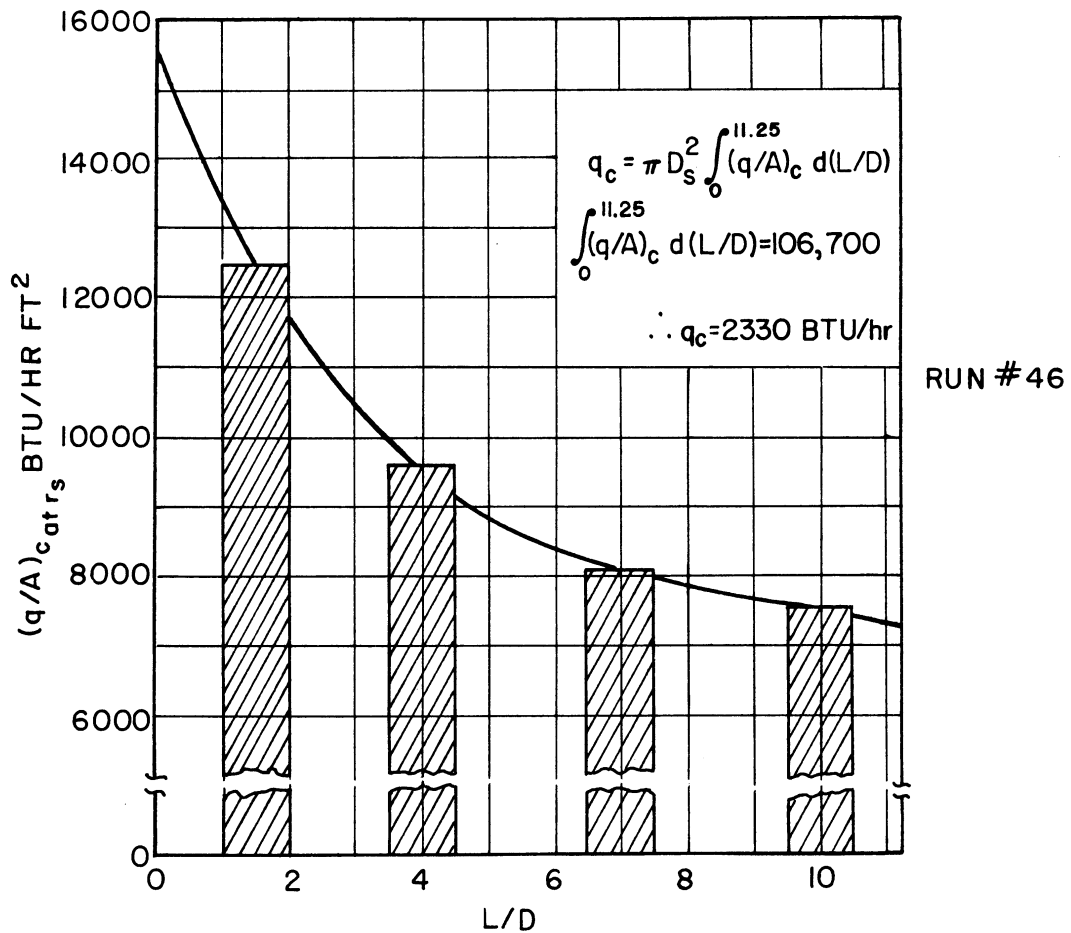
Two good checks on the amount of heat transferred are available. One is from a water side heat balance and the other is from an integration of the locally obtained fluxes over the inside of the tube. Similar calculations as the one illustrated above are used to find the local convective fluxes at the other three measuring stations. The results of these calculations are:

<u>L/D</u>	<u>Convective Flux, Btu/hr ft<sup>2</sup> °F</u>
1.5	12,475
4	9,520
7	8,040
10	7,540

The above results are plotted against L/D, which is shown at the bottom of Figure 17. The best "equal area" line is drawn through the above fluxes (which represent the average flux measured over a distance of one tube diameter), and a graphical integration was then



a) Temperature Profiles in Tube Wall



b) Integration of Fluxes to Compute Heat Transferred

Figure 17. Graphical Calculations for Run No. 46

performed. The results and method of these calculations are shown directly on Figure 17 itself, from which  $q = 2330$  Btu/hr.

The second check on the amount of heat transferred, as mentioned previously, is the water side heat balance. From the original data, the total water temperature difference, for a flow rate of 4 gpm, is  $(67.94 - 66.69) = 1.25^\circ\text{F}$ . Supplementary readings with the gas flow shut indicated that a correction of  $0.15^\circ\text{F}$  was necessary to account for the effects of conduction from the adiabatic sections and room temperature. Thus, the net water temperature difference  $\Delta t_w$  is  $(1.25 - .15) = 1.10^\circ\text{F}$ .

$$q_w = W_w c_p \Delta t_{w_{\text{net}}} = 500 \text{ (gpm)} \Delta t_{w_{\text{net}}} \text{ for a } c_p \text{ of 1.}$$

Hence,

$$q_w = 500 (4) (1.15) = 2200 \text{ Btu/hr.}$$

The above is in excellent agreement with the 2330 Btu/hr calculated from an integration of the fluxes, the deviation being only about 5 percent.

#### Calculation of Local Reynolds Number

The Reynolds number is equal to  $(DG/\mu)$ . From the data for this run,  $W = 43.6$  lbs/hr of air,  $G = W/A$ , and since the cross sectional area of the tube is  $.00545 \text{ ft}^2$ ,  $G = 7970$  lbs/hr  $\text{ft}^2$ . The bulk viscosity for the gas at  $L/D = 1.5$ , as previously indicated, is  $0.0886$  lb/ft hr, and the tube diameter equals  $1/12$  foot. Hence

$$Re_b = (1/12)(7970)/(0.0886) = 7500.$$

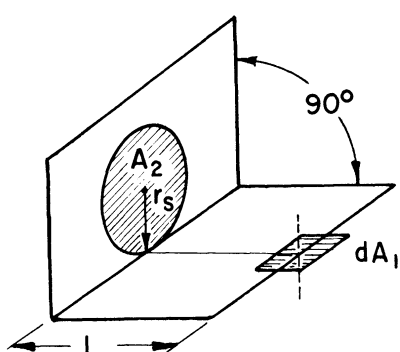


APPENDIX C

DERIVATIONS AND PROOFS

Derivation of Radiation Interchange Factor

For the configuration of a plane point source  $dA_1$  and a plane disk  $A_2$ , where the planes of  $dA_1$  and  $A_2$  intersect at right angles and the plane of  $dA_1$  is tangent to the circumference of the disk  $A_2$ , Hamilton and Morgan<sup>14</sup> give the formula



$$F_{12} = 1/2 \left[ \frac{(L/r)^2 + 2}{[(L/r)^2 + 4]^{1/2}} - (L/r) \right] \quad (68)$$

For simplification, the dummy variable  $\underline{E}$  will be used in place of  $L/r$  in the following derivations.

It will be seen that the situation above represents the present case if  $dA_1$  is assumed to lie on the inside heat transfer surface of the test unit and  $A_2$  represents the platinum screens at either end. Equation (68) would be adequate if only the point flux were desired; however, since the amount of radiation intercepted by a finite segment of the tube wall is desired, it will be necessary to invert the expression above so that it is based on  $A_2$  rather than  $dA_1$ . Since the amount of radiation exchanged must be the same, independent of the reference area used,

$$F_{12}A_1 = F_{21}A_2 \quad (69)$$

or for the present case,

$$\iint F_{12} dA_1 = F_{21} A_2 \quad (70)$$

from which

$$F_{21} = \iint \frac{F_{12} dA_1}{A_2} \quad (71)$$

Since in the present case,  $dA_1$  lies on a cylindrical surface,

$$dA_1 = r_s dL d\Theta = r_s^2 dE d\Theta \quad (72)$$

after  $dE = dL/r_s$  or  $dL = r_s dE$  has been substituted.

Since

$$A_2 = \pi r_s^2, \quad (73)$$

substitution of the above, equation (68) and equation (72) into equation (71) leads to the expression

$$F_{21} = \int_0^{2\pi} d\Theta \int_{E_1}^{E_2} \frac{1}{2\pi} \left[ \frac{E^2 + 2}{(E^2 + 4)^{1/2}} - E \right] dE \quad (74)$$

where the angular integration is carried out for the whole circumference. This makes the result more general because if the radiation is to be intercepted by only a part of the circumference, the result need only be multiplied by that fraction of the circumference that is exposed to the radiation. Integration of equation (74) leads to the result

$$F_{21} = \int_{E_1}^{E_2} \left[ \frac{E(E^2 + 4)^{1/2} - E^2}{2} \right] dE \quad (75)$$

which is to be evaluated between the limits of the measuring station in question, namely  $E_1$  and  $E_2$ . Since in the present case each measuring

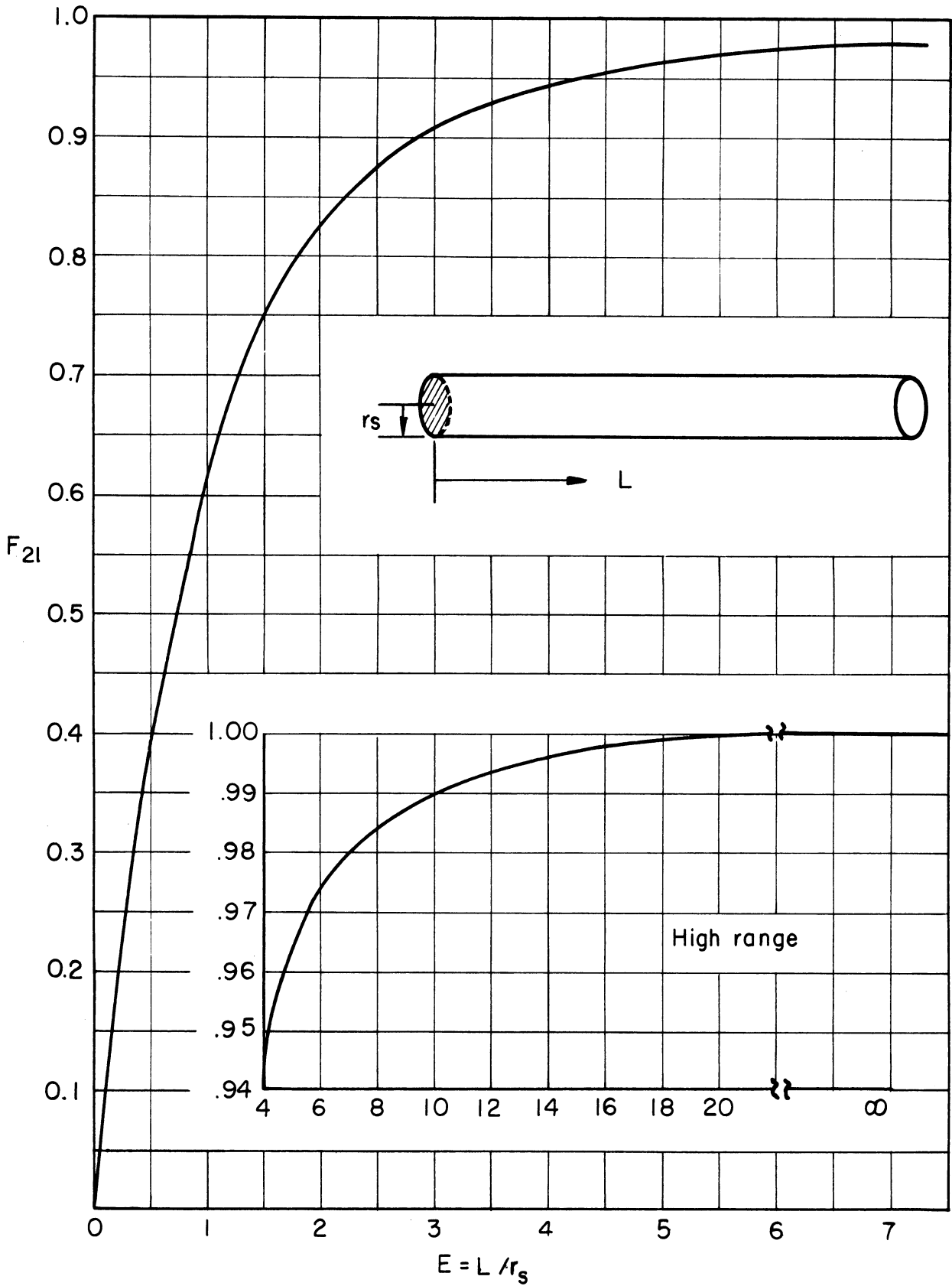


Figure 18. Geometric Interchange Factor for Radiation Emitted from the End of a Cylinder to the Cylinder Walls

station subtends an arc of only  $60^\circ$ , or  $1/6$  the circumference, the previous result must be multiplied by  $1/6$  to give equation (33) mentioned in the text. A check on the validity of the previous equation is that when it is evaluated between the limits of zero and infinity,  $F_{21}$  becomes unity, which is to be expected since all the radiation must have been intercepted.

For simplification of the calculations, a plot of  $F_{21}$  versus  $E$  (or  $L/r$ ) has been constructed by successively evaluating equation (75) between the limits of 0 and  $E$  for values of  $E$  up to 20 (which is equivalent to an  $L/D$  of 10). This is shown in Figure 17. To find the value of  $F_{21}$  between any two limits  $E_1$  and  $E_2$ , it is merely necessary to subtract the value obtained at  $E_1$  on the curve from that obtained at  $E_2$ .

Proof for Validity of Using Average Thermal Conductivity of Inconel

In the test, it has been stated that

$$(q/A)_s = \frac{k_{av} (T_o - T_s)}{r_s \ln r_o/r_s} \quad (76)$$

If  $k$  is used as a point function of temperature and this variation is assumed to be linear, then

$$(q/A)_{s_{actual}} = \frac{1}{r_s \ln r_o/r_s} \int_{T_o}^{T_s} k \, dt \quad (77)$$

where

$$k = k_i (1 + \alpha T) \quad (78)$$

Integration of equation (77) leads to

$$(q/A)_{s_{actual}} = \frac{k_i}{r_s \ln r_o/r_s} \left[ (T_s - T_o) + \frac{\alpha}{2} (T_s^2 - T_o^2) \right] \quad (79)$$

Dividing equation (76) by equation (77) yields

$$\frac{(q/A)_s}{(q/A)_{s_{\text{actual}}}} = \frac{k_{\text{av}} (T_s - T_o)}{k_i [(T_s - T_o) + 1/2 \alpha (T_s^2 - T_o^2)]} . \quad (80)$$

An evaluation of  $k_{\text{av}}$  is now required.

$$k_{\text{av}} = \frac{k_s + k_o}{2} = \frac{k_i (1 + \alpha T_s) + k_i (k + \alpha T_o)}{2} = \frac{k_i}{2} [2 + \alpha (T_s + T_o)] . \quad (81)$$

A substitution of the above value of  $k_{\text{av}}$  into equation (80), when simplified, leads to the result

$$\frac{(q/A)_s}{(q/A)_{s_{\text{actual}}}} = \frac{k_i [(T_s - T_o) + 1/2 \alpha (T_s^2 - T_o^2)]}{k_i [(T_s - T_o) + 1/2 \alpha (T_s^2 - T_o^2)]} = 1 . \quad (82)$$

Hence

$$(q/A)_s = (q/A)_{s_{\text{actual}}} \quad (83)$$

or absolutely no loss of generality has been obtained by use of  $k_{\text{av}}$  instead of integrating over point values of  $k$ .

#### Proof of the Effect of Thermocouple Holes on the Measured Flux

In the following derivation, all references will be to Figure 19. In a and b the actual situation present at each of the measuring stations is depicted.  $r_s = 500$  mils,  $r_o = 900$  mils.  $r_1$ , the radius of the bottom of the deepest hole = 530 mils, and the total angle subtended by each sector is  $\pi/6$  or  $60^\circ$ . In c, a degeneration of the sector is depicted where the worst possible location of a hole could occur, that is, a hole whose presence would affect the heat flux the greatest. This would be a hole running at a constant radius of  $r_1$ , the deepest part reached by the actual hole that is slanted towards the

bottom. The effect of this hole is so predominant that the other two are neglected for the purposes of this analysis. The proof offered below is a modification of one first used by Churchill.<sup>5</sup>

Since this is a steady state operation, the heat conduction equation in cylindrical coordinates is

$$\frac{\partial^2 T}{\partial r^2} + \frac{1}{r} \frac{\partial^2 T}{\partial \Theta^2} + \frac{\partial^2 T}{\partial Z^2} = 0 . \quad (84)$$

A harmonic transformation corresponding to the complex transformation  $W = \ln Z$ , in which case  $U = \ln r$  and  $V = \Theta$ , will be substituted into the above equation, when then becomes

$$\frac{\partial^2 T}{\partial U^2} + \frac{\partial^2 T}{\partial V^2} + \frac{\partial^2 T}{\partial Z^2} = 0 \quad (85)$$

with respect to the transformed coordinates. This harmonic transformation opens up the cylindrical element into a rectangular box as is shown in d. If this block is now rotated by 90°, it is analogous to an infinite bar whose cross section is the former r-z plane. This is shown in e, and the problem has now been reduced to a purely two dimensional one which can be attacked in normal fashion by conformed techniques. A table of some pertinent transformed values will now be given below.

	<u>r</u>	<u>U</u>
	original units	transformed units
Inside radius	500	6.22
Outside radius	900	6.80
Midpoint of hole	530	6.28
Diameter of hole	20	0.0378

Since the purpose of these manipulations is to apply a conformal transformation which will ultimately make the hole vanish and then find the solution of the heat conduction equation in this transformed plane, it will first be necessary to bring the cross section shown in f down to the u axis so that the hole is centered at the origin and to enlarge the whole cross section so that the hole is of unit radius. This is accomplished by the conformal transformation

$$W' = T (W + S) \quad , \quad (86)$$

where application of the transformed units shown in the above table shows that  $T = 26.5$  and  $S = -6.28$ . The result of this is shown in g, where the z limits have been left off since they are of little importance, as will subsequently be shown. In this enlarged version, the u limits of the cross section are 13.75 and -1.85.

In order to remove the hole, the complex transformation

$$W'' = W' + 1/W' \quad , \quad (87)$$

which collapses the unit circle into a line stretching from +2 to -2, is applied, under this transformation

$$U'' = U' \left( 1 + \frac{1}{U'^2 + Z'^2} \right) \quad (88)$$

and

$$Z'' = Z' \left( 1 - \frac{1}{U'^2 + Z'^2} \right) \quad . \quad (89)$$

Examination of the previous two equations will show that the distortion of the rectangle under the transformation of equation (87) will be such as to make the U coordinates bulge out and the Z coordinates being pinched in, the greatest amount of distortion for any one variable

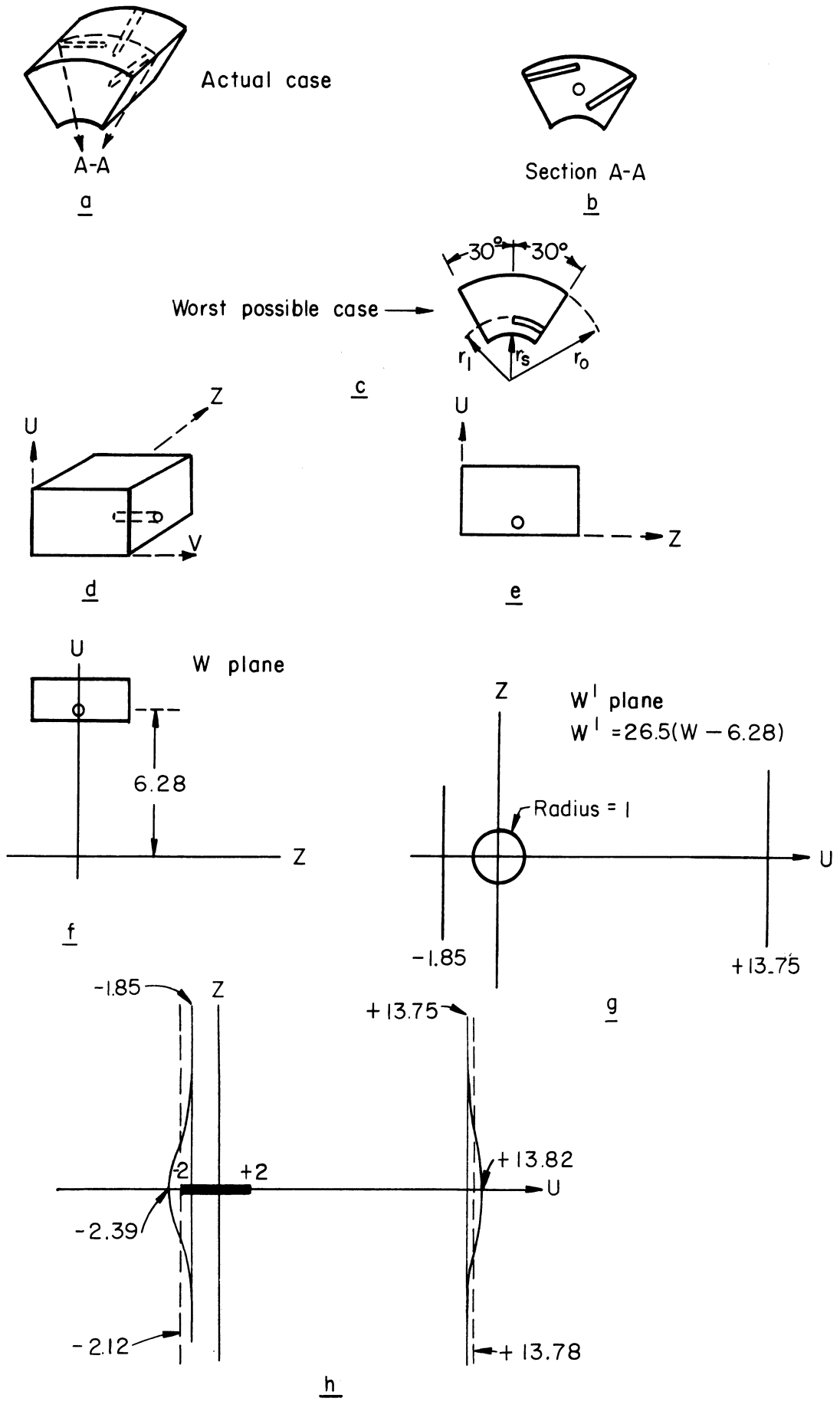


Figure 19. Illustration of Conformal Mapping Procedure



occurring when the other is equal to zero. The best rectangle will then be fit to the thus slightly distorted rectangle and a prototype solution will be set up for this new rectangle. However, the pinching in of the  $Z''$  coordinate with respect to  $Z'$  is negligible, as will be shown.

Up to now no fixed value has as yet been assigned to  $z$  since in the original harmonic transformation it was left unchanged. Originally, the  $Z$  width of the test sector was 980 mils, or 49 times the width of the original hole of 20 mils. It will now be assumed that under the first transformation, the ratio of  $Z$  to the hole size was left unchanged. Hence, after the transformation of equation (86), the relative size of  $Z$  must still remain unchanged, so that in the transformed units  $Z$  varies from 49 to -49. Substitution of this value into equation (89) for the case of  $U' = 0$  (maximum distortion), yields the result that  $Z''_{\min}/Z' = 0.999584$  which certainly justifies setting this quantity equal to unity and assuming no distortion on the  $Z'$  axis.

Substitution of  $Z' = 0$  into equation (88) gives the maximum distortion of the  $U$  lines bounding the rectangle. The maximum negative end now becomes -2.39 and the corresponding positive displacement is to 13.82. In each case these curves will rapidly approach asymptotically the previous limits of -1.85 and 13.75, respectively, so that the present figure is almost like a rectangle except that there are two slight bulges in the middle. The bulges will now be replaced by two straight lines which will be placed at the average coordinates between the bulge and the asymptote so that an approximate rectangle will have been formed. The result of all these manipulations is depicted in h. The new boundaries of the rectangle thus formed are -2.12 and 13.78.

A prototype solution in the  $W''$  plane can now be set up.

Using the simple conduction equation

$$q = \frac{k A (T_s - T_o)}{L} \quad (90)$$

and knowing that the area cross-sectional to the flow is proportional to  $Z''$ , the solution for the maximum flux in the  $W''$  plane becomes

$$q'' = 2 k Z''_{\min} (T_s - T_o) / (U''_s - U''_c). \quad (91)$$

A similar solution for the  $W'$  plane can be set up under the assumption that no hole is present (which corresponds to the assumption that is being validated in this proof). This solution becomes simply

$$q' = 2 k Z' (T_s - T_o) / (U'_s - U'_o). \quad (92)$$

Thus  $q''$  represents the heat flux taking the hole into account and  $q'$  the flux under the assumption that the hole doesn't exist. Division of equation (91) by equation (92), setting  $Z''_{\min}/Z'$  equal to unity, as demonstrated previously, and cancellation leads to

$$\frac{q_{\text{hole}}}{q_{\text{no holes}}} = \frac{(U'_s - U'_o)}{(U''_s - U''_o)}. \quad (93)$$

Substitution of the actual values into the above equation results in

$$\frac{q_{\text{hole}}}{q_{\text{no holes}}} = \frac{(13.75 + 1.85)}{(13.78 + 2.12)} = 0.982.$$

Hence the maximum error induced by discounting the holes amounts to 1.8%.

This certainly represents an absolute upper bound because the material in the hole was assumed to be a perfect non-conductor of heat ( $k = 0$ ), and the type of geometry chosen was for the worst possible case. Since

the deepest thermocouple hole slants upward and does not remain at the assumed constant low radius and the material filling the hole is not of zero thermal conductivity, the total alteration in flux due to the thermocouple holes should certainly be far below the above computed maximum error of 1.8%.

Derivation for Use of Geometric Mean Radius to Account for Effect of Separately Located Thermocouple Wires

In one case, it was found that the two wires forming the thermocouple junction had become fastened in the thermocouple hole at two different positions. In the analysis below it is assumed that the thermocouple reading produced will be that for the arithmetic mean temperature, which comes very close to the true value.

The radial temperature distribution in the test object wall is given by

$$T = C_1 \ln r + C_2 \quad . \quad (94)$$

Let the thermocouple positions be denoted by  $r_1$  and  $r_2$  and the corresponding temperatures  $T_1$  and  $T_2$  respectively. Then

$$T_1 = C_1 \ln r_1 + C_2$$

and

$$T_2 = C_1 \ln r_2 + C_2 \quad .$$

The arithmetic mean temperature  $T_{av}$  is  $\frac{T_1 + T_2}{2}$  and hence

$$T_{av} = \frac{(C_1 \ln r_1 + C_2) + (C_1 \ln r_2 + C_2)}{2} = \frac{C_1}{2} \ln r_1 r_2 + C_2 \quad . \quad (95)$$

However,  $T_{av}$  must correspond to a reading at some mean radius,  $r_m$ , or

$$T_{av} = C_1 \ln r_m + C_2 . \quad (96)$$

Equating equations (95) and (96),

$$\frac{C_1}{2} \ln r_1 r_2 + C_2 = C_1 \ln r_m + C_2$$

from which

$$r_m = \sqrt{r_1 r_2} . \quad (97)$$

APPENDIX D

PROPERTIES OF MATERIALS AND CALIBRATIONS

TABLE III. COMPOSITION AND THERMAL CONDUCTIVITY OF INCONEL

Composition	
	Percent Wt.
Nickel	77.0
Chromium	15.0
Iron	7.0
Manganese	0.25
Copper	0.2
Silicon	0.25
Carbon	0.08
Sulfur	0.007

Thermal Conductivity	
Temperature °F	k Btu/hr ft °F
32	8.87
212	9.44
392	9.92
572	10.40
752	10.89
932	11.61
1112	12.10

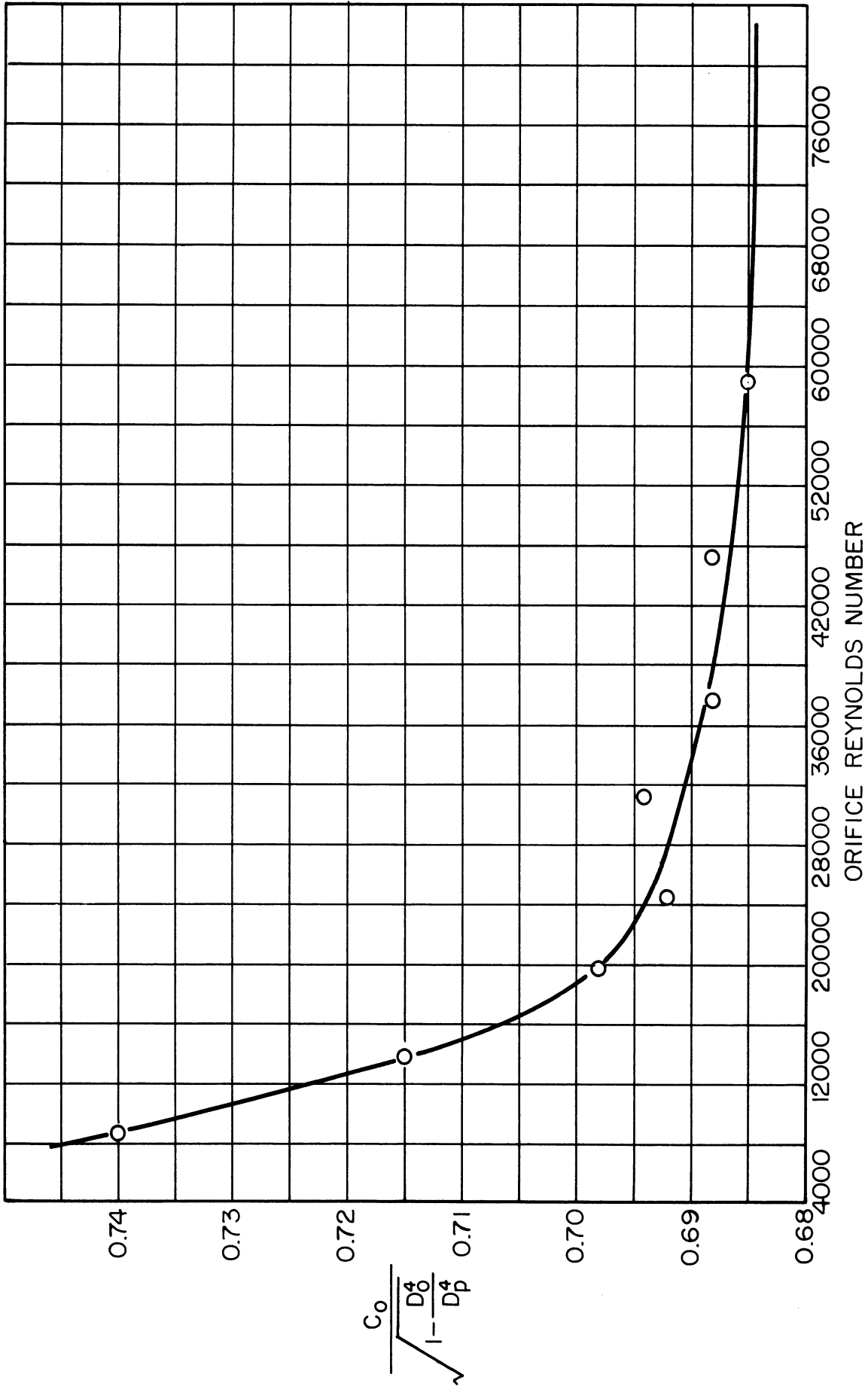


Figure 20. Calibration Curve for Inconel Orifice

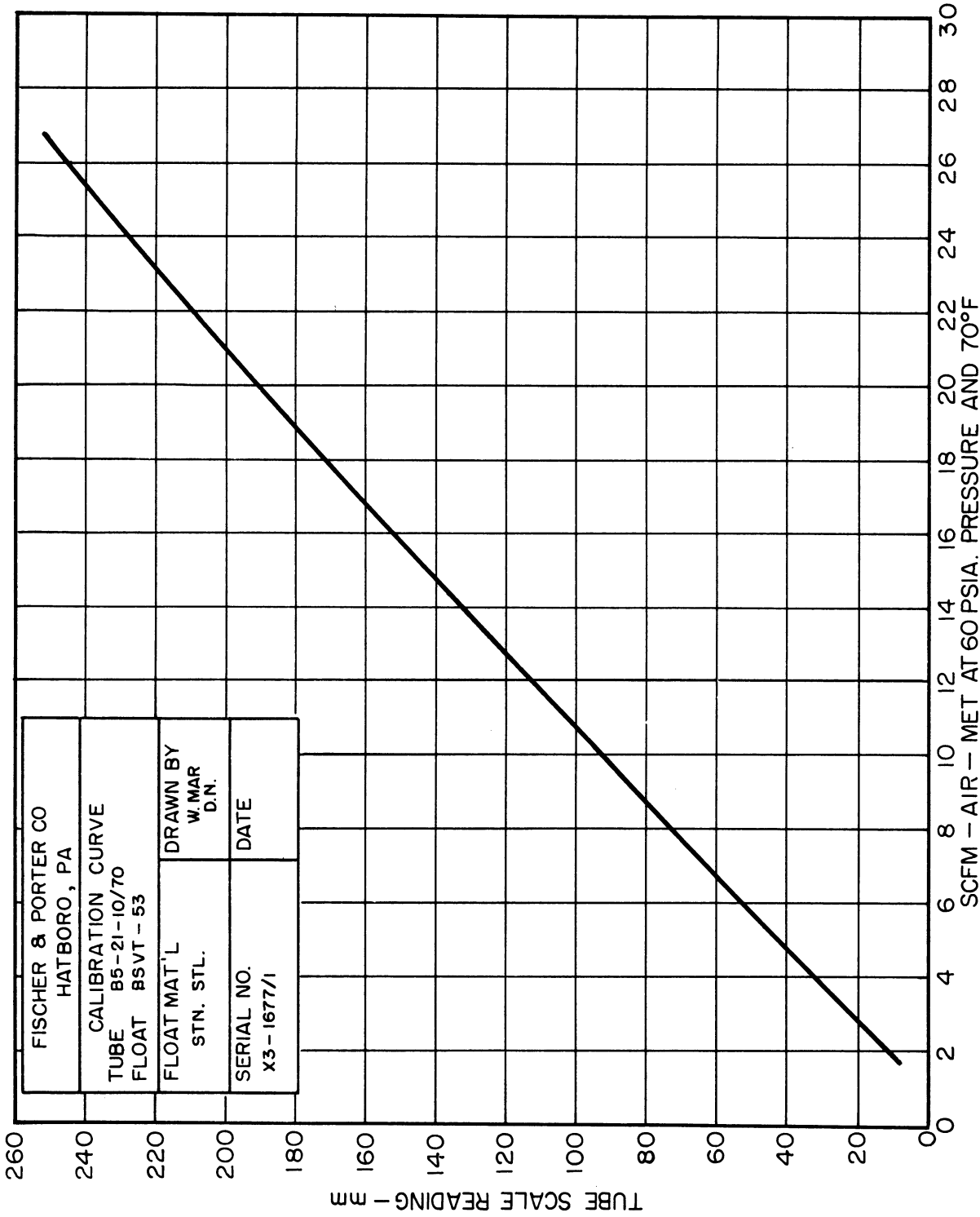


Figure 21. Calibration Curve for Air Rotameter

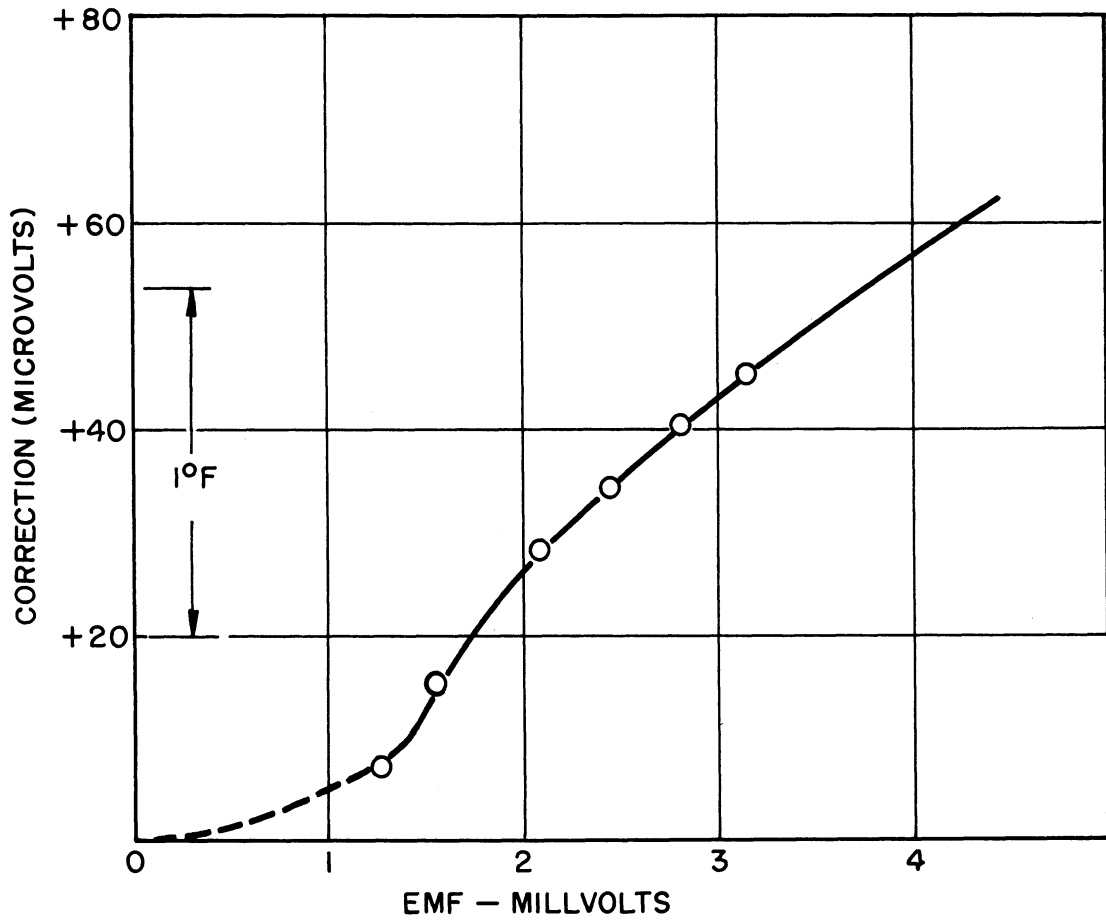


Figure 22. Calibration Curve of TC-7 in the Test Object



APPENDIX E

TABLE IV. SOURCES OF EQUIPMENT AND MATERIALS

Item	Source (Company)	Type
<u>Gas Supply System:</u>		
Air	Building Service System	90 psig.
Calcium Chloride	Mallinkrodt Chemical Co.	4 mesh dessicant quality
Pressure Regulator	Moore Products Company	Nullmatic #42-50
Rotameter	Fisher and Porter Co.	Figure 735
Thermometer	Consolidated Ashcroft Hancock Company	---
Pressure Gauges	Champion Gauge Company	Bourdon
<u>Gas Heating Unit:</u>		
Furnace	Harry W. Dietert Co.	Electric Resistance
Globar Element	The Carborundum Co.	Silicon Carbide
Inconel Tube	Steel Sales Company	Schedule 40
Tabular Alumina Balls	Aluminum Co. of America	T-80
Ceramic Rings	McDanel Refractory Co.	Alumina
Transite	University Plant Dept.	---
High Temperature Insulation	Johns-Manville Co.	Diatomaceous Earth
Platinum Screens	Eberbach and Son, Co.	52 Mesh
Thermocouple Pro- tective Tubing	Stupakoff Ceramic and Mfg. Company	Single Perforation

TABLE IV. (Cont.)

Item	Source (Company)	Type
Thermocouples	Hoskins Mfg. Company	Chromel-Alumel 28 gauge
Direct Reading Pyrometer	Hoskins Mfg. Company	0-1400 °C
<u>Heat Transfer Test Unit:</u>		
Inconel	Steel Sales Company	Hot Rolled
Special Thermocouples	Thermo-Electric Co.	Chromel-Constantan, 36 gauge Quadruple Teflon Enamel Coated
Silicone Resin Insulation	Dow-Corning Company	Type 994
Rotary Thermocouple Selector Switch	Foxboro Company	20 points, 2333 R
Precision Potentio- meter	Leeds and Northrup Co.	Portable Type 8662
<u>Cooling Water Circulation System:</u>		
Circulating Pump	Visking Pump Company	Internal Gear
Pump Motor	Star Electric Motor Co.	2 H.P., 3 Phase
Control Valves	Walworth Company	#95
Storage Tanks	University Plant Dept.	55 gal. Drums
Thermometer	Consolidated Ashcroft Hancock Company	---
Rotameter	Fischer and Porter Co.	Figure 735

## BIBLIOGRAPHY

1. Baines, W. D., and Peterson, E. G., Transactions of the American Society of Mechanical Engineers, 73, 467 (1951).
2. Bakhmeteff, B. A., The Mechanics of Turbulent Flow, Princeton University Press (1941).
3. Boelter, L. M. K., Young, G., and Iversen, H. W., National Advisory Committee for Aeronautics Technical Note 1451 (July 1948).
4. Cholette, A., Chemical Engineering Progress 44, 81 (1948).
5. Churchill, S. W., Convective Heat Transfer from a Gas Stream at High Temperature to a Cylinder Normal to the Flow, Ph.D. Thesis, University of Michigan (1952).
6. Deissler, R. G., National Advisory Committee for Aeronautics Technical Note 2138 (July 1950).
7. Deissler, R. G., National Advisory Committee for Aeronautics Technical Note 2242 (December 1950).
8. Deissler, R. G., National Advisory Committee for Aeronautics Technical Note 2410 (July 1951).
9. Deissler, R. G., National Advisory Committee for Aeronautics Technical Note 3016 (October 1953).
10. Deissler, R. G., and Eian, C. S., National Advisory Committee for Aeronautics Technical Note 2629 (February 1952).
11. Dow Corning Company, Midland, Michigan, Private Communication.
12. Groeber, H., Forschungs Arbeiten auf dem Gebiete des Ingenieurwesens 130, 1 (1912).
13. Groeber, H., Erk, S., and Grigull, U., Die Grundgesetze der Waermeuebertragung, Third Edition, Springer Verlag, Berlin (1955).
14. Hamilton, D. C., and Morgan, W. R., National Advisory Committee for Aeronautics Technical Note 2836 (December 1952).
15. Hilsenrath, J., et al., Tables of Thermodynamic Properties of Gases, National Bureau of Standards Circular 564 (Nov. 1, 1955).
16. Humble, L. V., Lowdermilk, W. H., and Desmon, L. G., National Advisory Committee for Aeronautics Report 1020 (1951).
17. Keenan, J. H., and Kaye, G. W. C., Thermodynamic Properties of Air, Wiley and Sons, New York (1945).

18. McAdams, W. H., Heat Transmission, Second Edition, McGraw-Hill Book Company, New York (1942).
19. Nusselt, W., Gesundheits-Ingenieur, 38, 477 (1915).
20. Nusselt, W., Zeitschrift des Vereines Deutscher Ingenieure, 61, 685 (1917).
21. Nusselt, W., Technische Mechanik und Thermodynamik, 1, 277 (1930).
22. Perry, J. H., Editor, Chemical Engineers' Handbook, Third Edition, McGraw-Hill Book Company, New York (1950).
23. Pigford, R. L., Chemical Engineering Progress Symposium Series 51, No. 17, Published by the American Institute of Chemical Engineers, New York City (1955).
24. Ramey, H. J., Henderson, J. B., and Smith, J. M., Preprint No. 10 for Heat Transfer Symposium, Annual Meeting of the American Institute of Chemical Engineers, St. Louis, Missouri (Dec. 13, 1953).
25. Rubesin, M. W., and Johnson, H. A., Transactions of the American Society of Mechanical Engineers, 71, 383 (1949).
26. Sieder, E. N., and Tate, G. E., Industrial and Engineering Chemistry, 28, 1429 (1936).
27. Stearns, R. F., et al., Flow Measurement with Orifice Meters, "Esso Series", D. Van Nostrand Company, Inc., New York (1951).
28. Thomassen, L., Professor of Chemical and Metallurgical Engineering, University of Michigan, Private Communication.
29. von Karman, T., Journal of the Aeronautical Sciences, 1, 1 (1934).
30. Weiland, W. F., and Lowdermilk, W. H., National Advisory Committee for Aeronautics Research Memorandum E53E04 (July 9, 1953).







UNIVERSITY OF MICHIGAN



**3 9015 03529 8549**